CURRENT UNDERSTANDING ON CYTOCHROME BD QUINOL OXIDASE OF *ESCHERICHIA COLI* A MUTAGENESIS, KINETICS AND SPECTROSCOPIC STUDY

BY

KE YANG

DISSERTATION

Submitted in partial fulfillment of the requirements
for the degree of Doctor of Philosophy in Biochemistry
in the Graduate College of the
University of Illinois at Urbana-Champaign, 2009

Urbana, Illinois

Doctoral Committee:

Professor Robert B. Gennis, Chair
Professor Robert B. Gennis, Director of Research
Professor Deborah E. Leckband
Associate Professor Satish K. Nair
Assistant Professor Maria Spies

ABSTRACT

Time-resolved kinetics study on the cytochrome *bd* quinol oxidase from *Escherichia coli* was carried out by stopped-flow techniques. The natural substrate, ubiquinol, was used to turnover the enzyme in the fast catalysis successfully for the first time. The results excluded the fully oxidized form of the enzyme from the rapid catalytic cycle of cytochrome *bd* oxidase. A re-investigation by both Flow-Flash and EPR on the previously reported mutant at Glu445 in subunit I, uncovered the dithionite-resistant ferric heme b_{595}. Electrometrics data further suggested a series of protonatable groups forming a proton channel located in the membrane to facilitate the proton translocation from cytoplasm to the heme b_{595} / heme *d* binuclear center. With help of the increasing database of available cytochrome *bd* oxidase sequences, site-directed mutagenesis studies were carried out on the highly conserved residues of the enzyme. Mutations on two highly conserved acidic residues in subunit I – Glu99 and Glu107 were characterized in detail. The glutamine substitution at Glu107 was managed to obtain the FTIR redox difference spectra regarding its relatively intact binuclear center. Glu107 was shown to be protonated at pH 7.6 and that it was perturbed by the reduction of the heme b_{595} / heme *d* binuclear center at the active site. Mutations on Serine140, another structurally important non-acidic residue were also studied by FTIR. Mutant enzyme in which Serine140 was replaced with threonine was shown to perturb protonation of several acidic residues including Glu107 and/or Glu99. Due to their close proximity to the active site, Glu99,

Glu107 and Ser140 were suggested to be part of the proton channel. Two highly conserved residues in the Q-loop of subunit I – Glu257 and Asp239 were also examined for their possible involvement in substrate binding. The FTIR difference spectra indicated a reorganization of binding environment caused by Glu257 mutant, while besides contributing to substrate binding, Asp239 was also believed to play a critical role in maintaining the redox potential of heme b_{595} in a right level that rapid catalysis can be achieved.

To My Family

ACKNOWLEDGEMENTS

Every party has an ending, no matter what. Working towards a Ph.D. is also a party, sort of. It's just a little bit longer than a Friday beer, in most of the case, five years. Now, we have the finale.

I have never imagined that I would stay in Champaign-Urbana for such a long time. As a big city boy, this small Midwest college town didn't give me a great first impression when I arrived in January 2004. No landscape, no water, no green plant. Wait a second, Eureka! We do have something: endless corn, and the same endless science.

Five years in Gennis lab would be a wonderful memory that I will recall in the future with smile on my face. Bob is such a good guy that not only helps us with his patience and knowledge, but also supports our career development with superb personality and open mind. I do appreciate his mentorship deeply.

Being a traditional Chinese, family is always the most important part in my life. I often feel sorry that as the only son, I cannot go home to see my parents very often due to busy experiment schedule and other uncontrollable issues. Thank my parents for their understanding and endless love.

Life always hides on the corner of next block, waiting to give you a surprise. Working and publications are not the only theme in small town. Two high schoolmates met in the other end of the Pacific and fell in love. Yes, my wife and I didn't know each other back to high school; even it's very likely we went to the same cafeteria every day

for three years. World is so big. World is so small.

Science is not a solo show any more, since many years ago. Especially when you are the only one knows the project in the whole group, you do need help. I have to thank Jie, the former “bd” girl in our group, whose lab notes served as my bible in my first two years, for her short but efficient instructions. Ahmet, our FTIR specialist, helped me to identify the subtle changes in the spectra. Jim, who dedicated to genomic sequencing, supported my research with evolutionary evidence.

Collaboration outside the group is another driving force in my research, and a great opportunity to learn from the scientist all over the world. Dr. Hellwig from Germany introduced me to the FTIR application; Dr. Konstantinov in Moscow taught me the basic about surface analysis of rapid kinetics; Dr. Belevich and Dr. Verkhovsky amazed me with their creative experiment design during my stay in Helsinki. All these are the treasures in my journey of science.

Time flies. Five years just like a flash. This is the finale of my Ph.D. life. This is the premier of my new adventure.

TABLE OF CONTENTS

CHAPTER 1:INTRODUCTION

1.1 Overview:

Energy generation is always the key issue in the life cycle of all the living organisms which need to maintain homeostasis, growth and reproduction. Among three major ways to obtain energy – aerobic respiration, anaerobic fermentation and photosynthesis, the aerobic respiration is found to be the most common and efficient way for heterotrophic organisms to generate energy for their food source. In general, aerobic respiration is achieved through a series of reaction called Respiratory Chain (**Figure 1.1**), also known as Electron Transfer Chain (ETC). This is a comprehensive process which consists of four or five complexes that pass the electrons from organic substance to the terminal acceptor, usually oxygen, during which energy is released and used for ATP synthesis or other energy-consuming process. Cytochrome oxidase, also known as terminal oxidase or complex IV, which is a group of heme proteins that can accept and pass electrons by changing their heme iron valences, is the crucial component in this process. Up to date, all the cytochorme oxidases can be classified into two major groups – the heme-copper oxidase superfamily and the tri-heme oxidase family. In *Escherichia coli*, the target organism of our study, there are two types of cytochrome oxidases involved in aerobic respiration – cytochrome bo_3 quinol oxidase from the heme-copper family and cytochrome *bd* quinol oxidase from the tri-heme family (Anraku and Gennis 1987).

1.2 Cytochrome *bd* quinol oxidase:

The cytochrome *bd* quinol oxdiase is expressed during both aerobic and anaerobic growth and achieves the highest expression level under the microaerophilic growth condition (Rice and Hempfling 1978; Cotter, Chepuri et al. 1990; Fu, Iuchi et al. 1991). The enzyme is a membrane-integrated heterodimer (**Figure 1.2**), with the two subunits being encoded by cydA (subunit I; 57 kD) and cydB (subunit II; 43 kD) (Miller, Hermodson et al. 1988). There is no sequence homology between either CydA or CydB and the subunits of the heme-copper oxidase superfamily (e.g., cytochrome *c* oxidases) (Calhoun, Thomas et al. 1994; Garcia-Horsman, Barquera et al. 1994). Both the heme-copper oxidases and the cytochrome *bd* oxidases are respiratory oxidases and catalyze the 4-electron reduction of O_2 to 2 H_2O. In both types of oxidases, the redox chemistry is coupled to the generation of a proton electrochemical gradient across the membrane (proton motive force). In both groups of oxidases, the sources of electrons and protons that are brought together with O_2 to generate water at the active site are on opposite sides of the membrane. Electrons come from the oxidation of electron donors at sites located at the periplasmic side and protons taken from the cytoplasm. This generates a transmembrane voltage coupled to enzyme turnover.

Despite of the physiological similarity to heme-copper oxidase described above, cytochrome *bd* is the only well-studied member of the tri-heme oxidase family (Jünemann 1997; Mogi, Tsubaki et al. 1998). Although increasing number of cytochrome *bd* oxidase has been found in prokaryotes and archaea, there is still lack of copy from eukaryotes (Osborne, 1999). There are three major structural and functional uniqueness of this enzyme that distinguish it from the heme-copper superfamily other than no

sequence homology. First, there is no copper in cytochrome *bd*, which is the main reason it's separated from the heme-copper oxidase family. Instead of a copper in the active site, another d-type heme is involved in the catalytic reaction. Second, cytochrome *bd* does not function as a transmembrane proton pump (Puustinen, Finel et al. 1991), which is one of the characteristics of the heme-copper oxidases. The fact that the enzyme does not pump proton may contribute to its exceptionally high affinity for oxygen and high catalytic efficiency (Puustinen, Finel et al. 1991; Jünemann, Butterworth et al. 1995). Third, in contrast to heme-copper oxidases' high sensitivity to cyanide, cytochrome *bd* is insensitive to cyanide inhibition. Its K_i value is as high as 8 mM for respiratory particles containing cytochrome *bd* (Pudek and Bragg 1974), compared to micromolar or even submicromolar range in its heme-copper opponent (Jones, Weiner et al. 1984; Kita, Konishi et al. 1984). All these unique features of cytochrome *bd* oxidase have made it an interesting target for enzymological study for decades (Zhang 2002).

Currently, there are over 1000 sequences of the cytochrome *bd* genes available from genomic data and from environmental sequencing projects. Cytochrome *bd* is much more prevalent in the genomic sequences than in the environmental sequences, which may indicate a biased presence in pathogenic bacteria which have been a major focus of genomic projects. Indeed, a number of publications have indicated a role of cytochrome *bd* in virulence and in the ability of pathogenic bacteria to survive as intracellular parasites (Loisel-Meyer, Jimenez de Bargues et al. 2005; Yamamoto, Poyart et al. 2005; Shi, Sohaskey et al. 2005; Way, Sallustio et al. 1999; Endley, McMurray et al. 2001).

A phylogenetic analysis of the sequences of both CydA and CydB indicates that the *bd*-type oxidases group in four phylogenetically coherent families (**Figure 1.3**)

(Hemp and Gennis, manuscript in preparation). It has been shown that subunit II has evolved significantly faster than subunit I, leading to more sequence diversity in subunit II (Hao and Golding 2006). Many prokaryotes have representatives of more than one of these families, suggesting that they may play distinct roles in the physiology of the organisms. The *E. coli* genome encodes two *bd*-type oxidases (*cyd*AB and *cyx*AB). CyxAB (previously called *app*BC), together with *app*A, consititutes the acid phosphatase regulon (Dassa, Fsihi et al. 1991), and the enzyme appears to be optimally expressed under anaerobic or near anaerobic conditions (Brondsted and Atlung 1996). The enzyme has not been extensively studied, but it has been isolated and characterized (Sturr, Krulwich et al. 1996). The CydAB oxidase has been more extensively studied, and is optimally expressed under microaerophilic conditions. CydAB is the predominant oxidase in *E. coli* grown to stationary phase or grown under conditions of limiting O_2 (Govantes, Orjalo et al. 2000; Govantes, Albrecht et al. 2000; Tseng, Albrecht et al. 1996; Iuchi and Lin 1991). CydAB is part of a closely related subgroup of *bd*-type oxidases that contains an insertion in the C-terminus of the Q-loop, a large periplasmic "loop" connecting transmembrane helices VI and VII (out of 9 predicted transmembrane helices) (**see Figure 1.4 and Figure 1.5**)(Osborne and Gennis 1999; Kusumoto, Sakiyama et al. 2000; Sakamoto, Koga et al. 1999). The Q-loop has been implicated by many experimental techniques as being involved in ubiquinol binding and oxidation (Matsumoto, Murai et al. 2006; Mogi, Akimoto et al. 2006; Dueweke and Gennis 1990; Dueweke and Gennis 1991).

All of the well-studied *bd*-type oxidases so far contain three heme prosthetic groups (**Figure 1.2**). Heme b_{558} is a low-spin protoheme IX (**Figure 1.6**) and located

within CydA, ligated to I-H186 and I-M393 (**Figure 1.4**), predicted to be near the periplasmic surface (Fang, Lin et al. 1989; Kaysser, Ghaim et al. 1995). Reduced heme b_{558} has absorption peaks at 560, 530, and 430 nm (**Figure 1.7**). The role of heme b_{558} appears to be to facilitate electron transfer from the reduced quinol substrate. The binding of quinone-analogues such as antimycin (Jünemann and Wrigglesworth 1994) or aurachin D (Mogi, Akimoto et al. 2006; Meunier, Madgwick et al. 1995) cause a red-shift of the absorption spectrum of heme b_{558}. Heme b_{595} is a high-spin protoheme IX (**Figure 1.6**), with absorption peaks at 595 and 560 nm and a recently characterized peak at around 440 nm in the reduced state (**Figure 1.7**). Heme *d* is a high-spin chlorin (**Figure 1.6**) with an α-absorption band at 628 nm and an uncharacterized Soret peak (**Figure 1.7**). Ferrous heme *d* binds stably to O_2 (heme *d* Fe^{2+}-O_2) and, upon the addition of two more electrons, forms a heme *d* $Fe^{4+}=O^{2-}$ oxoferryl species (plus –OH) (Lorence and Gennis 1989). When isolated, the enzyme is a mixture with hemes b in oxidized form, and heme *d* in ferrous-oxy and oxoferryl forms (Kahlow, Loehr et al. 1993) at a ratio around 70 to 30. The protein ligand of heme *d* is not known. Heme b_{595} does not stably bind to exogenous ligands (Borisov, Arutyunyan et al. 1999), such as CO, and its role in the catalytic mechanism is not known. It could be present simply as an electron donor, or it could play a role in capturing and activating O_2. Heme b_{595} is ligated to I-H19 in CydA (**Figure 1.4**) (Sun, Kahlow et al. 1996), also located at the periplasmic surface (Zhang, Barquera et al. 2004). Heme *d* and heme b_{595} are adjacent and since heme b_{595} is located to the periplasmic surface, it follows that the heme *d* / heme b_{595} active site must be located near the periplasmic side of the membrane (Zhang, Barquera et al. 2004).

Both heme-copper and tri-heme oxidases utilize protons from the bacterial cytoplasm. In the case of the heme-copper oxidases, distinct proton-conducting channels have been structurally and functionally identified (Branden, Gennis et al 2006; Brändén, Tomson et al. 2002; Gennis 1998; Konstantinov, Siletsky et al 1997; Ostermeier, Harrenga et al. 1997; Tsukihara, Aoyama et al. 1996). The D and K channels are used from proton input, and both lead from the bacterial cytoplasm to the vicinity of the enzyme active site. Highly conserved residues contribute to these channels. In the case of cytochrome *bd* oxidase, Electron transfer from heme b_{558} to the heme *d* / heme b_{595} active site generates a transmembrane voltage (positive outside) (Belevich, Borisov et al. 2005). This cannot be a direct result of the electron transfer itself because heme b_{558} and the heme *d* / heme b_{595} active site are both located near the periplasmic surface. Hence, the voltage must be generated by the coupled movement of protons across the membrane from the cytoplasm to the active site on the opposite side of the membrane. This is the basis for predicting a proton-conducting channel to facilitate this proton translocation. Unfortunately, there is no X-ray structure of a *bd*-type oxidase. However, with the large number of sequences now available, one can search for highly conserved residues that might be candidates for such a role. Several years ago, on the basis of sequence alignments, two glutamic acid residues were picked out as prime candidates as being components of a proton-conducting channel, E107 and E99 (*E. coli*) (Osborne and Gennis 1999). These are both predicted to be in transmembrane regions and are conserved. In this thesis, the effects of mutations in these, as well as other acidic residues, are reported.

The isolated cytochrome *bd* appears to have a single binding site for quinols. Unlike the heme-copper oxidases that utilize ubiquinol as a substrate, such as cytochrome bo_3 from *E. coli*, there is no evidence of a high affinity binding site for a quinone which does not readily exchange with the quinone pool in the membrane. Hence, the fully reduced form of cytochrome *bd* contains three electrons, corresponding to the ferrous forms of each of the three hemes.

After decades of intensive study on cytochrome *bd* oxidase, a lot of basic facts have been revealed, while more others remain mysterious. There are still some obvious questions need answers: What is the 3D structure of this enzyme? How does heme *d* reside in the membrane? What is the role of heme b_{595}? How do the proton from cytoplasm translocate to the reactive site couple with the electrons from the donors? How is the substrate quinol bound to the enzyme? Is fully oxidized heme *d* an essential state in the fast turnover? Some of these questions are addressed in this dissertation. Various experimental approaches, such as site-directed mutagenesis, EPR, FTIR and Flow-Flash, etc. are employed to explore the nature of cytochrome *bd* oxidase, and they are proven to be highly productive.

1.3 Scope of dissertation:

This dissertation focuses on the cytochrome *bd*-I quinol oxidase from the *E. coli* respiratory chain. By means of mutagenesis study of the highly conserved residues, as well as various spectroscopic studies of the wild type enzyme, more knowledge on the structure-function relationship of this evolutionarily unique enzyme is obtained.

The first chapter provides background information and serves as an introduction. Chapter 2 presents the novel rapid catalysis model based on the kinetics study of the wild type enzyme, where the fully oxidized, ferric state, is excluded in the latest version. The next three chapters form a series study on the putative proton channel comprised of three chapters: Chapter 3 complements a previous identified important residue, I-E445, near the Q-loop in the highly conserved "GRPQW" region, which is necessary in maintaining proper function of heme b_{595}. Mutation on this site specifically prevents the reduction of heme b_{595} without affecting the other two hemes. EPR spectra and electrometric data raise the discussion on the putative but "must-have" proton channel, which facilitates the proton uptake from cytoplasm to the enzyme reaction center. In Chapter 4, two highly conserved acidic residues, I-E99 and I-E107 have been identified in the spatial proximity of the bi-nuclear center. The comparative FTIR study of I-E107 mutants and wild type enzyme reveals the importance of E107's protonation status during the proton translocation. To further explore, Chapter 5 presents the FTIR and Flow-Flash work on another highly conserved residue, I-S140, which sits right below I-E99 and I-E107. Mutation on this residue specifically impairs the protonation of I-E107 / I-E99, as well as perturbs the fast kinetics through peroxy state. Chapter 6 and Chapter 7 focus on two highly conserved acidic residues, I-D239 and I-E257, which are involved in the quinol binding. Chapter 8 summaries all the findings and serves as the conclusion.

1.4 Figures and tables:

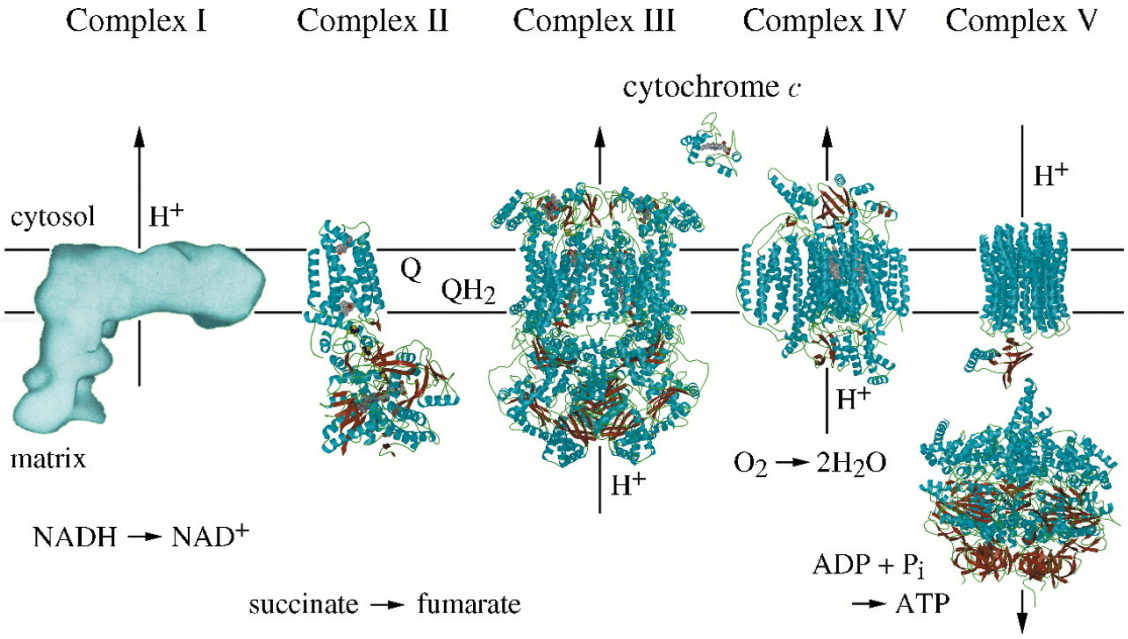

Figure 1.1 The mitochondrial respiratory chain.
Structures are of mitochondrial enzymes or bacterial analogs. ATP synthase was named as Complex V in this figure. (from B. E. Schultz and S. I. Chan, 2001)

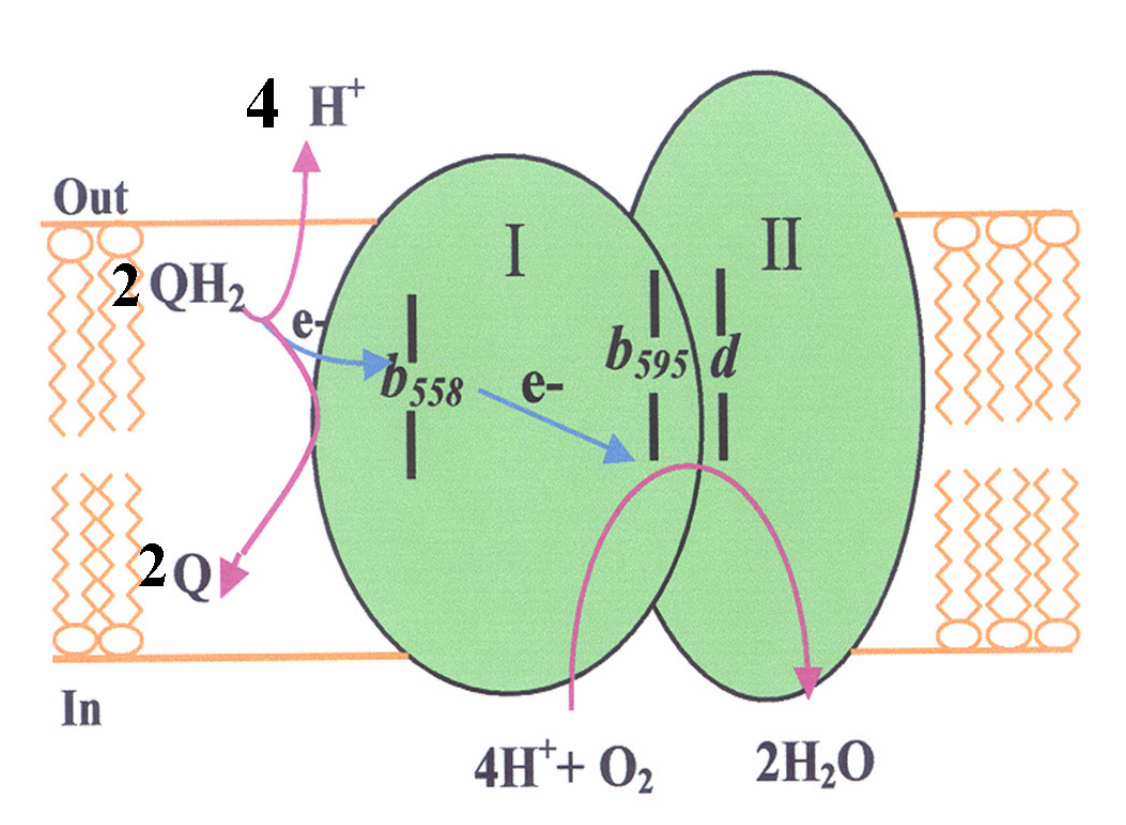

Figure 1.2 A model of cytochrome *bd* quinol oxidase structure.
The periplasm and cytoplasm are referred as "out" and "in" respectively. All the prosthetic groups are shown, with heme b_{558} located in subunit I, and heme b_{595}-heme *d* binuclear center at the interface between subunit I and II. The electron pathway is marked with blue, and proton pathway marked with magenta. Note the proton gradient across membrane is generated through scalar reactions with no proton pumping involved. (modified from dissertation of J. Zhang, 2002)

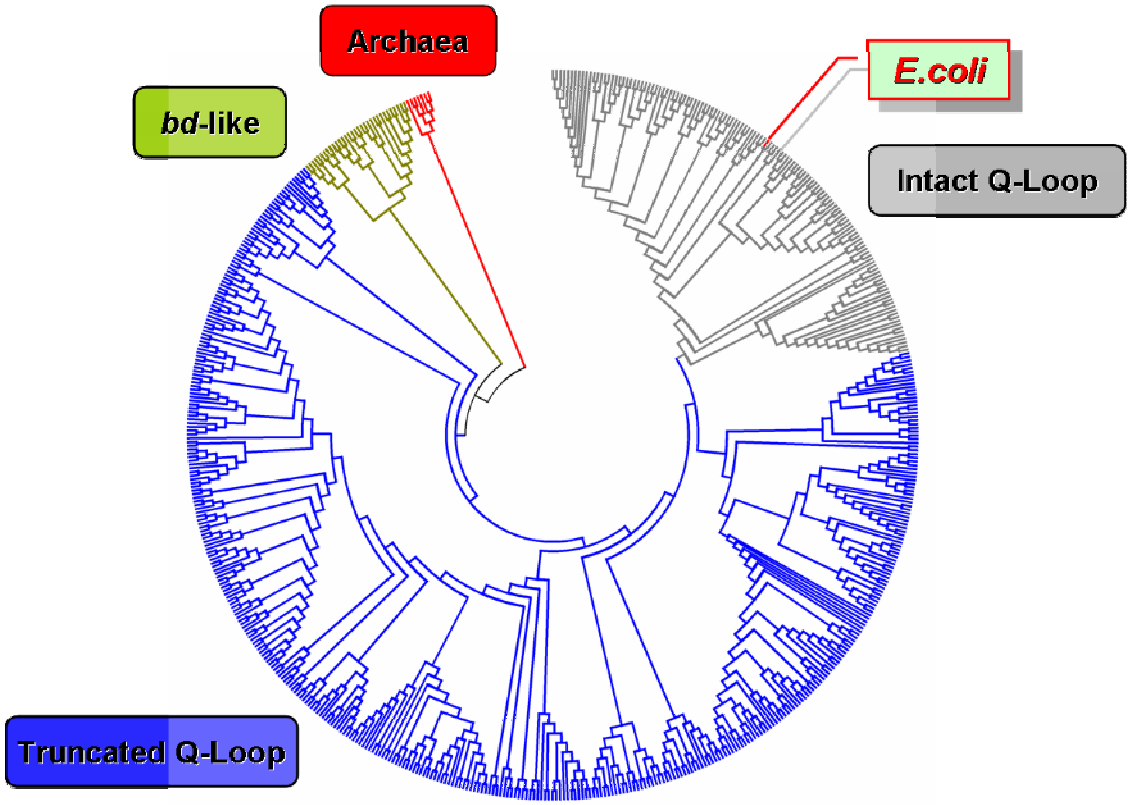

Figure 1.3 Evolutionary tree of cytochrome *bd* quinol oxidase.
Over 1000 cytochrome *bd* oxidase sequences from both genomic data and environmental sequencing projects were used to generate this tree. Four phylogenetically coherent families are marked with colors: family that has intact Q-loop including *E. coli* is in grey; family that have truncated Q-loop is in blue; family of *bd*-like oxidases is in yellowish green; family of archaea is in red.

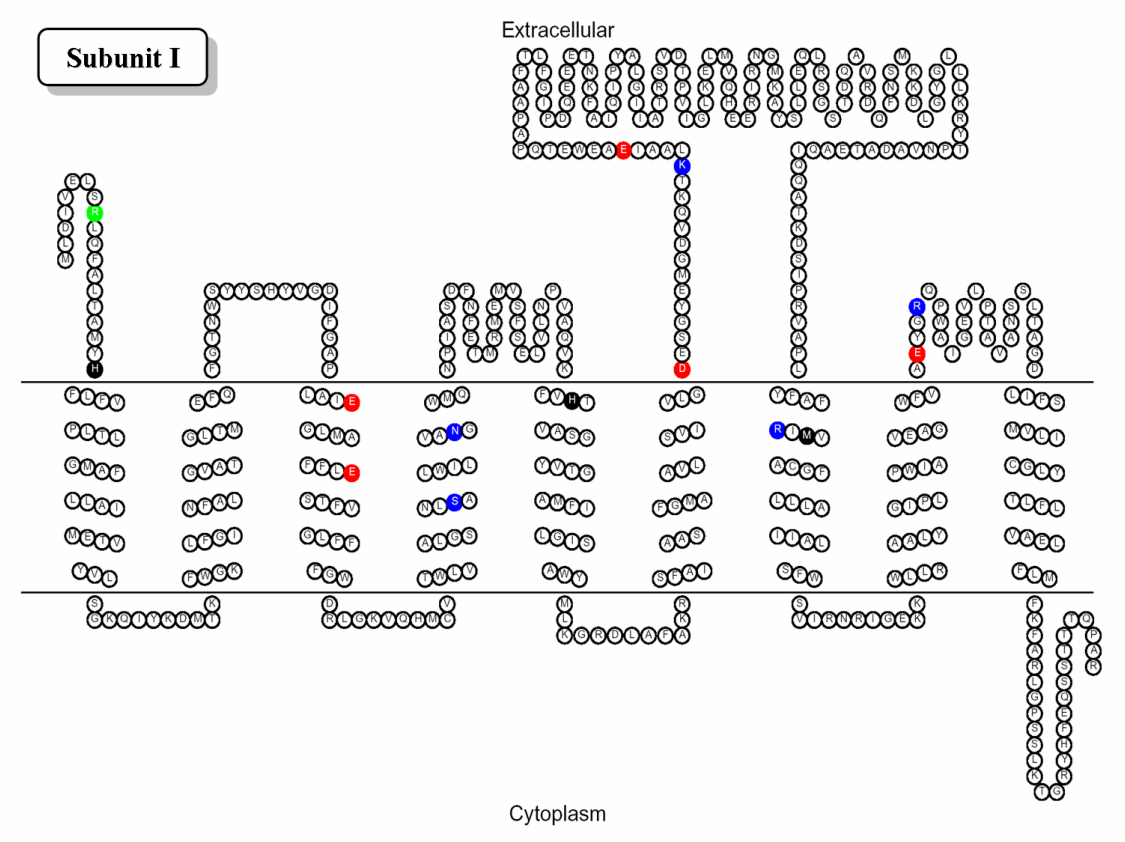

Figure 1.4 Membrane topology model of subunit I of cytochrome *bd* oxidase from *E. coli*.
The highly conserved residues are marked with colors: the heme ligands (H19, H186 and M393) are in black; the acidic residues are in red; the others are in blue. TMHMM 2.1 and TOPO2 programs were used to generate the model.

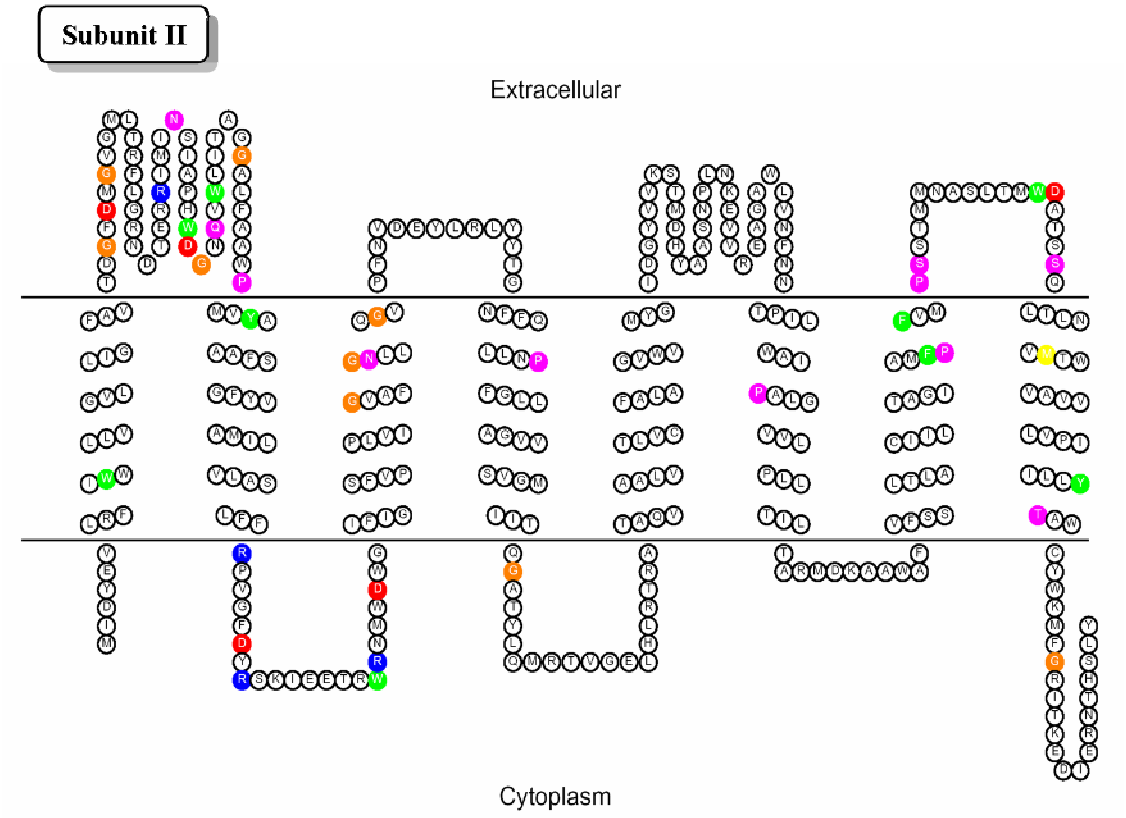

Figure 1.5 Membrane topology model of subunit II of cytochrome *bd* oxidase from *E. coli*.
Since subunit II is more evolutionarily diverse (James Hemp, unpublished data), the highly conserved residues within *E. coli* subfamily are marked in colors. TMHMM 2.1 and TOPO2 programs were used to generate the model.

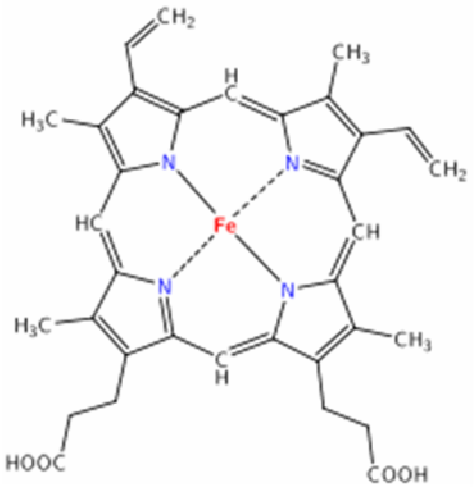

Protoheme IX
(Heme *b*)

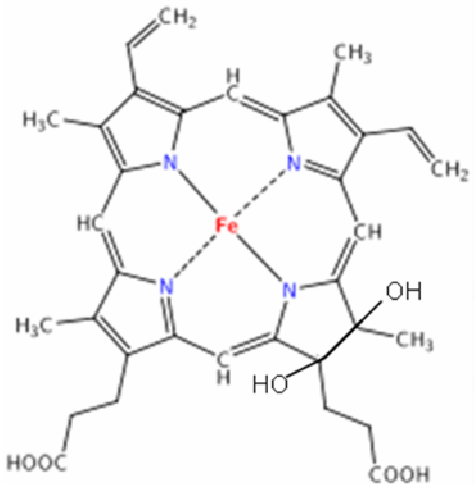

Heme *d*

Figure 1.6 The structures of heme *b* and heme *d*.
Heme *d*, a chlorin, is derived from heme *b* by the addition of two hydroxyl groups to a double bond in the porphyrin macrocycle. The axial ligands of the ferric ions are not shown. (modified from dissertation of J. P. Osborne, 1999)

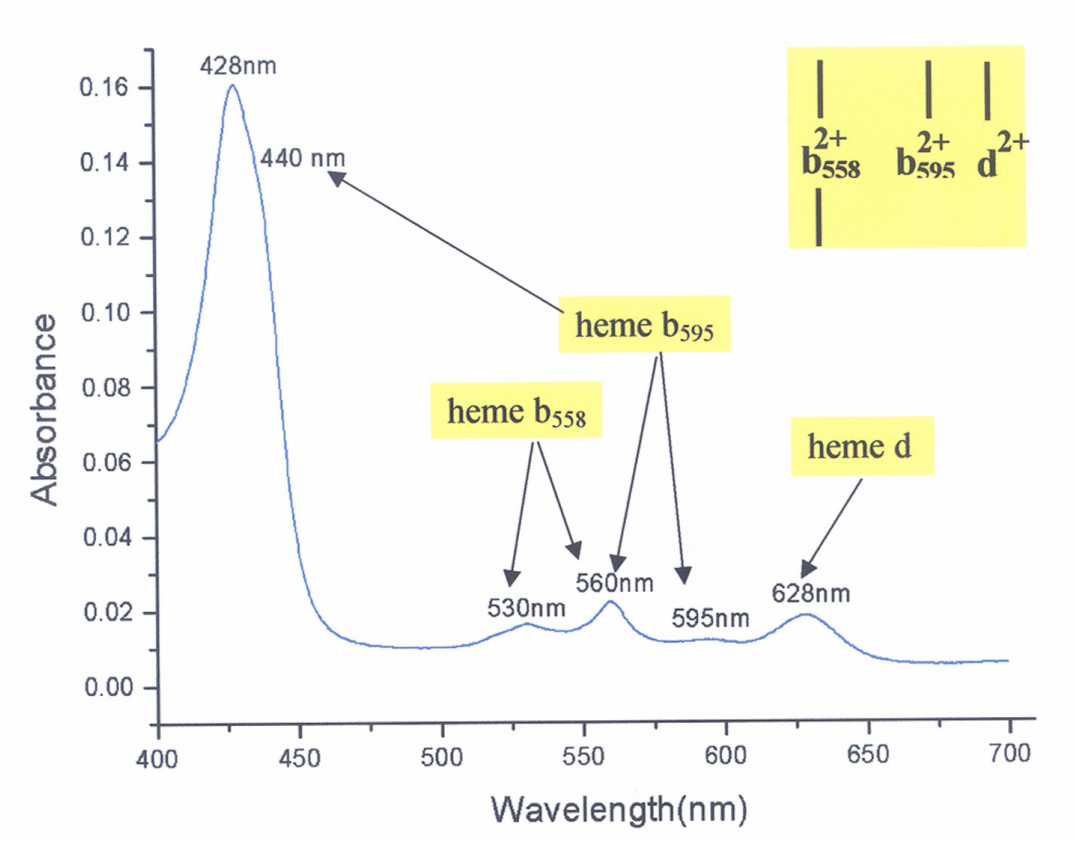

Figure1.7 UV-Vis spectrum of dithionite-reduced cytochrome *bd* oxidase.
The numbers indicate the positions of the absorption peaks of each heme. All hemes contribute to the absorption at 428 nm. (modified from dissertation of J. Zhang, 2002)

CHAPTER 2: EXCLUSION OF THE FULLY OXIDIZED FORM OF CYTOCHROME *BD* QUINOL OXIDASE FROM CATALYTIC CYCLE

2.1 Introduction:

Cytochrome *bd* contains three heme prosthetic groups: heme b_{558}, heme b_{595} and heme *d*. Heme b_{558} is a low spin heme near the quinol binding site and is involved in the oxidation of ubiquinol. Heme b_{595} and heme *d* constitute a binuclear center, and spectroscopic studies indicate they are within 10Å from each other (Arutyunyan, Borisov et al 2008). Both heme b_{595} and heme *d* are high spin hemes. Heme *d* is where O_2 binds and is reduced to water, and heme b_{595} appears to function primarily to transfer electrons to heme *d*.

The question being addressed in this chapter concerns the steady state mechanism by which the isolated enzyme converts oxygen to water using ubiquinol-1 as the substrate. Five different states of heme *d* have been characterized in cytochrome *bd*. These are 1) oxidized, Fe^{3+}; reduced, Fe^{2+}; ferrous-oxy complex, Fe^{2+}-O_2; 4) oxoferryl, Fe^{4+}=O^{2-}; and 5) peroxy, Fe^{3+}-OOH. The peroxy complex has been observed spectroscopically (Belevich, Borisov et al. 2007), but only transiently upon the addition of O_2 to the fully reduced enzyme, and its structure is a reasonable speculation, but requires further confirmation. Each of the other four forms of heme *d* can be generated as stable or metastable forms that can be examined and characterized. These forms suggest a sequence of events at heme *d* as O_2 is converted to water (**Figure 2.1**).

It has been a long-time controversial topic that the all-ferric form of the enzyme is not part of the catalytic cycle. Two mechanisms have been proposed which are closely related. The initial proposal also suggested that the ferrous-oxy complex of heme *d* was also not part of the catalytic cycle, but this has been argued as being unreasonable in view of the rapid internal electron transfer that has been observed in the enzyme. The analysis of the steady state kinetics, however, must take into account the redox status of the other two heme prosthetic groups, heme b_{558} and heme b_{595}, which can be present either as the Fe^{2+} or Fe^{3+} states, and also the fact that ubiquinol is a 2-electron donor. In this chapter, a slightly modified form of the proposed catalytic cycle from Matsumoto et al is shown in **Figure 2.2**. The modification is simply to explicitly add the ferric-hydroperoxy form of heme *d*, which had not been observed at the time of the initial proposed catalytic cycle.

The model shown in **Figure 2.2** would be reasonable if one assumes that the rate of reduction of the all-ferric form of the enzyme is slow. If it were rapid, the enzyme would readily form the 2-electron reduced species, which would rapidly react with O_2 and provide a possible alternate catalytic cycle with different species present as catalytic intermediates than those in **Figure 2.2**. However, a pulsed radiolysis study examined the rate of electron transfer from heme b_{558} to the heme b_{595} / heme *d* binuclear center (Kobayashi, Tagawa et al. 1999). The generation of a strong 1-electron reductant in this experiment resulted in the rapid reduction of reduced heme b_{558} and rapid equilibration within 10 μs between heme b_{558} and b_{595}, followed by electron transfer to heme *d* with a rate constant of about 5×10^2 s^{-1}. The rates were the same for heme *d* in either the ferric (Fe^{3+}) or oxoferryl ($Fe^{4+}=O^{2-}$) forms. In contrast, the 1-electron transfer to heme *d* in the ferrous-oxy form ($Fe^{2+}O_2$) was about 100-fold slower. Taken at face value, these data

raise questions about the catalytic competence of the ferrous-oxy complex as an intermediate, and suggest that the all-ferric form should be reconsidered as a possible intermediate during steady state analysis. One important different between the steady state and pulse radiolysis experiments is that the former utilizes a 2-electron substrate whereas the latter utilizes a 1-electron reductant. This was pointed out by Matsumoto et al, in reference to the slow electron transfer to the ferrous oxy complex.

In the current chapter, stopped-flow methods were used to monitor the rate of reaction of ubiquinol-1 / ascorbate reduced TMPD with the all-ferric form of cytochrome *bd* and with the as-isolated form of the enzyme, which contains a mixture of 80% ferrous-oxy and 20% oxoferryl forms of heme *d*, with the ferric forms of heme b_{558} and heme b_{595}. The results show very slow reduction by ubiquinol-1 of the all-ferric enzyme, and very rapid reduction of the as-isolated form of the enzyme. It is concluded that, as postulated, the all-ferric form of the enzyme is not part of the catalytic cycle, and that the ferrous-oxy form of the enzyme is part of the cycle, as shown in **Figure 2.2**.

2.2 Materials and methods:

2.2.1 Strains and plasmids:

E. coli strain CLY (*cyo::kan*, *rec*A), which lacks cytochrome bo_3 quinol oxidase (Yep 2005) was used as the host strain for expressing the wild type cytochrome *bd* on a plasmid. To obtain wild type cytochrome *bd*, plasmid pTY1 (Yang 2007) was introduced to the strain. This plasmind is a derivative of pET17b and contains the whole operon of wild type *bd* as well as ampicillin resistance gene for selection.

2.2.2 Cell growth and protein sample preparation:

Large scale cell growth of strains that grow aerobically (i.e. expressing wild type or some complementary mutants) was carried out in 24 2-liter flasks shaking at 220 rpm 37 °C using two Innova 4330 incubator shakers (New Brunswick Scientific). Strain expressing wild type was grown in LB containing 100 μg/mL Amp, 50 μg/mL Kan, and 0.5mM IPTG was added 4 hours after the inoculation. Wild type cytochrome *bd* oxidase was purified from the membrane of CLY/pTY1 using the same method as described previously (Miller and Gennis 1986), with the modification that the hydroxyapatite column was omitted. Fractions were collected from the Fast-Flow Sepharose DEAE column with an A_{412}/A_{280} ratio greater than 0.5. The pooled fractions were concentrated using an Amicon concentrator with a 50 kDa molecular weight cut-off filter and then dialyzed three times against 50 mM sodium phosphate buffer, pH 7.8, containing 5 mM EDTA, 0.05% N-lauroylsarcosine. Both wild type and mutant cytochrome *bd* samples were then examined, using the same dialysis buffer for appropriate dilution unless specified otherwise.

2.2.3 Ubiquinol-1 and TMPD oxidase activity assay:

Cytochrome *bd* wild type was assayed both in isolated membranes, in which there is no other quinol oxidase, and with the purified enzyme. For membranes, samples were homogenized in 25 mM Tris HCl, 1 mM EDTA disodium salt, pH 7.5. Purified protein samples were dialyzed against 50 mM NaPi buffer, pH 7.8, containing 5 mM EDTA disodium salt and 0.05 % N-lauroyl sarcosine. Various dilutions of either the homogenized membrane samples or pure protein samples were added to 1.8 mL of the

respective buffer containing either 2 mM dithiothreitol or 4 mM ascorbate that had been equilibrated to 37 °C in a Clark-type oxygen electrode (Yellow Springs Instrument CO.). A baseline was taken and the reaction was initiated by addition of ubiquinol-1 (kindly provided by Hoffman-LaRoche) or TMPD to a final concentration of 245 μM and 1 mM, respectively. Activities were determined assuming a value of 237 μM O_2 for air-saturated buffer at 37 °C.

2.2.4 Stopped-Flow spectroscopic and kinetic measurements:

All the work was performed at 20 °C using an Applied Photophysics model SX with a photodiode array detector as well as single-wavelength detection. The flow system was flushed thoroughly with Argon-saturated buffer (50 mM sodium phosphate, 5 mM EDTA and 0.05% N-lauroylsarcosine, pH 7.8) before the experiments. The whole system was kept anaerobic by flowing Argon during the experiments. The mixing ratio of the two solutions being mixed was all 1:1. All concentrations reported are the initial concentrations before mixing.

Since each species of heme *d* in the catalytic cycle of cytochrome *bd* have been characterized optically, the formation and the decay of the heme *d* species can be monitored spectrophotometrically. The reduction by ubiquinol of the "as isolated" enzyme was carried out by generated the "as isolated" enzyme *in situ*. This was done by typically starting with one solution containing 5 μM enzymes with an excess concentration of 200 μM ubiquinone and 6 mM DTT in Argon-saturated buffer (50 mM sodium phosphate, 5 mM EDTA disodium salt and 0.05% N-lauroyl sarcosine, pH 7.8). This solution was rapidly mixed with an equal volume of a solution containing

approximately 5 μM O_2 in the same buffer. The conditions were adjusted so that the O_2 rapidly oxidized the enzyme which was then, in turn, reduced by the excess ubiquinol-1 that was present. The oxidation reaction was too fast to resolve but most of the reduction was monitored to obtain rate constants. Spectroscopic analysis of the product of the reaction of O_2 with the reduced enzyme showed that it contained approximately 80% oxoferryl and 20% ferrous-oxy complex.

To investigate the reduction of the ferric cytochrome *bd*, 5 μM enzymes was incubated with 16 μM tetrachlorobenzoquinone, a lipophilic strong and effective oxidant (Borisov, Smirnova et al. 1994) for 20 minutes in Argon-saturated buffer (50 mM sodium phosphate, 5 mM EDTA and 0.05 % N-lauroyl sarcosine, pH 7.8). This generated the fully oxidized (all ferric) form of the enzyme. This form of the enzyme was rapidly mixed with an equal volume of 200 μM ubiquinone-1 and 6 mM DTT in the same buffer, or with an equal volume of 1 mM TMPD and 20 mM ascorbate in the same buffer. For all experiments reported, at least three runs were performed for each time scale, and 1600 spectra were collected from 300 nm to 1200 nm.

2.2.5 Data analysis:

The data were first analyzed with the use of Pro-Kineticist software package "ProK for PC" (Applied Photophysics) and selected data were imported into Origin 7 (Microcal) for further analysis and preparation of the figures.

2.3 Results:

2.3.1 Oxidation/Re-reduction of fully reduced / oxidized wild type with ubiquinol-1:

Figure 2.3 compares the kinetics of reduction of heme *d* in the oxoferryl and all-ferric forms of cytochrome *bd*. From the spectra/time surface collected, the kinetics at a wavelength pair 628 nm and 719 nm ($\Delta A_{628-719}$) was extracted to monitor the reduction of heme *d*. The kinetics of the reduction of the all-ferric form of the enzyme by UQH_2-1 is extremely slow and non-homogeneous, reaching only about 25% of the expected maximum in 2 s, the maximal observation period in the experiment shown. This is in contrast to the extremely rapid reduction of heme *d* in the all-ferric enzyme (k~ 3,400 s^{-1}), reported in the pulsed radiolysis experiments of Kobayashi et al. Reduction of hemes b_{558} and b_{595} in the same experiment was even slower that reduction of heme *d*, with either (DTT + ubiquinol) or (ascorbate + TMPD) as electron donors (data not included) and took about about 60 s for completion, whereas heme *d* reduction was complete in 20 to 30 s. Hence, it is likely that it is electron entry into the enzyme (reduction of b_{558}), rather than intramolecular electron transfer, that limits the rate of reduction of ferric heme *d* in the all-ferric enzyme.

In order to examine the reactivity of the oxoferryl state of cytochrome *bd*, this form of the enzyme was generated *in situ* in the stopped flow mixing chamber by oxidation of the fully reduced cytochrome *bd* with stoichiometric amount of O_2.

$$b_{558}^{2+}b_{595}^{2+}d^{2+} + O_2 \leftrightarrow b_{558}^{2+}b_{595}^{2+}d^{2+}{-}O_2 \qquad (1)$$

$$2H^+ + b_{558}^{2+}b_{595}^{2+}d^{2+}{-}O_2 \rightarrow b_{558}^{3+}b_{595}^{3+}d^{4+}{=}O^{2-} + H_2O \qquad (2)$$

Formation of the oxycomplex (reaction 1) and subsequent oxidation of the reduced cytochrome *bd* by bound oxygen (reaction 2) are complete within the mixing time, in agreement with the known rate constants. At 2.5 μM oxygen (final concentration after mixing), the expected rate for the reaction with O_2 is about 2×10^9 $M^{-1}cm^{-1} \times 2.5$ μM O_2 $= 5 \times 10^3$ s^{-1}, τ ~200 μs (Hill, Hill et al. 1994), and the oxidation yields largely the oxoferryl state of the enzyme (at least 80%). This was most clearly seen in the spectra from the experiments in which reduced TMPD was used as the reductant (data not shown), since the subsequent reduction of the enzyme in this case is much slower than with UQH_2-1.

The oxoferryl form of the enzyme is reduced quite rapidly by UQH_2-1, and the reaction is completed in about 10 ms (**Figure 2.3A**). During this time, up to 12 time-resolved spectra could be collected. The major part of the transiently oxidized cytochrome *bd* is actually reduced within the dead time of the mixing apparatus and only the tail end of this rapid reduction could be monitored with the current instrumentation. Global analysis of the spectra/time surface for the resolved part of the reduction process gave a rate constant of ~200 - 300 s^{-1}, which is close to enzyme turnover rate (~1000 electrons s^{-1}) when multiplied by 4 electrons required to convert enzyme from the oxoferryl to the all ferrous state.

2.3.2 Rapid phase of the ubiquinol-1 reduction:

The difference spectrum of the rapid phase of the reduction, as resolved by global analysis, is shown in **Figure 2.4**. The spectrum shows clearly simultaneous disappearance of the oxoferryl state (trough around 670 nm - 680 nm) and appearance of reduced heme

d (peak at ~630 nm), as well as reduced heme b_{558} and heme b_{595} (the peaks at 595 nm, 560 nm and 530 nm in the visible, and an asymmetric Soret band with a maximum at 431 nm and a shoulder around 438 nm). These data imply that the reaction monitored involves reduction of the enzyme by two equivalents of UQH_2-1, since four electrons are required to generate the fully reduced form of the enzyme ($b_{558}^{2+}b_{595}^{2+}d^{2+}$) from the oxoferryl state ($b_{558}^{3+}b_{595}^{3+}d^{4+}=O^{2-}$). The first equivalent of UQH_2-1 produces a partially reduced form of the enzyme ($b_{558}^{3+}b_{595}^{3+}d^{2+}$), so these results imply that the rate of reduction by the second equivalent of UQH_2-1 of the partially reduced enzyme ($b_{558}^{3+}b_{595}^{3+}d^{2+}$) is about as fast as the reaction of the oxoferryl species ($b_{558}^{3+}b_{595}^{3+}d^{4+}=O^{2-}$) with the first equivalent of UQH_2-1.

2.3.3 Oxidation/Re-reduction of fully reduced / oxidized wild type with TMPD:

The reduction kinetics of the enzyme with a single electron donor TMPD reduced by excess ascorbate was also examined (**Figure 2.3B**). Reduction of the all-ferric enzyme in this case is also very slow. As in the case of ubiquinol, the reaction of reduced TMPD with the oxoferryl form is more rapid than with the all-ferric form of the enzyme, although it is still much slower than observed with UQH_2-1. The reduction of the all-ferric cytochrome *bd* by reduced TMPD occurs on a time scale of 0.1-0.5 s, not in milliseconds. It cannot be excluded that the reaction of cytochrome *bd* with reduced TMPD is rate-limited by the oxidation of TMPD, since TMPD is a much poorer electron donor than UQH_2-1.

2.4 Discussion and conclusions:

The data clearly show that the reduction of heme *d* in the oxidized (all-ferric) form of cytochrome *bd* by its natural 2-electron substrate, ubiquinol, is much too slow to be part of the catalytic cycle. In contast, the reaction of the oxoferryl form of cytochrome *bd* with ubiquinol is rapid and results in formation of the fully reduced enzyme. Presumably, the reaction proceeds in 2 sequential two-electron steps which are not time-resolved under the conditions of our experiments at a UQH_2-1 concentration of 100 μM (the final concentration after mixing).

$$UQH_2\text{-}1 + (b_{558}{}^{3+}b_{595}{}^{3+}d^{4+}{=}O^{2-}) \leftrightarrow UQ\text{-}1 + H_2O + (b_{558}{}^{2+}b_{595}{}^{2+}d^{2+}) \qquad (3)$$

$$UQH_2\text{-}1 + (b_{558}{}^{3+}b_{595}{}^{3+}d^{2+}) \leftrightarrow UQ\text{-}1 + (b_{558}{}^{2+}b_{595}{}^{2+}d^{2+}) \qquad (4)$$

The rate of reaction 4 must be at least as fast as reaction 3 under the conditions of these experiments, since the appearance of reduced heme *d* and the reduced hemes b occur in the same time window. However, in the presence of excess of O_2, the very rapid rate of binding of O_2 with the 1-electron reduced enzyme (microseconds) is expected to result in formation of the 1-electron ferrous-oxy complex.

$$(b_{558}{}^{3+}b_{595}{}^{3+}d^{2+}) + O_2 \leftrightarrow (b_{558}{}^{3+}b_{595}{}^{3+}d^{2+}{-}O_2) \qquad (5)$$

Hence, when the concentration of O_2 is high, reaction 5 would prevail, followed by reaction 6.

$$(b_{558}{}^{3+}b_{595}{}^{3+}d^{2+}{-}O_2) + UQH_2\text{-}1 \leftrightarrow (b_{558}{}^{2+}b_{595}{}^{2+}d^{2+}{-}O_2) \quad (6)$$

The product of reaction 6 has sufficient electrons to split the O-O bond (reaction 2), provided protons are available.

Under microaerophilic growth conditions, in which cytochrome *bd* is normally expressed in *E. coli* (Govantes, Orjalo et al. 2000), the reactions of the one-electron reduced enzyme ($b_{558}{}^{3+}b_{595}{}^{3+}d^{2+}$) with O_2 (reaction 5) and with UQH_2-1 (reaction 4) might occur in the reverse order, which, however, makes no difference to the final outcome of the reaction cycle. It is interesting that the heme *d* ferrous-oxy complex ($b_{558}{}^{3+}b_{595}{}^{3+}d^{2+}$-$O_2$) is very stable, being the major form of the enzyme as it is isolated (Lorence, Koland et al. 1986). The dissociation of oxygen in the form of superoxide (O_2^-), which would be deleterious to the cell, is negligible. On the other hand, 2-electron reduction of the all-ferric cytochrome *bd* by UQH_2 and its subsequent oxidation by oxygen could give rise to an unstable peroxide adduct of the ferric enzyme that could dissociate releasing hydrogen peroxide, or produce hydroxyl radicals in case of homolytic scission of the O-O bond. Hence, the intermediate states of cytochrome *bd* with an odd number of electrons relative to the all-ferric form appear to be preferred in the catalytic cycle of the enzyme. These catalytic intermediate forms contain +3, +1 and -1 electrons relative to the all-ferric enzyme: a) +3 electrons = all-ferrous ($b_{558}{}^{2+}b_{595}{}^{2+}d^{2+}$); b) +1 electron = oxycomplex ($b_{558}{}^{3+}b_{595}{}^{3+}d^{2+}$-$O_2$); c) -1 = oxoferryl ($b_{558}{}^{3+}b_{595}{}^{3+}d^{4+}{=}O^{2-}$).

The expectation from the previous work of Jünemann et al. and of Matsumoto et al., based on steady state kinetics, that the all-ferric form of cytochrome *bd* is not part of

the catalytic cycle of the enzyme is directly verified by pre-steady state kinetics. It remains to be seen why the one-electron reductant formed during the pulsed radiolysis experiments by Kobayashi et al. reacts with the all-ferric enzyme rapidly. The explanation might be simply that the N-methylnicotinamide radical and solvated electron generated under the conditions of pulse radiolysis are much stronger reductants than the one-electron donor used in the current work, TMPD (E_m = 260 mV) as well as than the ubiquinol / ubisemiquinone couple that serves as an initial reductant for cytochrome *bd* during the reaction of the enzyme with ubiquinol. One might also note that the all-ferric forms of cytochrome *bd* were obtained by different methods in this work, compare to previous publication (Kobayashi, Tagawa et al. 1999), but it is highly unlikely that a variance in the preparations can account for the ~ 1000-fold difference in reactivity of heme *d*.

The observation that UQH_2-1 is a poor reductant for the all-ferric form of the enzyme, but a good reductant for the oxoferryl ($b_{558}^{3+}b_{595}^{3+}d^{4+}$ - O^{2-}) and one-electron reduced enzyme ($b_{558}^{3+}b_{595}^{3+}d^{2+}$) suggests that the redox state of heme *d* plays a role in determining the rate of reduction of heme b_{558} (and, perhaps, of heme b_{595} as well). Further work is needed to clarify the mechanism of this effect. Recent work has shown that the redox state of heme b_{558} and heme b_{595} regulate the accessibility of heme *d* by O_2 (Belevich, Borisov et al. 2007), thus, reciprocal regulation of the reactivity of the two hemes *b* by the redox and/or ligand-binding state of heme *d* may be a reasonable speculation. Evidently, the interactions between the three hemes play a critical role in determining the sequence of reactions in the catalytic cycle.

2.5 Figures and tables:

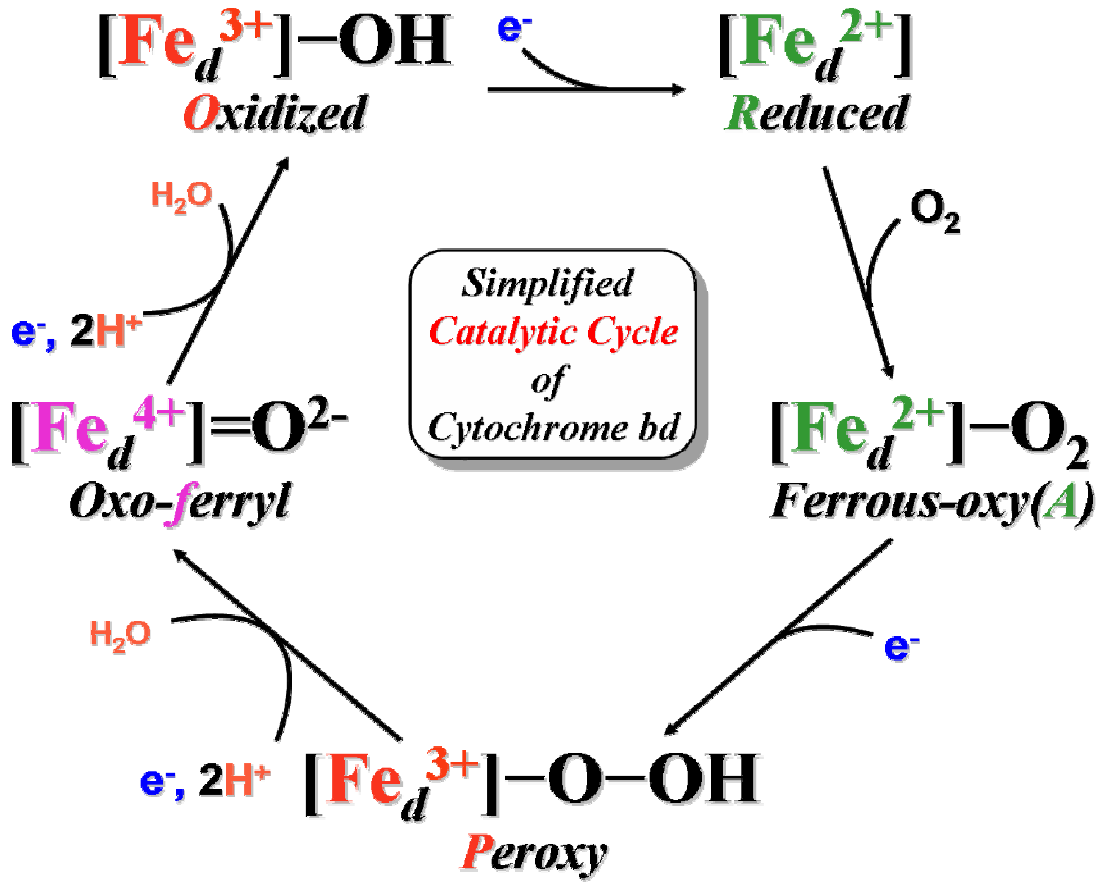

Figure 2.1 Simplified catalytic cycle of cytochrome *bd* oxidase.
Only the ferric ion on heme *d* is shown. All the intermediates have been identified optically. (modified from dissertation of J. Zhang, 2002)

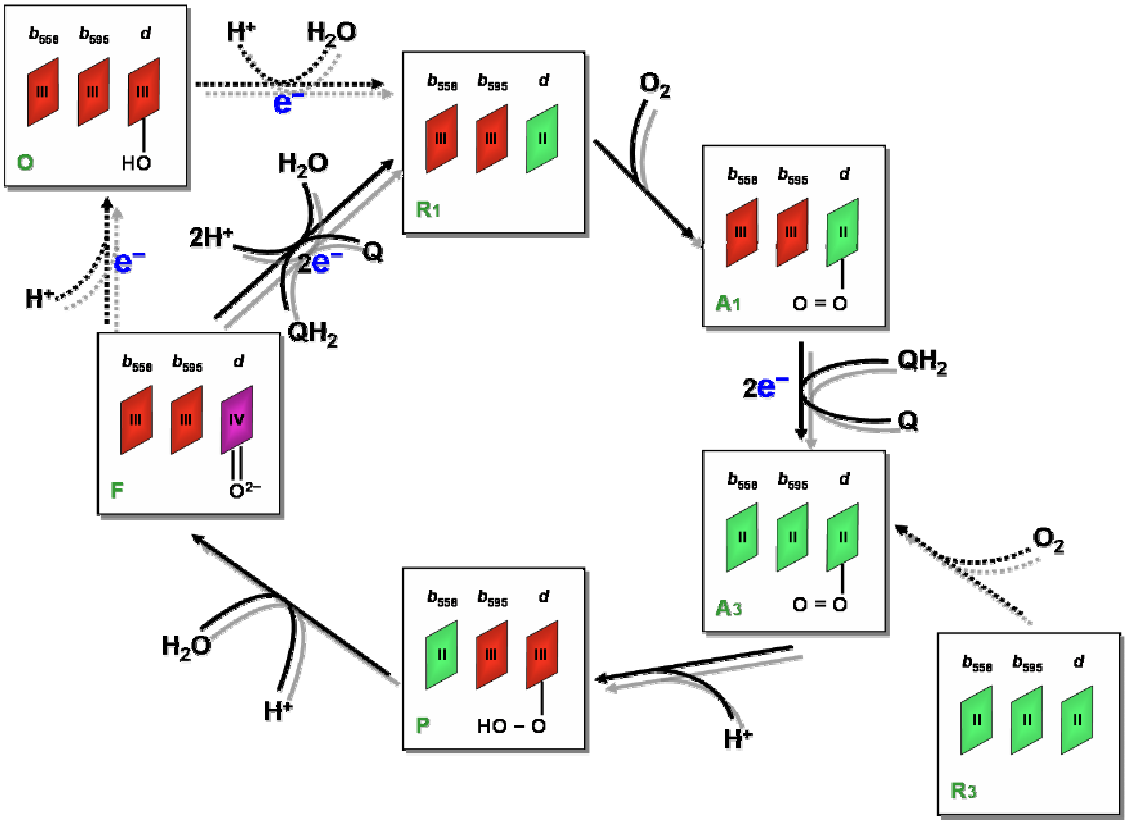

Figure 2.2 Modified catalytic cycle of cytochrome *bd* oxidase.
The new scheme is based on the work of Jünemann et al. and Matsumoto et al. All-ferric form (O) of the enzyme has been excluded from the rapid turnover (solid arrows) using ubiquinol as the substrate.

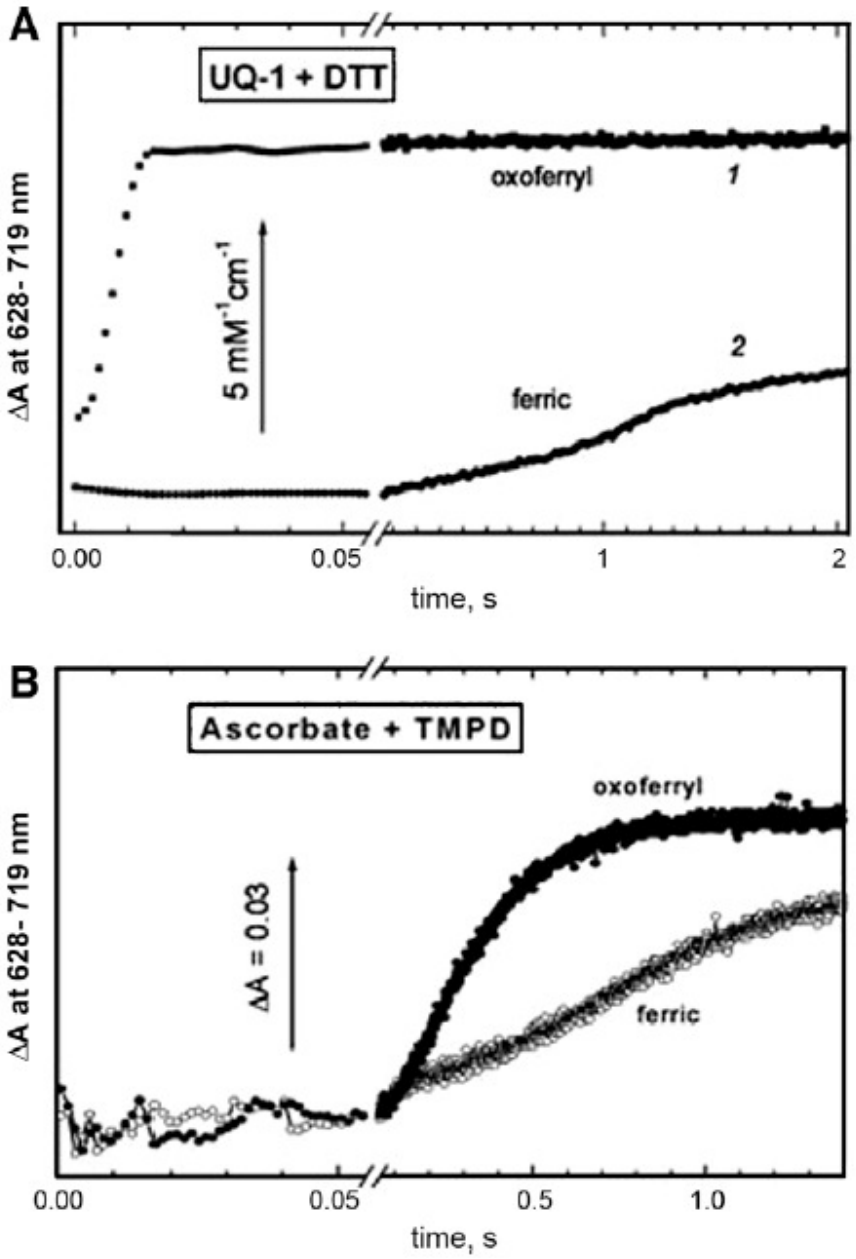

Figure 2.3 Kinetics of reduction of heme *d* in the oxoferryl and the all-ferric forms of cytochrome *bd*.
Panel A. Reduction by UQH_2-1: heme d in the oxoferryl form is reduced within about 10 ms, compatible with the turnover of the enzyme. No significant reduction of heme *d* in the all-ferric enzyme is observed in the same time range.
Panel B. Reduction by TMPD: the reduction of the all-ferric form is significantly slower than the reduction of heme *d* in the oxoferryl form of the enzyme. Heme *d* in the oxoferryl form is reduced by TMPD much more slowly than with UQH_2-1.

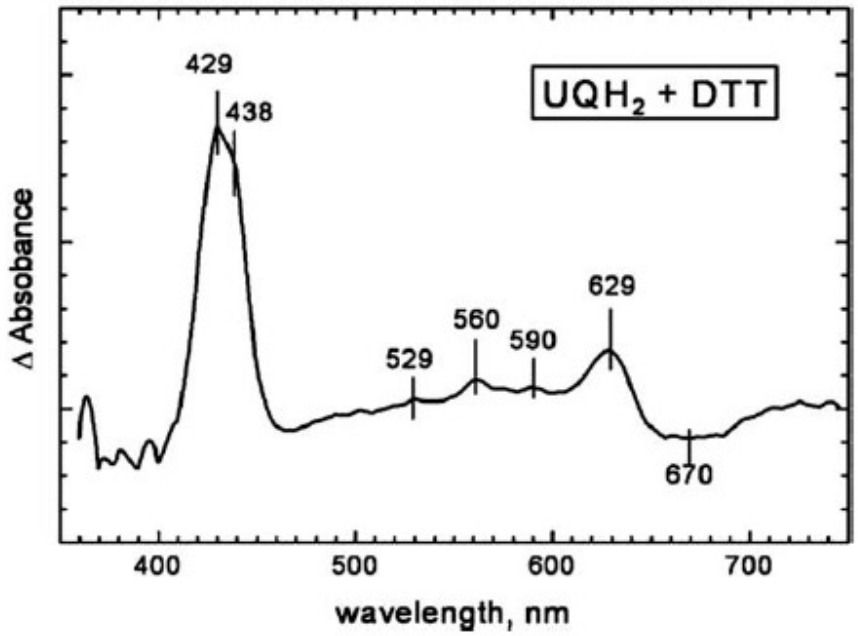

Figure 2.4 Global analysis of the spectra/time surface of very early stage reaction. Difference spectrum of the rapidly reduced component of cytochrome *bd* in the reaction of the oxoferryl form reduced by UQH_2-1 has been found by global analysis of the spectra/time surface. The spectrum is that of major product of the reaction formed in the first 50 ms minus the initial spectrum, which is primarily the oxoferryl form of the enzyme.

CHAPTER 3: TIME-RESOLVED ELECTROMETRIC AND OPTICAL STUDIES SUGGEST A MECHANISM OF ELECTRON-PROTON COUPLING IN THE DI-HEME ACTIVE SITE

3.1 Introduction:

As the only well known member of the tri-heme terminal oxidases so far, cytochrome *bd* has been intensively studied in order to understand how the same function of heme-copper oxidases is fulfilled by such a distinctive structure design. Due to the difficulty of solving the three dimensional information, site-directed mutagenesis became the most powerful tool to explore the structural and functional relationships of this enzyme. With the help of increasing sequences available from the bioinformatics research, a number of highly conserved residues have been identified and well studied. For our interest in the scope of this thesis, a series of highly conserved acidic amino acids have been mapped out in subunit I (**Figure 1.4**).

In previous work, a highly conserved region – (440) **GWXXXEXGRQPW** (451) - (*E. coli* numbering; bold letters indicate strictly conserved residues) in subunit I was discovered, which is predicted to be in a region near the C-terminus of the Q-loop on the periplasmic side of the membrane. As already mentioned in Chapter 1, the Q-loop is a highly hydrophilic group locted int eh periplasmic side of the membrane, and was believed to be involved in substrate quinol binding and oxidation (Kranz and Gennis 1984; Dueweke and Gennis 1990; Dueweke and Gennis 1991). The importance of the highly conserved region was examined by site-directed mutagenesis, and one of the mutants of acidic residues, E445A, was characterized in detail (**Figure 3.1**). The results

showed that one of the heme prosthetic groups, heme b_{595} was greatly perturbed, and was essentially missing from most preparations of the mutant enzyme, while other two hemes, b_{558} and d appear undisturbed (Zhang and Gennis 2001). This was particularly surprising given the indications that heme b_{595} and heme *d* are in close proximity (Hill, Alben et al. 1993; Hill, Hill et al. 1994). The use of di-heme as binuclear center opposed to heme-copper used in other terminal oxidases has long been the interest of the cytochrome *bd* research, and attempts trying to specifically perturb heme b_{595} have inevitably resulted in loss of both hemes.

In this chapter, a re-visit of this surprising mutant has been carried out using UV-vis, electron paramagnetic resonance (EPR), and spectrophotometric methods, as well as time-resolved electron transfer and charge separation approaches. In the current work, the high-spin heme b_{595} is found to be retained by the enzyme in contrast to the original proposal, but it is not reducible even by excess of dithionite. Furthermore, in our new hypothesis, E445 is believed to be one of the two redox-linked ionizable groups required for charge compensation of the di-heme oxygen-reducing site (b_{595}, *d*) upon its full reduction by two electrons.

3.2 Materials and methods:

3.2.1 Strains and plasmids:

E. coli strain CLY (*cyo::kan*, *rec*A), which lacks cytochrome bo_3 quinol oxidase (Yep 2005) was used as the host strain for expressing the wild type cytochrome *bd* on a plasmid.. To obtain wild type cytochrome *bd*, plasmid pTY1 (Yang 2007) was introduced

to the strain. This plasmind is a derivative of pET17b and contains the whole operon of wild type *bd* as well as ampicillin resistance gene for selection.

Mutants of cytochrome *bd* were expressed using *E. coli* strain GO105 (*cyd*AB::*kan*, *cyo*, *rec*A), which lacks both cytochrome bo_3 and cytochrome *bd* quinol oxidases (Kaysser, Ghaim et al. 1995) was used as the host strain. To obtain mutant cytochrome *bd*, plasmid pTK1 (Zuberi 1993) was introduced to the strain. This plasmid is a derivative of pBR322 and contains the whole operon of wild type *bd* as well as ampicillin resistance gene for selection.

3.2.2 Site-directed mutagenesis using Quik-Change method:

The Stratagene Quik-Change mutagenesis kit was used to construct mutants. Plasmid pTK1 was used as template. The oligonucleotide primers were synthesized by Operon (Alamdeda, CA) with melting temperature around 80 °C based on the Stratagene formula, and were diluted in pure water to 100 ng/μL for Quik-Change reaction. Thermocyclings were conducted on PTC-100 Programmable Thermal Controller (MJ Research Inc.). The protocol was as follows: 95 ˚C for 2 min, 1 cycle; 18 cycles of 95 °C for 1 min, 54 °C for 1 min, and 68 °C for 8 min; then 68 °C for 7 min, 1 cycle. The samples were digested with 1 μL *Dpn*I for 3 ~ 4 hours. All mutants were confirmed by DNA sequencing.

3.2.3 Complementation test for the mutant cytochrome *bd*:

The complementation test was carried out as follows: Plasmid DNA from confirmed mutants was used to transform GO105 using TSS method (Chung, Niemela et

al. 1989). Cells were grown anaerobically for selection of ampicillin and kanamycin resistance. The strains exhibiting both amplicillin and kanamycin resistance were restreaked to obtain single colonies, and were grown on M63 (Cohen and Rickenberg 1956) minimal plates supplemented with 0.3 % lactate and 0.3 % succinate. Also added were 100 μg/mL ampicillin and 50 μg/mL kanamycin to maintain the plasmid and the strain. Complementation was defined by aerobic growth within 48 ~ 72 hours of incubation at 37 °C.

3.2.4 Cell growth and protein sample preparation:

Large scale cell growth of strains that grow aerobically (i.e. expressing wild type) was carried out in 24 2-liter flasks shaking at 220 rpm 37 °C using two Innova 4330 incubator shakers (New Brunswick Scientific). Strain expressing wild type was grown in LB containing 100 μg/mL Amp, 50 μg/mL Kan, and 0.5mM IPTG was added 4 hours after the inoculation. Strain expressing E445A mutant, which could not grow aerobically, was grown at the Fermentation Facility at the University of Illinois, at 37 °C, pH 7, in a 20-liter fermenter using LB containing 100 μg/mL Amp, 50 μg/mL Kan, and 0.3 % glucose. Both wild type and E445A mutant cytochrome *bd* oxidases were purified from the membrane of either CLY/pTY1 or GO105/pE445A as described previously (Miller and Gennis 1986), with the modification that the hydroxyapatite column was omitted. Fractions were collected from the Fast-Flow Sepharose DEAE column with an A_{412}/A_{280} ratio greater than 0.5. The pooled fractions were concentrated using an Amicon concentrator with a 50 kDa molecular weight cut-off filter and then dialyzed three times against 50 mM sodium phosphate buffer, pH 7.8, containing 5 mM EDTA, 0.05% N-

lauroylsarcosine. Both wild type and mutant cytochrome *bd* samples were then examined, using the same dialysis buffer for appropriate dilution unless specified otherwise.

3.2.5 Ubiquinol-1 and TMPD oxidase activity assay:

Cytochrome *bd* wild type and mutants were assayed both in isolated membranes, in which there is no other quinol oxidase, and with the purified enzyme. For membranes, samples were homogenized in 25 mM Tris HCl, 1 mM EDTA disodium salt, pH 7.5. Purified protein samples were dialyzed against 50 mM NaPi buffer, pH 7.8, containing 5 mM EDTA disodium salt and 0.05 % N-lauroyl sarcosine. Various dilutions of either the homogenized membrane samples or pure protein samples were added to 1.8 mL of the respective buffer containing either 2 mM dithiothreitol or 4 mM ascorbate that had been equilibrated to 37 °C in a Clark-type oxygen electrode (Yellow Springs Instrument CO.). A baseline was taken and the reaction was initiated by addition of ubiquinol-1 (kindly provided by Hoffman-LaRoche) or TMPD to a final concentration of 245 μM and 1 mM, respectively. Activities were determined assuming a value of 237 μM O_2 for air-saturated buffer at 37 °C.

3.2.6 Heme analysis:

The heme *b* contents of both wild type and E445A mutant cytochrome *bd* were measured by the pyridine hemochromogen assay, using an extinction coefficient for the wavelength pair 556.5−540 nm = 23.98 mM^{-1} cm^{-1} (Berry and Trumpower 1987). The heme *d* content was determined from the reduced minus "as isolated" difference spectrum with the $\Delta\varepsilon_{628-607\ nm}$ = 10.8 mM^{-1} cm^{-1} (Borisov, Arutyunyan et al. 1999). The

concentration of the wild type cytochrome *bd* was determined from the reduced minus as isolated difference spectra, using $\Delta\varepsilon_{560-580\,nm}$ = 21.4 mM^{-1} cm^{-1} (Tsubaki, Hori et al. 1995). Since the "as isolated" enzyme contains varying amounts of ferrous heme *d*-oxy complex and oxoferryl heme *d* species, the heme *d* content was also determined by the absolute spectrum of the fully reduced enzyme, using the extinction coefficient $\Delta\varepsilon_{628-670\,nm}$ = 25 mM^{-1} cm^{-1} (Borisov, Arutyunyan et al. 1999). The concentration of the E445A mutant protein was determined by the BCA assay using wild type cytochrome *bd* as standard. All the measurements were repeated at least three times.

3.2.7 UV-Vis spectroscopic measurements:

All the absorbance spectra in the UV-Vis region were obtained with a DW2000 spectrophotometer (Aminco) using a 1 cm pathlength cuvette. The series of absorbance spectra for mid-point potential measurements were taken using UV-2101PC scanning spectrophotometer (Shimadzu).

3.2.8 EPR spectroscopic measurements:

X-band (9.521 GHz) EPR spectra were acquired on a Bruker ESP 300 equipped with an Oxford liquid helium cryostat and ITC4 temperature controller. Spectra were recorded with samples of both air-oxidized and fully dithionite-reduced wild type (100 μM) and E445A mutant cytochrome *bd* (100 μM) of the enzyme at 9 K. The modulation frequency is 100 KHz. The microwave power is 1 mW.

3.2.9 Time-resolved spectrophotometric measurements:

Time-resolved spectrophotometric measurements were performed using a home-built CCD-based instrument. The setup allows acquiring absorption change surfaces with a time resolution of 1 μs between the spectra. Details of the methodology can be found in previous work by Morgan et al. (1993). To obtain the CO complex of the ferrous enzyme, the as-isolated enzyme was (i) deoxygenated by argon equilibration, (ii) reduced under anaerobic conditions with 2.5 mM sodium ascorbate and 5 μM TMPD, and (iii) equilibrated with 1% CO. The ferrous-CO enzyme was transferred to the stopped flow module in a gastight Hamilton syringe preflushed with argon and then mixed with oxygen. CO photolysis was initiated by a laser flash (Brilliant B; Quantel, Les Ulis, France; frequency-doubled YAG, 532 nm; pulse energy, 120 mJ).

3.2.10 Electrometric Time-resolved measurements of membrane potential generation:

The direct, time-resolved electrical measurement is based on a method originally developed by Drachev and co-workers (Drachev, Jasaitis et al. 1974; Drachev, Kaulen et al. 1979). In the present system, $Ag/AgCl_2$ electrodes record the voltage between the two compartments of a cell separated by a measuring membrane consisting of a lipid-impregnated, stretched Teflon mesh vesicles, into which the enzyme has been reconstituted, are forced to associate with this measuring membrane (Verkhovsky, Morgan et al. 1997). The voltage across the measuring membrane follows the $\Delta\Psi$ across the vesicle membranes proportionally, allowing the kinetics of charge translocation to be

recorded. The method is described in more detail in works by Verkhovskey et al. in 1997 and 1999.

3.2.11 Software for experiments and data analysis:

Instrumental software for experimental setups was written by Dr. I. Belevich (Helsinki, Finland). MATLAB (The Mathworks, South Natick, MA) was used for data analysis and presentation.

3.2.12 Sequence analysis and topology model generation:

The homologous sequences of subunit I of cytochrome *bd* were kindly provided by Dr. James Hemp in Grennis lab, Urbana, University of Illinois. The sequence alignment was performed by BioEdit Sequence Alignment Editor Ver.7.0.9.0 (Hall 1999).. The topology model of subunit I was generated by membrane topology prediction tool TMHMM 2.0 program (http://www.cbs.dtu.dk/services/TMHMM/). The graph was created by TOPO2 program based on the TMHMM result (http://www.sacs.ucsf.edu/TOPO-run/wtopo.pl).

3.3 Results:

3.3.1 Complementation test, heme analysis and optical spectra:

Complementation test was carried out by introducing the plasmid expressing the E445A mutant cytochrome *bd* into the *E. coli* strain without terminal oxidase. The ability to rescue the aerobic growth of the strain on minimal plate serves as a sign that how much the mutant enzyme retains its catalytic activity. E445A failed to support aerobic

growth as previously described by Zhang et al. (**Table 3.1**) This mutant also appears to be missing heme b_{595} as judged from UV-Vis spectra, which is consistent with previous observation (Zhang, Hellwig et al. 2001). The heme content of the E445A mutant was determined using the pyridine hemochromagen method. The conventional procedure of using the dithionite-reduced minus air-oxidized difference absorption spectrum appears to be error-prone because the mutant enzyme in the air-oxidized form has a much lower amount of the ferrous oxy species. Hence, the use of the $\Delta\varepsilon_{628-607}$ value of 10.8 mM^{-1} cm^{-1}, which correctly quantifies the content of heme *d* in the WT enzyme (Borisov, Arutyunyan et al. 1999), results in an incorrect value of heme *d* in the E445A mutant enzyme (Zhang, Hellwig et al. 2001). The use of this traditional method results in overestimation of heme *d* in the mutant enzyme. For this reason the content of heme *d* for the WT and mutant enzyme was determined from the ferrous heme *d* absorption spectra by using the wavelength pair 630 nm minus 670 nm ($\Delta\varepsilon_{628-670}$ of 25 $mM^{-1}\cdot cm^{-1}$) instead of the frequently used pair 630 nm minus 607 nm (Borisov, Arutyunyan et al. 1999). The ratio of hemes *b* / heme *d*, which used to be close to 1 in the previous study (Zhang, Hellwig et al. 2001), returns to around 2 in E445A mutant by using this new calculation. Thus, the hemes *b* content of the E445A mutant is not different from that of the wild type enzyme.

3.3.2 Ubiquinol-1 and TMPD oxidase activity of E445A mutant:

Consistent with the previous work (Zhang, Hellwig et al. 2001), the ubiquinol-1 oxidase activity was almost totally lost in E445A mutant enzyme (less than 1% of that of the wild type) (**Table 3.1**). The same was found also for the TMPD oxidase activity.

3.3.3 Flash photolysis of the CO adduct of the reduced E445A mutant:

Transient absorption changes in cytochrome *bd* were measured in the spectral region where the absorbance spectra of all the three hemes are well defined. The wild type, fully reduced, unliganded cytochrome *bd* shows peaks at 629 nm (α-band) of heme d^{2+}, 595 nm (α-band) of heme $b_{595}{}^{2+}$, 561 nm (α-band) of heme $b_{558}{}^{2+}$ and (β-band) of heme $b_{595}{}^{2+}$, and 531 nm (β-band) of heme $b_{558}{}^{2+}$.

Figure 3.2A compares the absorption changes following CO photolysis from heme d^{2+} in the dithionite-reduced wild type (solid line) and E445A mutant (dotted line) enzymes. For the wild type cytochrome *bd*, CO-recombination difference spectrum in the presence of 1% CO has a maximum at 642 nm, a minimum at 622 nm, and a bump around 540 nm that is consistent with CO rebinding to heme d^{2+}, similar to an earlier report (Jünemann, Wrigglesworth et al. 1997). In contrast, in the E445A mutant enzyme, the total kinetic spectrum of the CO recombining phase (dotted line) reveals not only CO rebinding to heme d^{2+}, but also some internal electron redistribution between hemes *d* and b_{595}. The latter is well illustrated by the difference between the two CO-recombination spectra shown in **Figure 3.2A**. This difference spectrum (**Figure 3.2B**) has maxima at 595 and 562 nm, and a minimum at 630 nm, and is almost identical to the reported spectrum of the reduced *minus* oxidized spectrum of heme b_{595} (Koland, Miller et al. 1984; Lorence, Koland et al. 1986), with the addition of a trough at 630 nm indicating the oxidation of heme *d*. Although the amount of reduced heme b_{595} is small (about 20% of the maximum possible), the spectroscopic identification of reduced heme b_{595} is clear.

This was an unexpected result since the E445A mutant enzyme was previously reported to be missing heme b_{595} (Zhang, Hellwig et al. 2001). This conclusion is

contradicted with the data in the current work, which shows that the E445A mutant does contain heme b_{595}, but in a strict ferric form, rather than losing it, even in the presence of dithionite. Photolysis of heme d^{2+}-CO in the dithionite-reduced E445A enzyme is followed by electron redistribution from heme d^{2+} to heme $b_{595}{}^{3+}$, which suggests that E445A mutant enzyme is in a unique two-electron reduced state, $b_{558}{}^{2+}b_{595}{}^{3+}d^{2+}$, even in the presence of strong reductant, such as dithionite.

3.3.4 EPR spectroscopy of dithionite reduced wild type and E445A mutant:

EPR spectra of the dithionite-reduced mutant enzyme supports the conclusion that heme b_{595} remains high spin ferric even in the presence of excess reductant. After addition of dithionite, there is still a signal in the low field region at g = 6 from a high spin ferric heme assigned unambiguously to the high spin ferric heme b_{595} but no any signal in the high field region (around g = 3) from a low spin ferric heme (**Figure 3.3**). The signal at g = 6 is very fast relaxing and does not show any saturation behavior on increase of microwave power up to 100 mW at 13 K and only at 4 K at such power it is slightly saturated. Control EPR experiments with the wild type enzyme show that, under the same conditions, the EPR spectrum of dithionite-reduced wild type cytochrome *bd* reveals no any heme signals.

3.3.5 Charge translocation during the reaction of O_2 with reduced enzymes:

Electrometric measurements of $\Delta\Psi$ generation associated with the reaction of both the wild type and the mutant enzymes with O_2 were made under the same experimental conditions. Typical recordings are shown in **Figure 3.4**. The kinetics of

the electrometric response of the fully reduced wild type enzyme (trace 1) can be reasonably modeled by three sequential reactions. The first reaction is an electrically silent lag phase with a time constant (k_1) dependent on the concentration of O_2 (Jasaitis, Borisov et al. 2000). Under the present experimental conditions $k_1 = 7.4 \times 10^4\ s^{-1}$ ($\tau_1 \sim 14\ \mu s$). This reaction reflects oxygen binding to the enzyme (**R**→**A** transition), where state **A** denotes the formation of the heme d^{2+}-O_2 adduct. The second phase with k_2 of $1.1 \times 10^4\ s^{-1}$ ($\tau_2 \sim 90\ \mu s$) is electrogenic and very similar to the value reported previously (Jasaitis, Borisov et al. 2000) corresponding to the transition of the ferrous-oxy intermediate (heme d^{2+}-O_2) to the oxoferryl state (heme d^{4+}=O^{2-}) (**A**→**F** transition). There is an additional third kinetic phase with k_3 of $1.65\times10^3\ s^{-1}$ ($\tau_3 \sim 600\ \mu s$) corresponding to the conversion of the oxoferryl state **F** to the oxidized enzyme (heme d^{3+}-$^-$OH) and/or to the **A** state (heme d^{2+}-O_2).

The amplitude of the **F**→**O** transition (~1.6 mV) is about half of that for the **A**→**F** transition (~3.2 mV). This is likely due to the loss of the bound quinone from a portion of the enzyme population during the vesicle reconstitution procedure. Enzyme lacking bound quinone will not have the reducing equivalents needed to proceed beyond the **F** state.

As shown in **Figure 3.4** (trace 2 and inset), the initial non-electrogenic binding of O_2 to the E445A enzyme is followed by a minor electrogenic phase (~0.36 mV) with the k value of $7.6\times10^2\ s^{-1}$ ($\tau \sim 1.3$ ms). After this small electrogenic phase, a large electrogenic event with the rate constant of about $80\ s^{-1}$ ($\tau \sim 12.5$ ms) and amplitude of ~1.7 mV is observed. Both phases probably reflect the conversion of **A** to **F** in different subpopulations of the enzyme. The conclusion that the final product

of this reaction is the **F** state was confirmed by the absolute absorption spectrum after completion of the reaction (2 sec), showing a peak at 680 nm, diagnostic of the heme *d* oxoferryl species (Kahlow, Zuberi et al. 1991). The huge delay of $\Delta\Psi$ generation in E445A mutant is a clear sign that the proton translocation from the cytoplasm to the reactive center is perturbed.

3.3.6 Electron backflow in one-electron reduced wild type and E445A mutant enzymes:

The wild type and E445A oxidases each readily forms the CO adduct of the one-electron reduced enzyme (heme d^{2+}-CO). Previous results (Jasaitis, Borisov et al. 2000) with the wild type enzyme show that photodissociation of CO results in electron redistribution from heme *d* to heme b_{558} and heme b_{595}, referred to as "backflow" electron transfer. The backflow electron transfer reactions were compared for the wild type and E445A mutant enzymes. Remarkably, the results are very similar.

Recombination of CO after photolysis of the mixed-valence enzyme includes not only CO rebinding (see **Figure 3.2**, solid line) but also the return of redistributed electrons to heme *d* from hemes b_{558} and b_{595} (Jasaitis, Borisov et al. 2000). Therefore, the spectrum of the CO-rebinding phase of the CO mixed-valence enzyme contains the spectral changes induced by the binding of CO to heme *d* (i.e., the CO binding spectrum) as well as the changes caused by the subsequent electron redistribution. The CO-binding spectrum can be determined by recording the spectral changes induced by photolysis of CO from the fully-reduced wild type enzyme, in which case

there is no electron redistribution. The spectral component due to electron transfer (**Figure 3.5)** was obtained by subtracting the CO-binding spectrum from the overall CO recombination spectra of the one-electron reduced wild type (solid line) and mutant (dotted line) enzymes. This spectrum shows the reduction of heme *d* and corresponding oxidation of hemes b_{558} and b_{595} as CO rebinds to heme *d*.

Using the appropriate extinction coefficients for hemes *d* and b_{558} (see Materials and Methods), it is possible to quantify the extent to which hemes *d* and b_{558} are reduced and oxidized, respectively, concomitant with CO rebinding. Approximately 25% of the heme *d* undergoes a redox change (initial oxidation followed by re-reduction as CO recombines) upon photolysis (Jasaitis, Borisov et al. 2000). If the amount of heme *d* that becomes reduced as CO rebinds is taken as 100%, the data show that only ~20% this reducing equivalent can be accounted for by the oxidation of heme b_{558} in the wild type and ~18% in the mutant enzymes. The remaining source of electrons must be heme b_{595}, since the bound quinone will have E_m value that is much lower than heme b_{595} (Koland, Miller et al. 1984). Hence, in both enzymes, the photolysis of CO from heme d^{2+} in the one-electron reduced enzyme results in partial reduction of heme b_{558} and heme b_{595} with most (~80%) of the internally redistributed electron residing on heme b_{595}. Since, under the solution conditions employed, both in the wild type and in the E445A mutant enzymes, of the two hemes *b*, heme b_{595} is the major contributor to electron redistribution between heme *d* resolved in optical measurements.

3.4 Discussion and conclusions:

One clear conclusion from this chapter is that the E445A mutant of *E. coli* cytochrome *bd* contains heme b_{595}. Although the enzyme contains heme b_{595}, the heme remains in the ferric form even in the presence of dithionite as it can be seen by EPR spectroscopy. This observation explains the activity lose of this mutant (Zhang, Hellwig et al. 2001). Remarkably, heme b_{595} can be reduced transiently by photolysis of the CO adduct of heme d^{2+}, either in the one- or two-electron reduced forms of the enzyme (**Figures 3.2 and 3.4**). Previous studies claiming that the E445A mutant enzyme had only one heme *b* per heme *d* were apparently incorrect due to a difference in the appropriate extinction coefficients needed to quantify heme *d* for the wild type and mutant strains (see Materials and Methods). It is also clear that the E445A mutation has a very dramatic effect selectively on this heme component of the enzyme.

When heme b_{595} is locked into the ferric form, the enzyme is incapable of rapid catalysis. The reaction of O_2 with the two-electron reduced E445A mutant is about 100-fold slower to form the oxoferryl species. Formation of oxoferryl species requires 4-electrons to split the O-O bond along with at least one proton. Since heme b_{595} remains in the ferric form in the ascorbate/TMPD-reduced enzyme, there are not enough electrons present to rapidly catalyze the reaction (which would normally utilize 1 electron each from heme b_{595} and heme b_{558} as well as 2 electrons from heme *d*). It is possible that sufficient electrons are present in the enzyme in the form of ubiquinol; in that case the very slow reaction suggests that rapid catalysis specifically

requires the ferrous form of heme b_{595} and/or that the reaction requires the proton delivered to E445 that would accompany reduction of heme b_{595}.

The backflow optical experiments show clearly that, upon the photolysis, the electron from heme *d* is redistributed predominantly to heme b_{595}. If the amount of transiently oxidized heme *d* in the photolyzed one-electron reduced enzyme is taken as 100%, ~80% of this reducing equivalent ends up on heme b_{595} and only about 20% - on heme b_{558}. Hence, in control electrometric experiments with two-electron reduced E445A enzyme one would expect that CO photolysis from the mutant in the absence of O_2 resulting in electron backflow from heme *d* to heme b_{595} will be linked to proportional electrogenic movement of *protons* with the amplitude of $\Delta\Psi$ generated as much as 80% of that in the one-electron reduced enzyme (i.e., without reductant). However, $\Delta\Psi$ generation after CO photolysis from the one-electron reduced E445A enzyme (~0.6-0.7 mV) decreases proportionally with reduction of heme b_{558} and in two-electron reduced state of the mutant the amplitude of $\Delta\Psi$ generation is close to zero although the electron backflow to heme b_{595} is still present (**Figure 3.2B**). These data suggest that generation of $\Delta\Psi$ caused by CO dissociation from heme *d* in the one-electron reduced enzyme is due to electron redistribution between heme *d* and heme b_{558} and protonation events associated with it, whereas redox equilibration between heme *d* and heme b_{595} (while the major event in optics) is not linked to electrogenic proton movement and it also proves that these two hemes positioned in the membrane at the same depth.

When the E445A mutant is treated with dithionite, heme *d* and heme b_{558} are reduced, but heme b_{595} remains oxidized. The fact that part of heme b_{595} is transiently

reduced upon photolysis of the heme d^{2+}-CO adduct suggests that the mutation does not specifically block the reduction of heme b_{595} but, rather, prevents the complete simultaneous reduction of both heme *d* and heme b_{595}.

Shown in **Figure 3.6** is the proposed scheme of electron and proton transfer pathways in cytochrome *bd* that can explain the two apparently conflicting observations of behavior of the E445A mutant: resistance of heme b_{595} towards reduction by dithionite and transient reduction of a fraction of heme b_{595} upon photolysis of CO from heme *d* in the mixed-valence enzyme.

It is proposed that there are two protonatable groups, denoted X_N^- and X_P^-. The protonation states of both of these groups are influenced by the redox state of hemes *d* and b_{595} (**Figure 3.6**). It is postulated that the pKa of X_N^- is higher than the pKa of X_P^- and that the X_N^- group is in protonic equilibrium with the bulk aqueous phase on the negative side of the membrane via a proposed proton-conducting channel. Proton transfer between the negative side of the membrane and the X_N^- site through this channel, normal to the plane of the membrane, is proposed to result in generation of $\Delta\Psi$.

Upon reduction of both the wild type and the mutant enzyme, the first electron transferring from heme b_{558} to the binuclear site is accompanied by the protonation of the X_N^- site ($X_N^- + H^+ \rightarrow X_NH$). For reduction of the binuclear site by the first electron, the E_m value of heme b_{595} in the mutant is similar to that in the wild type, because in both cases the first electron is compensated by simultaneous uptake of the first proton by the X_N^- group. The second electron from heme b_{558} entering the binuclear site completes reduction of the di-heme site, resulting in reduction of ~80% heme b_{595} and

~20% heme *d* in the wild type enzyme that is linked to uptake of the second proton by another shared proton-accepting group, X_P^-. The E445A mutation is proposed to specifically block the protonation of the X_P^- site. Consequentially, in the mutant enzyme, the complete reduction of the binuclear site becomes impossible as the second electron cannot be compensated by uptake of the second proton.

In principle, the proton delivered to X_P^- could come through the same channel as does the proton taken up by X_N^-. In this case, the proton delivery would be electrogenic and, presumably the proton would be used by the chemistry of forming water at the active site. The precise role of E445 is up to its location relative to the membrane. If E445 is embedded in the membrane, it's reasonable to assume that E445 itself is the X_P^- site. On the other hand, if E445 is located on the surface, it may be required for the proton transfer to X_P^-. In the latter case, the identity of the X_P^- site also needs to be established.

The E_m values of hemes *d* and b_{595} are pH-dependent (Lorence, Miller et al. 1984), consistent with the proposed model. Presumably, the protons taken up by one or both of these two groups are subsequently used to combine with O_2 in the catalytic reaction to form H_2O.

The addition of CO to the dithionite-reduced E445A mutant increases E_m of heme *d* so that one electron equilibrated between hemes *d* and b_{595} (80% : 20%) entirely moved on heme *d* (>99%). Photolysis to remove CO, results in the backflow of about 20% of the reducing equivalent transiently from heme *d* to heme b_{595}. When backflow between hemes *d* and b_{595} occurs, the redistributed electron is already

compensated by the proton which was taken up by the X_N^- site earlier. Hence this electron transfer is not associated with proton uptake and is nonelectrogenic.

The results obtained upon photolysis of heme d^{2+}-CO in the one-electron reduced enzyme are also explained by this model. Within the wild type enzyme, photolysis results in the redistribution of the electron that was initially on heme *d* to all three heme components. Of the 25% of heme *d* that is transiently oxidized, only approximately 20% of the reducing equivalent ends up on heme b_{558}. However, electron transfer from heme *d* to heme b_{558} is coupled to deprotonation of the group near heme *d* ($X_NH \rightarrow X_N^- + H^+$), which makes this step electrogenic.

Transient reduction of heme b_{558} following the photolysis of heme d^{2+}-CO in the one-electron reduced enzyme is also accompanied by H^+ uptake from periplasmic side. The extent of protonation of a proposed protonatable group (X_b^-) near heme b_{558} (**Figure 3.6**) is equal to that of deprotonation of X_N^- group near heme *d*. The protonation of the X_b^- site may also contribute to some extent to the backflow $\Delta\Psi$ generation provided that the site is located at some depth in the membrane.

The re-visit of E445A mutant in this chapter raises the argument of the presence of proton channel from the cytoplasma to the reactive center of cytochrome *bd* oxidase. Both X_P^- and X_N^- could be part of this pathway. With the help of sequence alignment, several strictly conserved residues are identified around the region in the membrane, which lead to further investigation in the following two chapters.

3.5 Figures and tables:

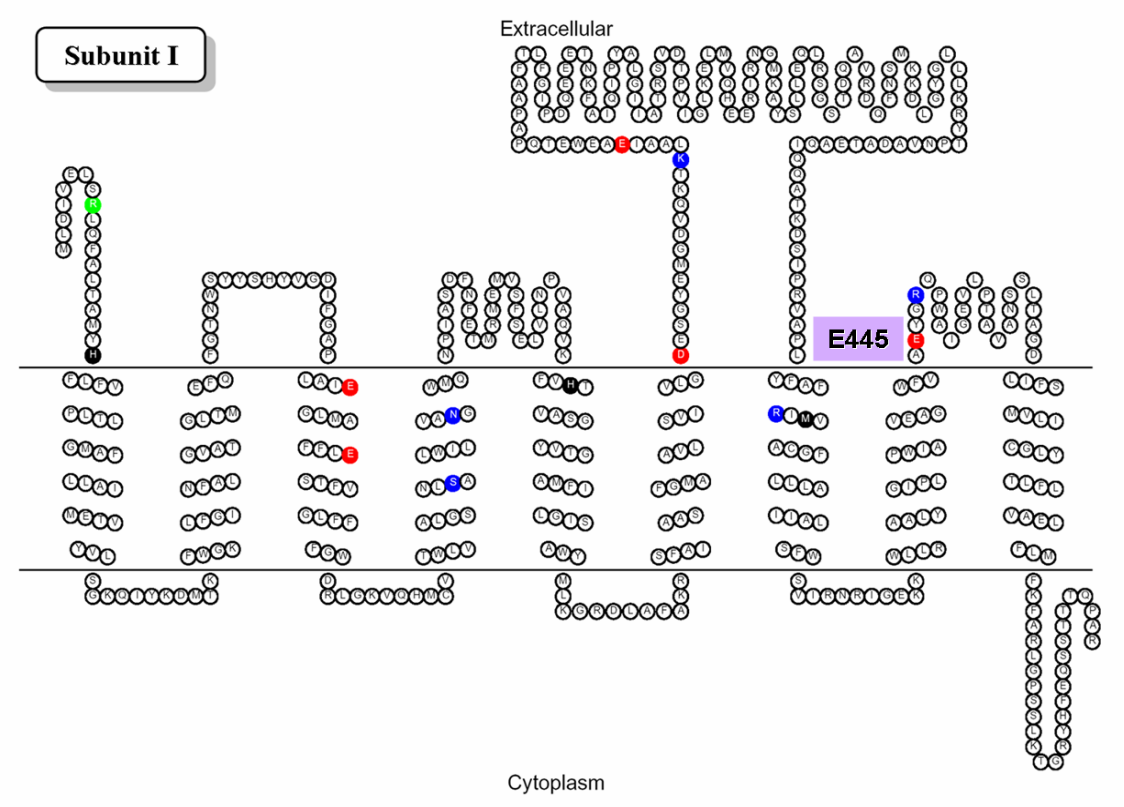

Figure 3.1 Membrane topology model of subunit I of cytochrome *bd* oxidase from *E. coli* with E445 marked out.

Table 3.1 Summary of the properties of the cytochrome *bd* E445 mutants

	Complementation of aerobic growth	Heme content (UV-Vis spectra)	UQ_1H_2 oxidase activity[a]	TMPD oxidase activity[b]
Wild type	Yes	All hemes present	100%	100%
E445A	No	No heme b_{595}	0%	0%
E445Q	No	No heme b_{595}	0%	3%

[a] 100% of ubiquinol-1 oxidase activity corresponds to a turnover of about $1450e^{-1}$/sec.
[b] 100% of TMPD oxidase activity corresponds to a turnover of about $100e^{-1}$/sec.

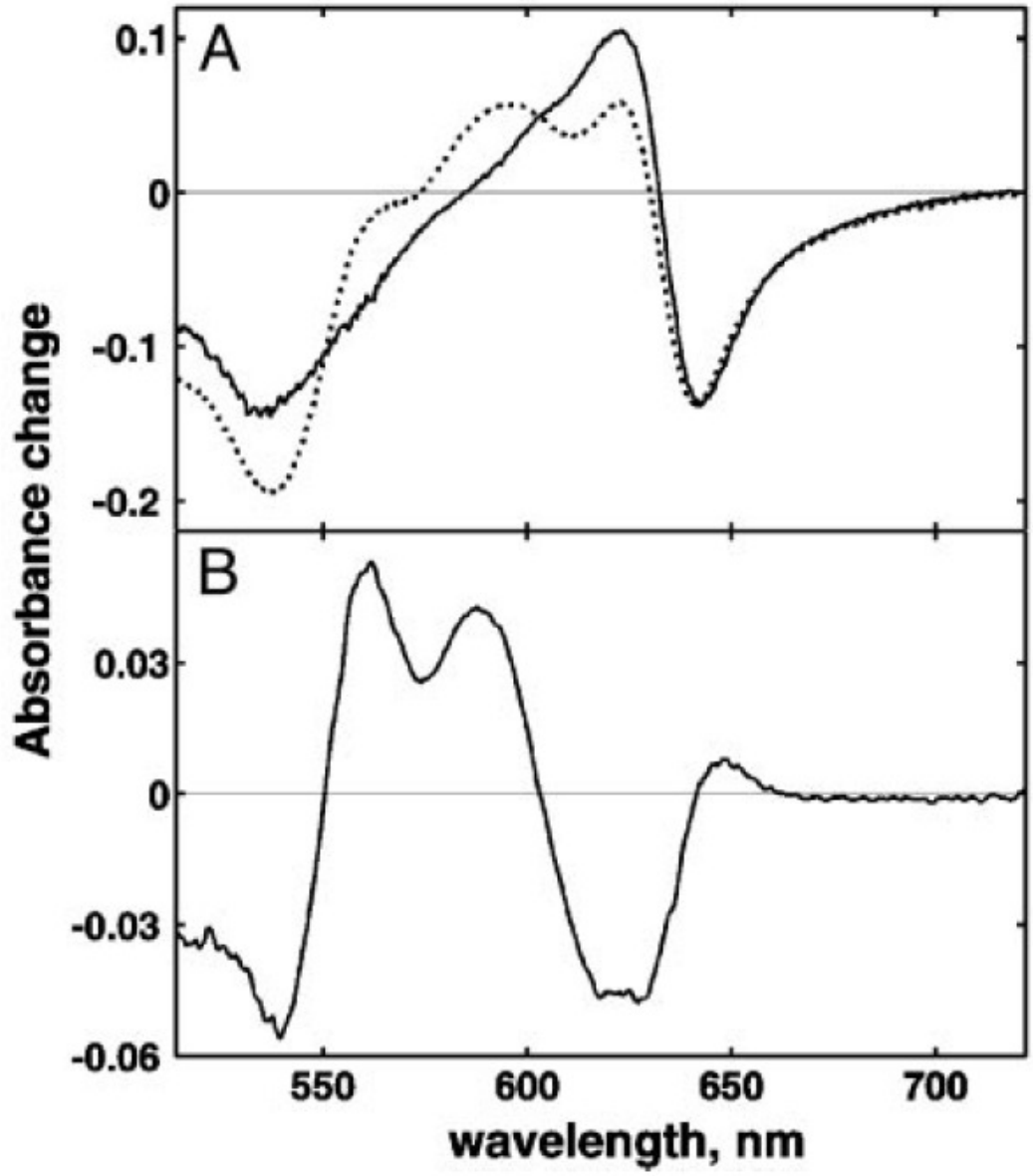

Figure 3.2 Absorption changes during CO recombination after flash photolysis of dithionite-reduced cytochrome *bd*.
(A) Spectrum of CO photolysis of the E445A mutant enzyme (dotted line) was adjusted to match the amplitude of photolysis of the WT enzyme (solid line). The spectrum is a difference between spectra before and after the flash. The spectrum before the flash is constant, but the spectrum after the flash was obtained by extrapolation of the CO recombination kinetics at each wavelength to zero time.
(B) Difference between CO recombination spectra of E445A mutant and WT. Conditions: cytochrome *bd*, 25 μM (WT) and 12 μM (E445A mutant); 0.1% Tween 20; 100 mM Hepes-KOH, pH 7.5; sodium dithionite, 0.1 mM (WT) and 3 mM (E445A mutant); 1% CO; 1-cm light path; room temperature.

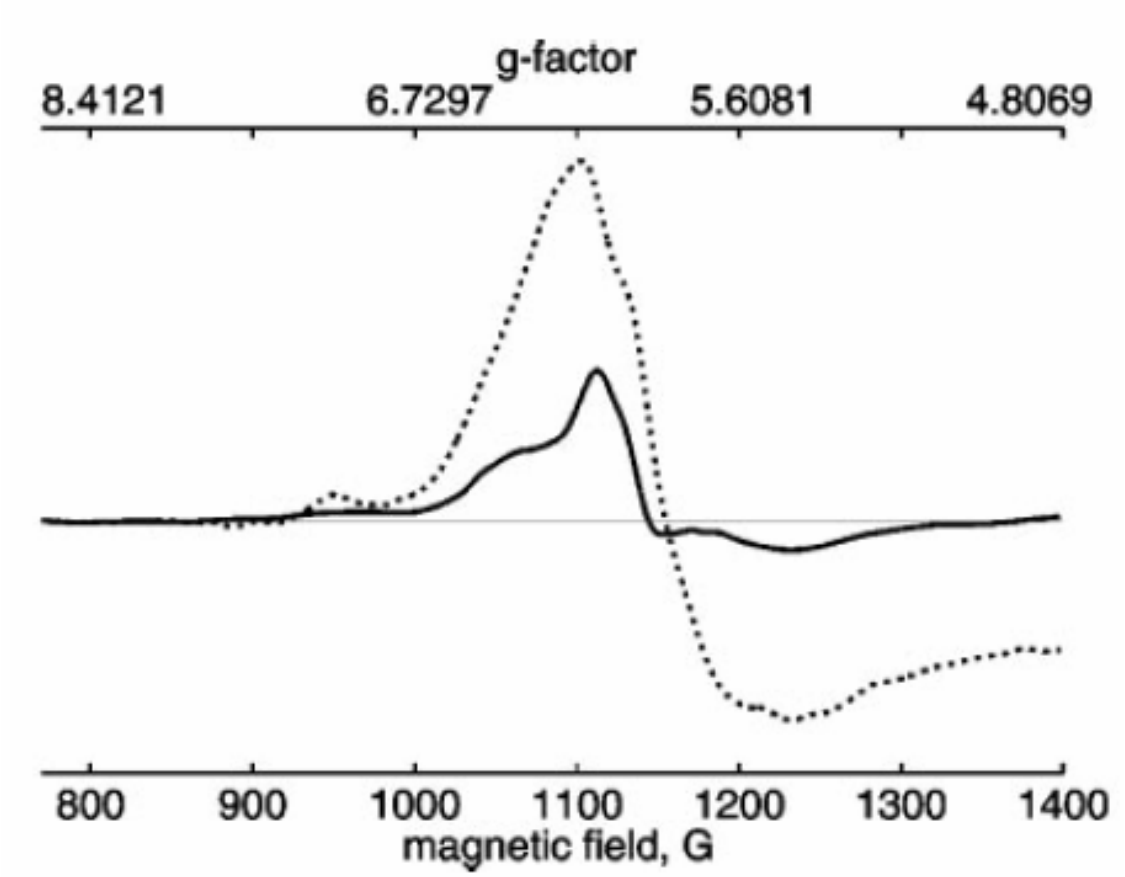

Figure 3.3 EPR spectra of air-oxidized (dotted line) and dithionite-reduced (solid line) cytochrome *bd* from E445A mutant enzyme.
EPR conditions: microwave power, 2 mW; microwave frequency, 9.429 GHz; modulation amplitude, 12 G; temperature, 12° K. Sample conditions: 26.6 μM enzyme; 20 mM Mops-KOH and 40 mM sodium phosphate, pH 7.6; 0.05% sarcosyl. Data indicated by the solid line were obtained in the presence of 5 mM sodium dithionite.

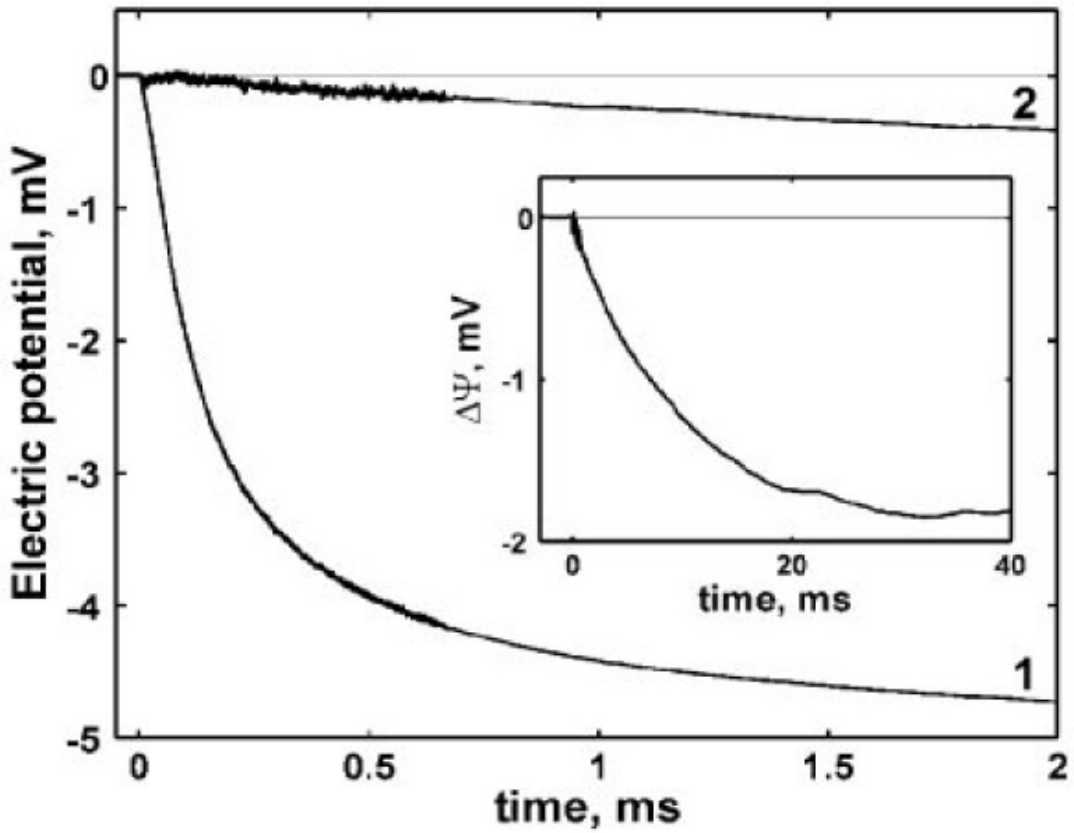

Figure 3.4 Generation of a membrane potential during the reaction of the reduced cytochrome *bd* with O_2.
Trace 1, WT enzyme. Trace 2, E445A mutant enzyme. Conditions: 100 mM Mops-KOH (pH 7.0), 10 μM TMPD, 50 mM glucose, 0.5 mg/ml catalase, 1.5 mg/ml glucose oxidase, and 1% CO. Reaction was started by a laser flash after 400 ms from the beginning of the injection of 100 μl of oxygen-saturated buffer ($[O_2]$ = 1.2 mM). The fit of the presented experimental curves gives the following parameters for the phases: Trace 1, R → A, $\tau \approx$ 13.5 μs with zero amplitude; A → F, $\tau \approx$ 90.9 μs, amplitude of –3.2 mV; F → O, $\tau \approx$ 606 μs, amplitude of –1.6 mV. Trace 2: R → A, $\tau \approx$ 13.5 μs with zero amplitude; A → F_1, $\tau \approx$ 1.3 ms, amplitude of –0.36 mV; A → F_2, $\tau \approx$ 12.5 ms, amplitude of –1.7 mV. (Inset) Generation of ΔΨ during the reaction of the reduced E445A mutant cytochrome bd with O_2 on the longer time scale.

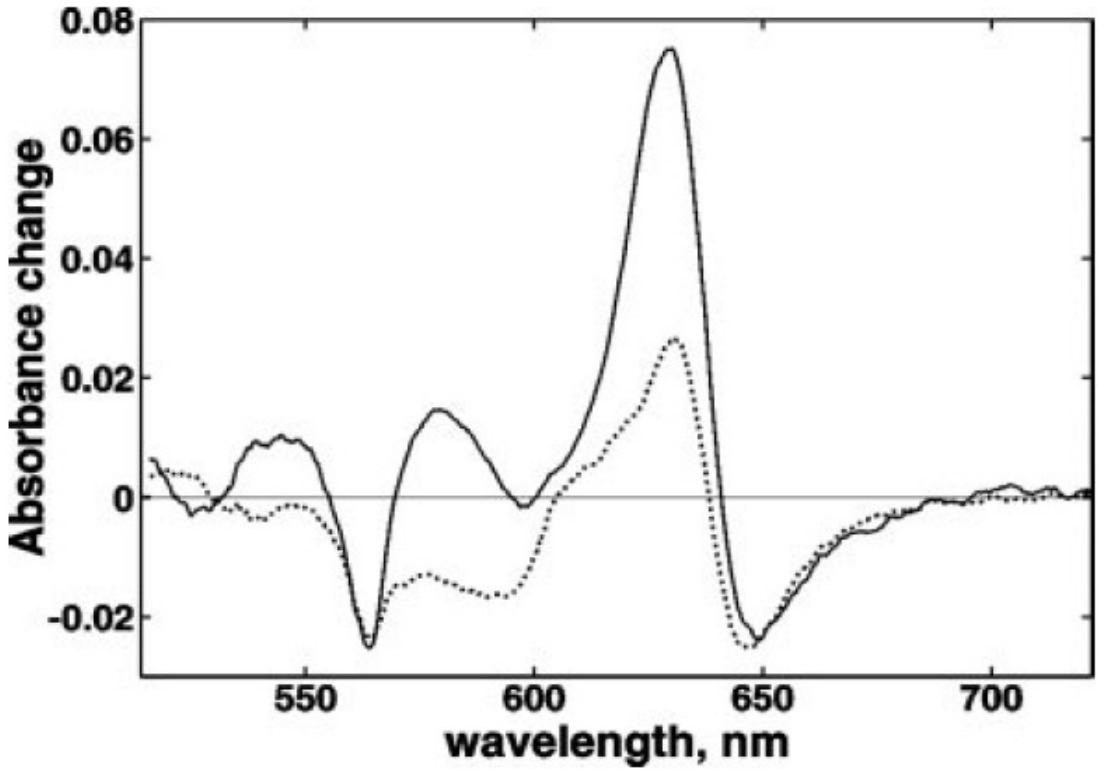

Figure 3.5 Spectra of electron backflow relaxation after CO photolysis from the one-electron-reduced WT (solid line) and E445A mutant (dotted line) enzymes.
The spectra were obtained by subtraction of the spectrum of CO rebinding to heme d (solid line of Fig. 1) from the total spectra of the CO recombining phase, the latter is a sum of the two processes (CO rebinding to heme d and intraprotein electron redistribution). The amplitudes of CO recombination phases of mixed valence enzymes were adjusted to match the amplitude of CO photolysis of fully reduced WT enzyme. Conditions are as in Fig. 3.2, except that no dithionite was added.

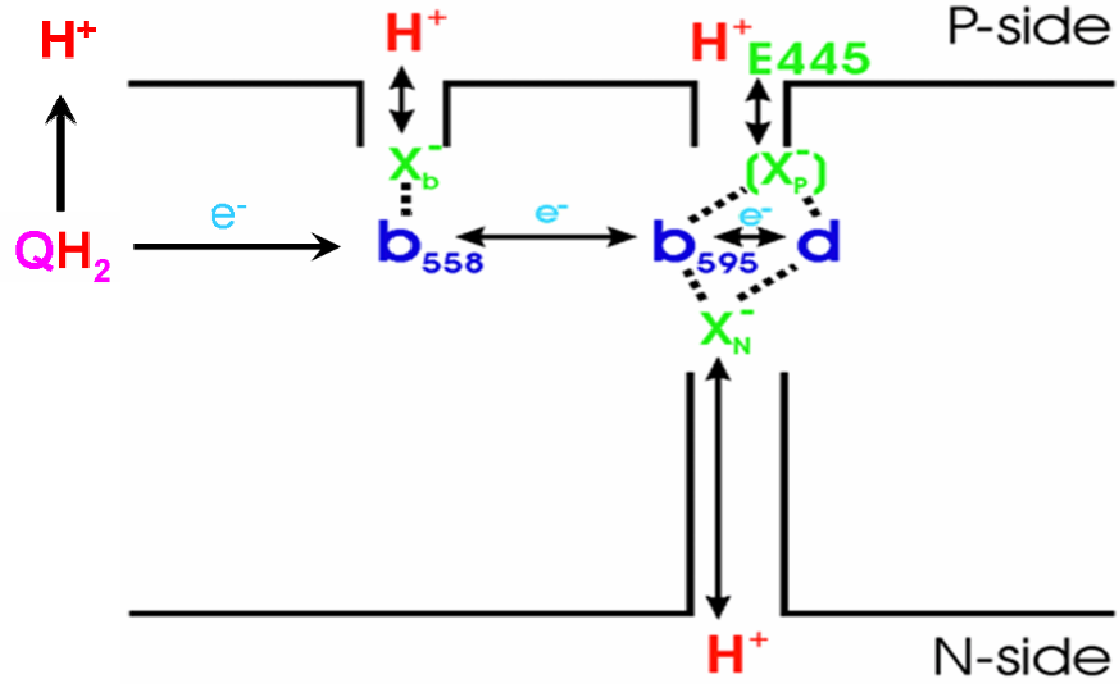

Figure 3.6 Possible scheme of electron and proton transfer pathways in cytochrome *bd* oxidase.
The mutation in the E445 residue prevents the complete two-electron reduction of the di-heme site by dithionite. The proton access to site Xp is pictured as being from the periplasmic side of the membrane (P-side). If this is the case, it is unlikely that this proton is used in the reaction catalyzed at the enzyme active site, but is re-released upon reoxidation of the hemes. N-side, negative side of the membrane.

CHAPTER 4: MUTAGENESIS AND FTIR SPECTROSCOPIC EVIDENCE FOR THE INVOLVEMENT OF TWO ACIDIC RESIDUES IN PROTON TRANSLOCATION

4.1 Introduction:

Cytochrome *bd* is a quinol oxidase from *Escherichia coli* which is optimally expressed under microaerophilic growth conditions. The enzyme catalyzes the 2-electron oxidation of either ubiquinol or menaquinol in the membrane and scavenges O_2 at low concentrations, reducing it to water. Previous work has shown that although cytochrome *bd* does not pump protons, turnover is coupled to the generation of a proton motive force. The generation of a proton electrochemical gradient result from the release of protons from the oxidation of quinol to the periplasm and the uptake of protons used to form H_2O from the cytoplasm. Since the active site has been shown to be located near the periplasmic side of the membrane, a proton channel must facilitate the delivery of protons from the cytoplasm to the site of water formation. Two conserved glutamic acid residues, E107 and E99, are located in transmembrane helix III in subunit I (**Figure 4.1**), and have been proposed to form part of this putative proton channel (see Chapter 3).

In this chapter, the results are reported for mutations in several conserved acidic residues: E99, E107 in CydA and D29 in CydB (**Figure 4.2**). The locations in the predicted topology of each subunit are shown in Figure 1. In the current work, it is shown that mutations in either of these residues results in the loss of quinol oxidase activity and can result in loss of the two hemes at the active site, heme *d* and heme b_{595}. One mutant, E107Q while being totally inactive, retains the hemes. FTIR redox difference

spectroscopy has identified absorption bands from the COOH group of E107. The data show that E107 is protonated at pH 7.6 and that it is perturbed by the reduction of the heme *d* / heme b_{595} binuclear center at the active site.

4.2 Materials and methods:

4.2.1 Strains and plasmids:

E. coli strain CLY (*cyo::kan*, *rec*A), which lacks cytochrome bo_3 quinol oxidase (Yep 2005) was used as the host strain for expressing the wild type cytochrome *bd* on a plasmid.. To obtain wild type cytochrome *bd*, plasmid pTY1 (Yang 2007) was introduced to the strain. This plasmind is a derivative of pET17b and contains the whole operon of wild type *bd* as well as ampicillin resistance gene for selection.

Mutants of cytochrome *bd* were expressed using *E. coli* strain GO105 (*cyd*AB::*kan*, *cyo*, *rec*A), which lacks both cytochrome bo_3 and cytochrome *bd* quinol oxidases (Kaysser, Ghaim et al. 1995) was used as the host strain. To obtain mutant cytochrome *bd*, plasmid pTK1 (Zuberi 1993) was introduced to the strain. This plasmid is a derivative of pBR322 and contains the whole operon of wild type *bd* as well as ampicillin resistance gene for selection.

4.2.2 Site-directed mutagenesis using Quik-Change method:

The Stratagene Quick-Change mutagenesis kit was used to construct mutants. Plasmid pTK1 was used as template. The oligonucleotide primers were synthesized by Roy J. Carver Biotechnology Center (Urbana, IL) with melting temperature around 80 ˚C based on the Stratagene formula, and were diluted in pure water to 100 ng/μL for Quick-

Change reaction. Thermocyclings were conducted on PTC-100 Programmable Thermal Controller (MJ Research Inc.). The protocol was as follows: 95 °C for 2 min, 1 cycle; 18 cycles of 95 °C for 1 min, 54 °C for 1 min, and 68 °C for 8 min; then 68 ˚C for 7 min, 1 cycle. The samples were digested with 1 μL *Dpn*I for 3 ~ 4 hours. All mutants were confirmed by DNA sequencing.

4.2.3 Complementation test for the mutant cytochrome *bd*:

The complementation test was carried out as follows: Plasmid DNA from confirmed mutants was used to transform GO105 using TSS method (Chung, Niemela et al. 1989). Cells were grown anaerobically for selection of ampicillin and kanamycin resistance. The strains exhibiting both amplicillin and kanamycin resistance were restreaked to obtain single colonies, and were grown on M63 (Cohen and Rickenberg 1956) minimal plates supplemented with 0.3 % lactate and 0.3 % succinate. Also added were 100 μg/mL ampicillin and 50 μg/mL kanamycin to maintain the plasmid and the strain. Complementation was defined by aerobic growth within 48 ~ 72 hours of incubation at 37 °C.

4.2.4 Cell growth and protein sample preparation:

Large scale cell growth of strains that grow aerobically (i.e. expressing wild type or E107D mutant) was carried out in 24 2-liter flasks shaking at 220 rpm 37 °C using two Innova 4330 incubator shakers (New Brunswick Scientific). Strain expressing wild type was grown in LB containing 100 μg/mL Amp, 50 μg/mL Kan, and 0.5mM IPTG was added 4 hours after the inoculation. Strains expressing those inactive mutants, which

could not grow aerobically, was grown at the Fermentation Facility at the University of Illinois, at 37 °C, pH 7, in a 20-liter fermenter using LB containing 100 μg/mL Amp, 50 μg/mL Kan, and 0.3 % glucose. Both wild type and mutant cytochrome *bd* oxidases were purified from the membrane of either CLY/pTY1 or GO105/pTK1 as described previously (Miller and Gennis 1986), with the modification that the hydroxyapatite column was omitted. Fractions were collected from the Fast-Flow Sepharose DEAE column with an A_{412}/A_{280} ratio greater than 0.5. The pooled fractions were concentrated using an Amicon concentrator with a 50 kDa molecular weight cut-off filter and then dialyzed three times against 50 mM sodium phosphate buffer, pH 7.8, containing 5 mM EDTA, 0.05% N-lauroylsarcosine. Both wild type and mutant cytochrome *bd* samples were then examined, using the same dialysis buffer for appropriate dilution unless specified otherwise.

4.2.5 Ubiquinol-1 and TMPD oxidase activity assay:

Cytochrome *bd* wild type and mutants were assayed both in isolated membranes, in which there is no other quinol oxidase, and with the purified enzyme. For membranes, samples were homogenized in 25 mM Tris HCl, 1 mM EDTA disodium salt, pH 7.5. Purified protein samples were dialyzed against 50 mM NaPi buffer, pH 7.8, containing 5 mM EDTA disodium salt and 0.05 % N-lauroyl sarcosine. Various dilutions of either the homogenized membrane samples or pure protein samples were added to 1.8 mL of the respective buffer containing either 2 mM dithiothreitol or 4 mM ascorbate that had been equilibrated to 37 °C in a Clark-type oxygen electrode (Yellow Springs Instrument CO.). A baseline was taken and the reaction was initiated by addition of ubiquinol-1 (kindly

provided by Hoffman-LaRoche) or TMPD to a final concentration of 245 μM and 1 mM, respectively. Activities were determined assuming a value of 237 μM O_2 for air-saturated buffer at 37 °C.

4.2.6 Heme analysis:

The heme *b* contents of both wild type and mutant purified cytochrome *bd* were measured by the pyridine hemochromogen assay, using an extinction coefficient for the wavelength pair 556.5−540 nm = 23.98 mM^{-1} cm^{-1} (Berry and Trumpower 1987). The heme d content was determined from the reduced minus "as isolated" difference spectrum with the $\Delta\varepsilon_{628-607\ nm}$ = 10.8 mM^{-1} cm^{-1} (Borisov, Arutyunyan et al. 1999). The concentration of the wild type cytochrome *bd* was determined from the reduced minus as isolated difference spectrm, using $\Delta\varepsilon_{560-580\ nm}$ = 21.4 mM^{-1} cm^{-1} (Tsubaki, Hori et al. 1995). Since the "as isolated" enzyme contains varying amounts of ferrous heme d-oxy complex and oxoferryl heme d species, the heme d content was also determined by the absolute spectrum of the fully reduced enzyme, using the extinction coefficient $\Delta\varepsilon_{628\text{-}670\ nm}$ = 25 mM^{-1} cm^{-1} (Borisov, Arutyunyan et al. 1999). The concentration of the mutant protein was determined by the BCA assay using wild type cytochrome *bd* as standard.

4.2.7 UV-Vis spectroscopic measurements:

All the absorbance spectra in the UV-Vis region were obtained with a DW2000 spectrophotometer (Aminco) using a 1 cm pathlength cuvette. The series of absorbance spectra for mid-point potential measurements were taken using UV-2101PC scanning spectrophotometer (Shimadzu).

4.2.8 Electrochemistry and FTIR difference spectroscopy:

FTIR difference spectra recorded at 5 °C as a function of applied potential with BioRad (now Varian, Inc.) FTS-6000 FTIR. Each FTIR difference spectrum consisted of 256 intereferograms at 4 cm^{-1} resolution and approximately 20 spectra were averaged to give better signal to noise. Triangular apodization is used for Fourier transformation. Equilibration at the applied potential is achieved in less than 10 min. FTIR spectra monitored until no change detected. Experimental conditions for *bd* quinol oxidase and electrochemical cell set-up is described in detail previously (Mansfield and Wiggins 1990; Mantele 1996). A mixture of 13 different mediators added to 40 μM final concentration 1,1'-dicarboxylferrocene, dimethylparaphenylendiamine (DMPPD), ferricyanide, quinhydrone, tetramethylparaphenylendiamine (TMPPD), tetrachlorobenzoquinone, 2,6-dichlorophenol indophenol, ruthenium hexamine chloride, 1,2-naphthoquinone, menadione, 2-hydroxy-1,4-naphthoquinone, benzyl viologen, methyl viologen.

4.2.9 Sequence analysis and topology model generation:

The homologous sequences of subunit I and subunit II of cytochrome *bd* were kindly provided by Dr. James Hemp in Grennis lab, Urbana, University of Illinois. The sequence alignment was performed by BioEdit Sequence Alignment Editor Ver.7.0.9.0 (Hall 1999). The topology models of subunit I and subunit II were generated by membrane topology prediction tool TMHMM 2.0 program (http://www.cbs.dtu.dk/services/TMHMM/). The graph was created by TOPO2 program based on the TMHMM result (http://www.sacs.ucsf.edu/TOPO-run/wtopo.pl).

4.3 Results:

4.3.1 Complementation test, heme analysis and UV-Vis spectra:

To test how much the mutation affect the catalytic activity of the enzyme, complementation test were performed. As shown in **Table 4.1,** except E107D, all the other mutants cytochrome *bd* were unable to rescue the aerobic growth of *E. coli* strain GO105, which lacks both of the terminal oxidases – an indication that the mutants cytochrome *bd* lost their terminal oxidase activity. The heme analysis showed that all I-E99 and II-D29 mutants completely lost the heme b_{595} / heme *d* binuclear center, while I-E107Q mutant retains about half of heme d that expected compared to the wild type. Surprisingly, the only mutant that passed the complementation test, E107D, also lost the heme b_{595} / heme *d* active site, indicating the mutation destabilizes the binding of heme *d* and heme b_{595} to a point where even isolation of the membranes results in loss of heme content. The UV-Vis spectra confirm the heme analysis optically.

4.3.2 Ubiquinol-1 and TMPD oxidase activity assay:

Consistent with the loss of binuclear center, none of the mutants showed ubiquinol oxidase activity (**Table 4.1**). It has been shown that TMPD donates electrons to a site distinct from ubiquinol and appears to be oxidized directly at the heme *d* / heme b_{595} active site. In our case, except E107Q who demonstrates a low activity with TMPD, all the other mutants lack the TMPD oxidase activity, suggesting a severe damage to their active site.

4.3.3 FTIR spectra of wild type and E107Q mutant:

The main goal of this work was to determine whether E107 and/or E99 carboxyl groups contribute to the FTIR redox difference spectrum previously reported (Zhang, Oettmeier et al. 2002; Yamazaki, Kandori et al. 1999). Only the E107Q mutant could be isolated with the heme content intact and approximating that of the wild type oxidase. **Figure 4.3** shows the oxidized-*minus*-reduced FTIR difference spectra (708 mV to -292 mV vs. SHE).of wild type and the E107Q mutant of anaerobically grown cytochrome *bd* oxidase. The spectra include the contributions of all hemes, the bound quinone, the backbone and all residues reorganising or changing protonation state concomitant with the redox reaction. The positive signals correspond to the oxidized form and the negative signals to the reduced state. The spectra of wild type oxidase have been previously described in (Zhang, Oettmeier et al. 2002) and include the contributions of several protonated acidic residues (i.e., COOH). It is noted that anaerobically grown *E. coli* contains primarily menaquinone as a component of its respiratory chain, whereas aerobically grown cells utilize ubiquinone. Cytochrome *bd* can utilize either menaquinol or ubiquinol as a substrate. The E107Q mutant enzyme, isolated from anaerobically grown cells, exhibits clear perturbations in the spectral region that is typical for protonated acidic residues, 1730 to 1750 cm^{-1} (Venyaminov and Kalnin 1990). Other components may also contribute to the FTIR spectrum in this region, including lipids (Hielscher, Wenz et al. 2006) and, possibly heme d, whose FTIR spectrum is unknown.

As shown in **Figure 4.3**, the FTIR redox difference spectrum of the mutant oxidase differs from that of the wild type oxidase. The absence of the negative band at 1753 cm^{-1} and the perturbations around 1738 cm^{-1} and 1700 cm^{-1} are highlighted in

double difference spectra in **Figure 4.4**. On the basis of these shifts, E107 can be assigned to the signal in the wild type spectrum with a negative trough near 1753 cm^{-1} and positive band at 1738 cm^{-1}. This sigmoid shaped band is most readily interpreted as being due to the reorganization of the environment around a protonated form of E107. The basic conclusion is that E107 must be protonated at the pH of the experiment (pH 7.6) and it is perturbed upon changing the redox state of one or more of the heme components of the enzyme. The frequencies observed for the residue indicate that E107 is in a hydrophobic environment and that there is stronger hydrogen bonding upon reduction (shift from 1751 cm^{-1} to 1738 cm^{-1}).

Additional spectroscopic shifts around 1700 cm^{-1} and 1685 cm^{-1} are observed in the spectra and these spectroscopic changes may include contributions from the heme propionates and the backbone. In the lower spectral range, only minor variations can be seen in the spectrum of the E107Q mutant oxidase, and these may be attributed to the small loss of heme *d* that is observed over the time required to complete the spectroscopic measurements.

4.3.4 Redox-induced perturbation of E107Q mutant using FTIR:

The redox-induced perturbation of the E107 environment was further examined over more narrow ranges of solution potential. **Figure 4.5** shows the double difference spectrum in the 1750 cm^{-1} region of the spectrum over the ranges -292 mV to +118 mV (vs. SHE), within which is the midpoint potential of cytochrome b_{558}, and +128V to +708 mV (vs. SHE) which will capture changes accompanying the oxidation/reduction of heme *d* and heme b_{595}. The midpoint potentials of heme *d* and heme b_{595} are sufficiently close

(256 mV and 223 mV vs SHE) so as to preclude resolving spectroscopic changes that can be attributed to either heme alone. The spectral alterations over the entire voltage range (-292 mV to +708 mV vs SHE) is also shown in **Figure 4.5**, which includes changes coupled to the reduction/oxidation of all three hemes plus the quinones. The results clearly show that the perturbation of the spectrum of E107 is associated with the redox changes of heme *d* / heme b_{595}. There are other changes in the 1750 cm^{-1} region of the spectrum of the wild type enzyme, suggesting the perturbation of other protonated acidic residues besides E107 coupled to the reduction/oxidation of the metal centers. E99 is a good candidate, but the loss of heme *d* / heme b_{595} from both the E99A and E99Q mutants rules out meaningful FTIR difference spectroscopy.

4.4 Discussion and conclusions:

Previously reported FTIR difference spectroscopy (Zhang, Oettmeier et al. 2002; Yamazaki, Kandori et al. 1999) has shown that more than one acidic residue is perturbed when the metal centers are reduced in cytochrome *bd* from *E. coli.* In addition, our new model of electron and proton transfer pathways inside the cytochrome *bd* put the argument of a proton translocation channel on the table. Two acidic amino acid residues are totally (>99%) conserved in all the sequences of the *bd*-type oxidases - E99 and E107. Their special locations on the transmembrane helices as well as close proximity to the hemes' ligands, make them good candidates for the role.

Both the E99A and E99Q mutant oxidases lose the heme *d* / heme b_{595} active site, and, therefore, were not useful for FTIR spectroscopy. It is reasonable to conclude that E99 is important for binding the di-heme center at the enzyme active site, as is E107. The

E107D and E107Q mutants both have labile heme *d* and heme b_{595}. In the case of E107Q, the heme content is about half the expected amount upon isolation, but after 12 hours at 4 °C at pH 7.6, the heme d content is significantly lower (about half). At higher pH, the lability of the hemes is increased, which is the case for the wild type oxidase as well. The E107D mutant oxidase is functional *in vivo*, but the activity is lost upon preparing membranes, and the isolated enzyme lacks heme d and heme b_{595}. Clearly, E107 is important for both function and for the structural integrity of the active site. Evidently, having an acidic residue at this location is not sufficient for stability since aspartate does not substitute for glutamate at this position. This is reflected in the sequence alignments which show only glutamates at equivalent positions to E99 and E107 (Osborne and Gennis 1999).

The E107Q mutant was sufficiently stable for FTIR difference spectroscopy. The results (**Figure 4.3**) show a substantial difference between the spectra of the wild type and the E107Q mutant. The double difference spectra (inset, **Figure 4.3**) clearly show that E107 absorbs at 1738 cm^{-1} in the oxidized form of the enzyme, but at 1752 cm^{-1} when the enzyme is fully reduced. The spectroscopic shift is coupled to the redox change of the heme *d* / heme b_{595} center (**Figure 4.5**). The position of the absorption demonstrates that E107 is in a hydrophobic environment and that it is protonated in both the reduced and oxidized forms of the enzyme. Furthermore, the shift to higher wave number indicates that the hydrogen bonding of E107 is strengthened when the enzyme is reduced. Clearly, the population of the enzyme lacking the heme *d* / heme b_{595} active-site hemes does not respond to any redox changes in these metal centers, so these data are not based on the fraction of the enzyme in which these hemes are lacking.

The data in this work indicate a cluster of acidic residues from both CydA and CydB that are important for the stable assembly of the heme *d* / heme b_{595} center. These include E99, E107 and D29 (CydB). Even conservative substitutions of glutamate for aspartate or *vice versa* are not tolerated. The ease of destabilizing the binding of heme *d* / heme b_{595} has been previously noted and speculated to possibly indicate that these hemes are present at the interface between CydA and CydB, susceptible to perturbations to that interface(Oden and Gennis 1991)). The current work is consistent with this possibility but does not rule out other possibilities.

The major motivation of this work was to investigate the possibility that E99 and E107 participate in conveying protons to the heme b_{595} / heme *d* active site. This remains possible, and the likely proximity of both E99 and E107 to heme *d* is consistent with this role. However, the structural importance of both E107 and E99 make it difficult at this point to make any conclusions about a certain role of these residues in proton translocation within a possible proton channel.

4.5 Figures and tables:

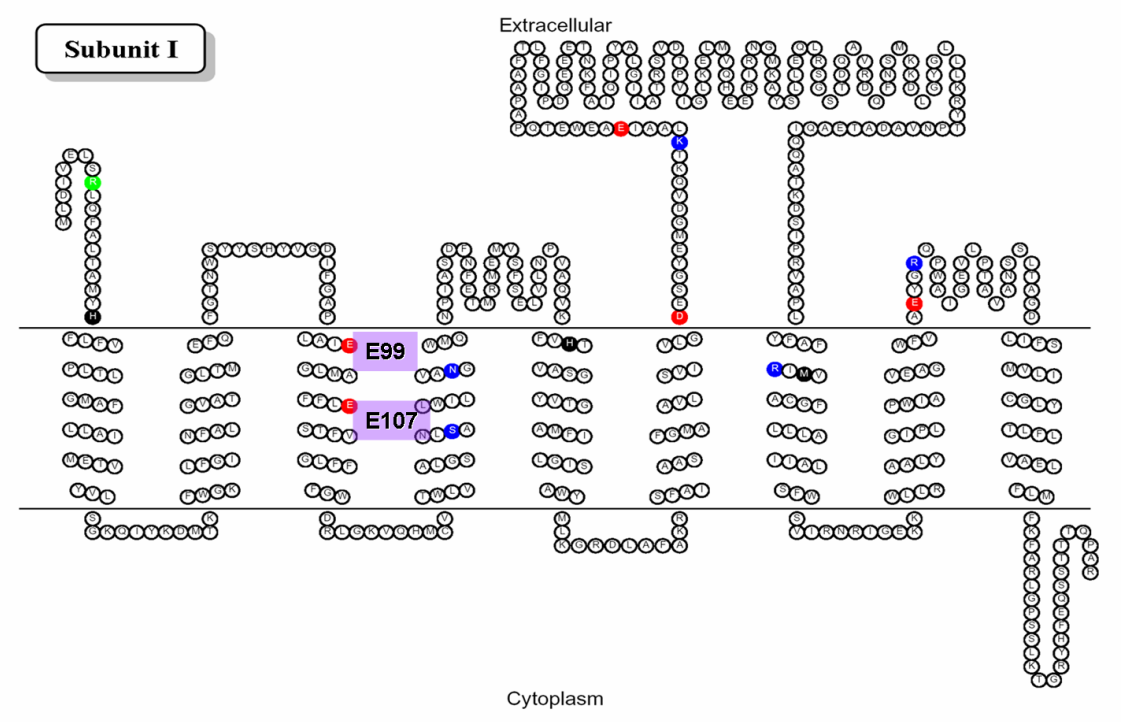

Figure 4.1 Membrane topology model of subunit I of cytochrome *bd* oxidase from *E. coli* with E99 and E107 marked out.

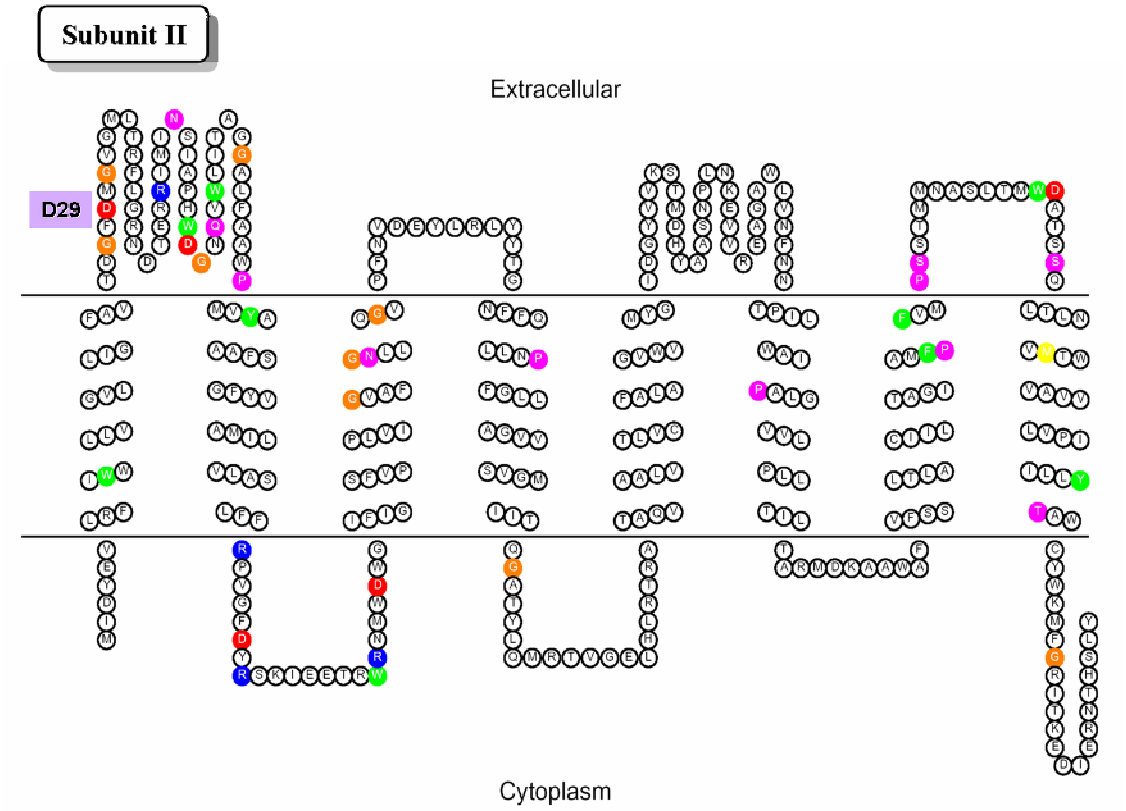

Figure 4.2 Membrane topology model of subunit II of cytochrome *bd* oxidase from *E. coli* with D29 marked out.

Table 4.1 Summary of the properties of the cytochrome *bd* E99, E107 and II-D29 mutants

	Complementation of aerobic growth	Heme content (UV-Vis spectra)	UQ_1H_2 oxidase activity[a]	TMPD oxidase activity[b]
Wild type	Yes	All hemes present	100%	100%
E107D	Yes	Little heme *d*/heme b_{595}	0%	0%
E107Q	No	Near wild type but heme *d*/heme b_{595} are labile and readily lost after purification	0%	22%
E99A	No	No heme *d*/heme b_{595}	0%	0%
E99Q	No	No heme *d*/heme b_{595}	0%	0%
II-D29E	No	No heme *d*/heme b_{595}	0%	0%

[a] 100% of ubiquinol-1 oxidase activity corresponds to a turnover of about $1450e^{-1}$/sec.
[b] 100% of TMPD oxidase activity corresponds to a turnover of about $100e^{-1}$/sec.

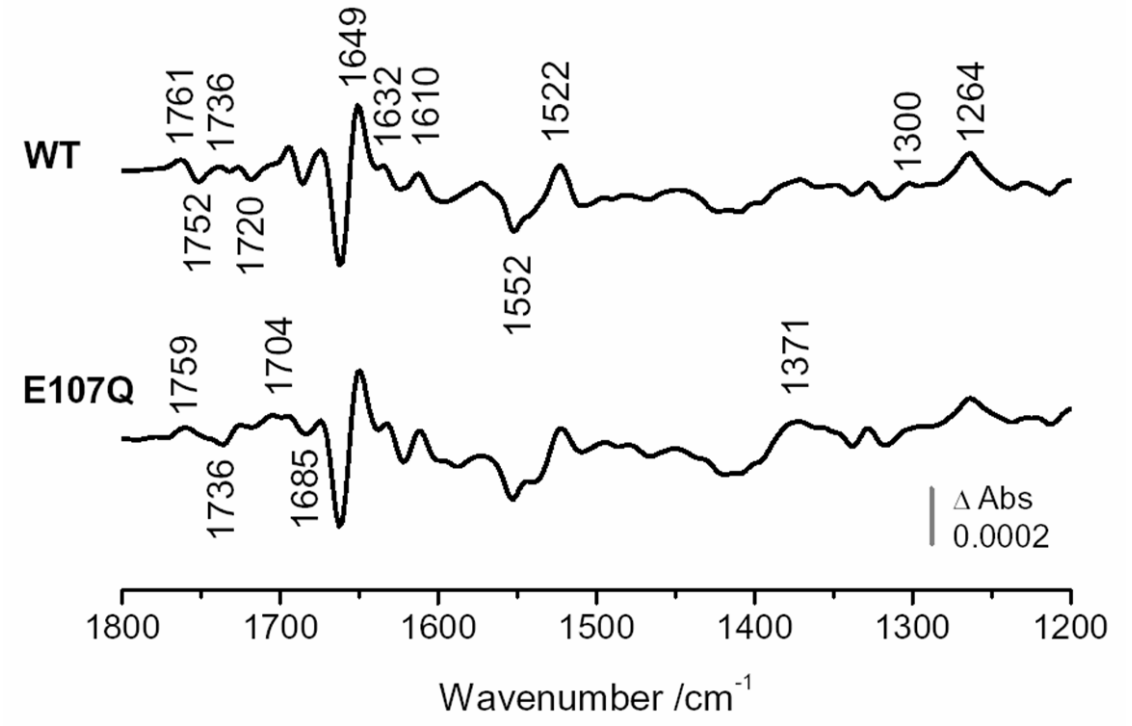

Figure 4.3 Oxidized-*minus*-reduced FTIR difference spectra of wild type and E107Q. Both wild type and E107Q mutant were grown anaerobically. The redox potential changed in steps from 708 mV to -292 mV vs. SHE.

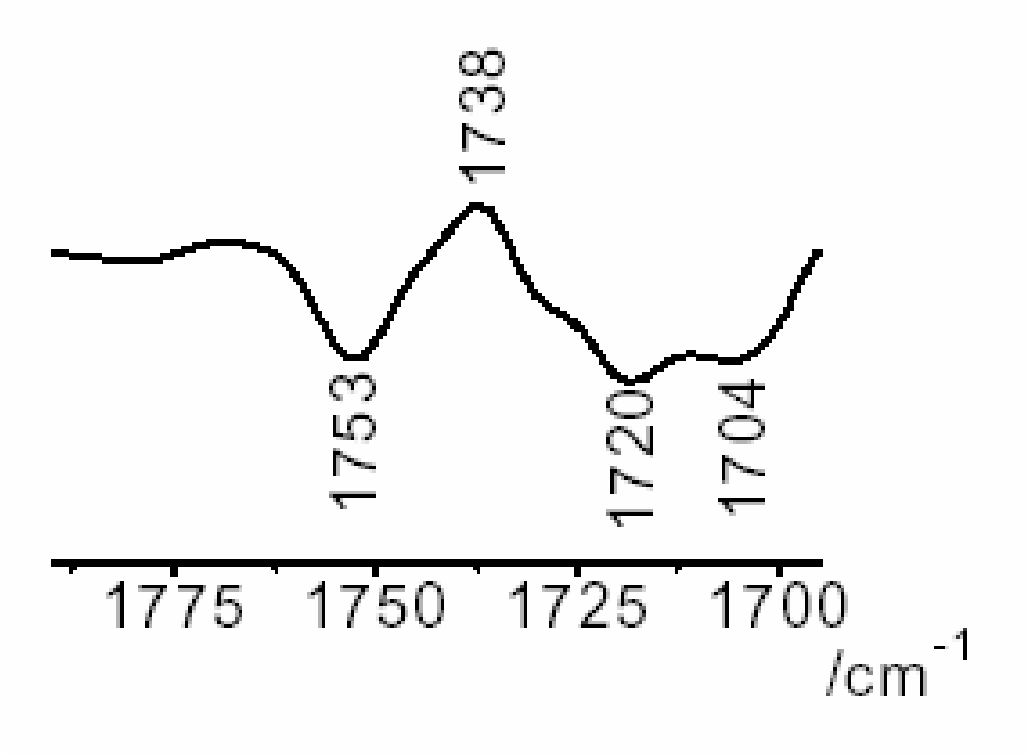

Figure 4.4 Wild type-*minus*-E107Q double difference spectrum.
The negative band at 1753 cm^{-1} and positive band at 1738 cm^{-1} are assigned to E107.

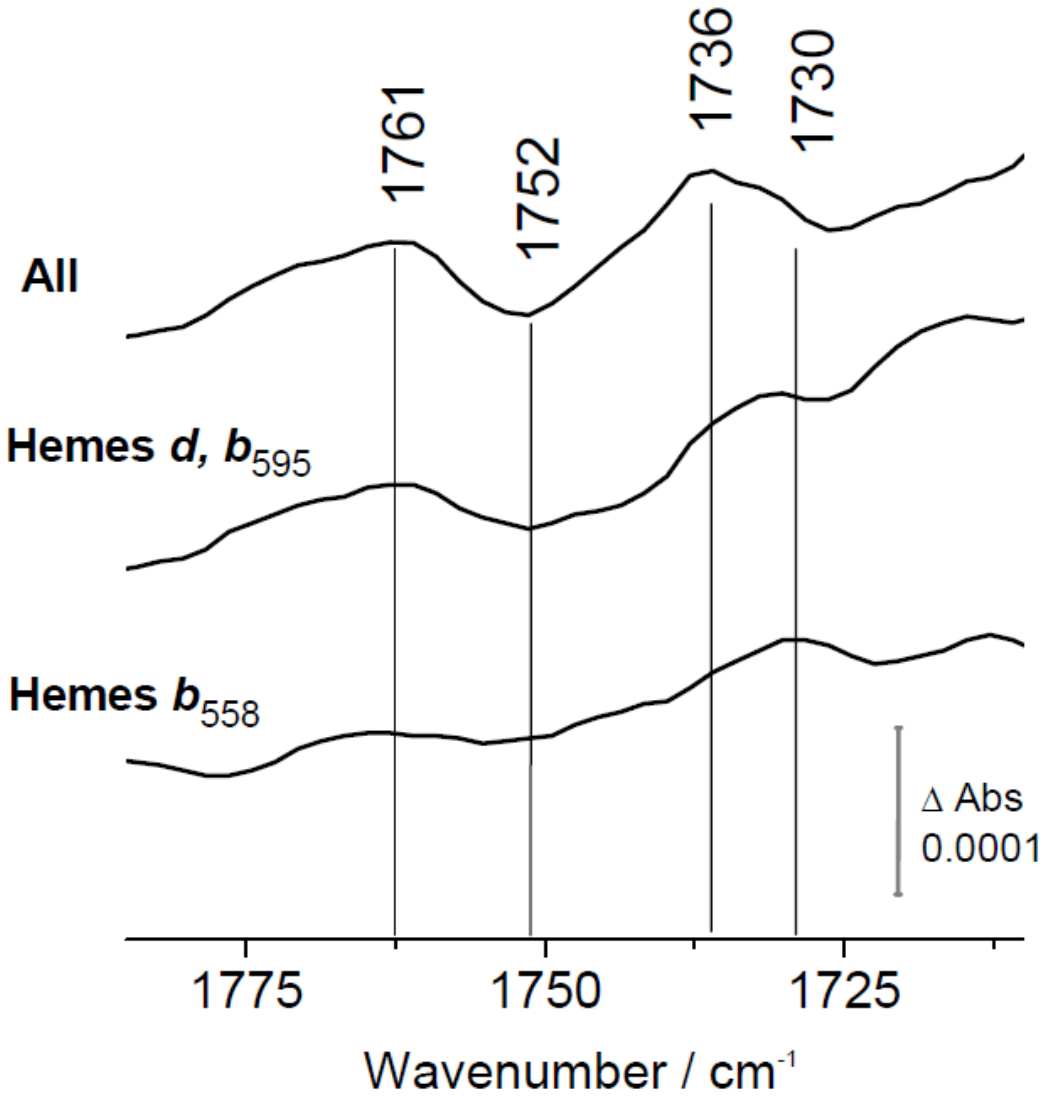

Figure 4.5 Oxidized-*minus*-reduced FTIR difference spectra of wild type cytochrome *bd* for selected potential steps.
The steps include the contributions from heme b_{558} (+118 to -292 mV), the active site (+708 to +128 mV vs. SHE) and a full potential step (+708 to -292 mV vs. SHE), which includes contributions from all cofactors plus the quinone.

CHAPTER 5: MUTAGENESIS AND FTIR EVIDENCE INDICATE A POSSIBLE ROLE OF A NON-ACIDIC RESIDUE IN PROTON UPTAKE

5.1 Introduction:

As a plausible proton channel has been outlined in the previous two chapters, more structural details are on demand for this translocation pathway. Other than strictly conserved acidic residues that have been discussed, two more non-acidic amino acids, S140 and N148, enter our view due to their high conservation in over 1000 cytochrome *bd* homologous sequences, as well as their close proximity to E99 and E107 (**Figure 5.1**).

In this chapter, we examined the importance of these highly conserved residues by site-directed mutagenesis. Seven mutants were made: S140A, S140L, S140T, S140H, S140C, N148A, and N148D. All the Serine 140 mutants are suffering from server impairment of aerobic growth, while all the Asparagine 148 mutants retain wild type activity. In vitro enzymatic assays showed that, two Serine mutants, S140L and S140T partially retain the ability to oxidize TMPD, an artificial electron donor, and are unable to catalyze the quinol oxidation reaction at all. This could be a sign that the mutations may perturb both the initial electron transfer from quinol to heme b_{558} and the downstream electron transfer or water formation in an electrogenic way. Further experiments conducted using Fourier transform infrared spectroscopy (FTIR), which provides more detailed characterization of S140T mutant enzyme is reported in this chapter.

5.2 Materials and methods:

5.2.1 Strains and plasmids:

E. coli strain CLY (*cyo::kan*, *rec*A), which lacks cytochrome bo_3 quinol oxidase (Yep 2005) was used as the host strain for expressing the wild type cytochrome *bd* on a plasmid.. To obtain wild type cytochrome *bd*, plasmid pTY1 (Yang 2007) was introduced to the strain. This plasmind is a derivative of pET17b and contains the whole operon of wild type *bd* as well as ampicillin resistance gene for selection.

Mutants of cytochrome *bd* were expressed using *E. coli* strain GO105 (*cyd*AB::*kan*, *cyo*, *rec*A), which lacks both cytochrome bo_3 and cytochrome *bd* quinol oxidases (Kaysser, Ghaim et al. 1995) was used as the host strain. To obtain mutant cytochrome *bd*, plasmid pTK1 (Zuberi 1993) was introduced to the strain. This plasmid is a derivative of pBR322 and contains the whole operon of wild type *bd* as well as ampicillin resistance gene for selection.

5.2.2 Site-directed mutagenesis using Quik-Change method:

The Stratagene Quik-Change mutagenesis kit was used to construct mutants. Plasmid pTK1 was used as template. The oligonucleotide primers were synthesized by Roy J. Carver Biotechnology Center (Urbana, IL) with melting temperature around 80 °C based on the Stratagene formula, and were diluted in pure water to 100 ng/μL for Quik-Change reaction. Thermocyclings were conducted on PTC-100 Programmable Thermal Controller (MJ Research Inc.). The protocol was as follows: 95 °C for 2 min, 1 cycle; 18 cycles of 95 °C for 1 min, 54 °C for 1 min, and 68 °C for 8 min; then 68 °C for 7 min, 1

cycle. The samples were digested with 1 μL *Dpn*I for 3 ~ 4 hours. All mutants were confirmed by DNA sequencing.

5.2.3 Complementation test for the mutant cytochrome *bd*:

The complementation test was carried out as follows: Plasmid DNA from confirmed mutants was used to transform GO105 using TSS method (Chung, Niemela et al. 1989). Cells were grown anaerobically for selection of ampicillin and kanamycin resistance. The strains exhibiting both amplicillin and kanamycin resistance were restreaked to obtain single colonies, and were grown on M63 (Cohen and Rickenberg 1956) minimal plates supplemented with 0.3 % lactate and 0.3 % succinate. Also added were 100 μg/mL ampicillin and 50 μg/mL kanamycin to maintain the plasmid and the strain. Complementation was defined by aerobic growth within 48 ~ 72 hours of incubation at 37 °C.

5.2.4 Cell growth and protein sample preparation:

Large scale cell growth of strains that grow aerobically (i.e. expressing wild type) was carried out in 24 2-liter flasks shaking at 220 rpm 37 °C using two Innova 4330 incubator shakers (New Brunswick Scientific). Strain expressing wild type was grown in LB containing 100 μg/mL Amp, 50 μg/mL Kan, and 0.5mM IPTG was added 4 hours after the inoculation. Strains expressing those inactive mutants, which could not grow aerobically, were grown microaerobically in the lab at the University of Illinois, at 37 °C, pH 7, in a 12 2-liter air-tight flasks using LB containing 100 μg/mL Amp, 50 μg/mL Kan, and 0.3 % glucose. Both wild type and mutant cytochrome *bd* oxidases were purified

from the membrane of either CLY/pTY1 or GO105/pTK1 as described previously (Miller and Gennis 1986), with the modification that the hydroxyapatite column was omitted. Fractions were collected from the Fast-Flow Sepharose DEAE column with an A_{412}/A_{280} ratio greater than 0.5. The pooled fractions were concentrated using an Amicon concentrator with a 50 kDa molecular weight cut-off filter and then dialyzed three times against 50 mM sodium phosphate buffer, pH 7.8, containing 5 mM EDTA, 0.05% N-lauroylsarcosine. Both wild type and mutant cytochrome *bd* samples were then examined, using the same dialysis buffer for appropriate dilution unless specified otherwise.

5.2.5 Ubiquinol-1 and TMPD oxidase activity assay:

Cytochrome *bd* wild type and mutants were assayed both in isolated membranes, in which there is no other quinol oxidase, and with the purified enzyme. For membranes, samples were homogenized in 25 mM Tris HCl, 1 mM EDTA disodium salt, pH 7.5. Purified protein samples were dialyzed against 50 mM NaPi buffer, pH 7.8, containing 5 mM EDTA disodium salt and 0.05 % N-lauroyl sarcosine. Various dilutions of either the homogenized membrane samples or pure protein samples were added to 1.8 mL of the respective buffer containing either 2 mM dithiothreitol or 4 mM ascorbate that had been equilibrated to 37 °C in a Clark-type oxygen electrode (Yellow Springs Instrument CO.). A baseline was taken and the reaction was initiated by addition of ubiquinol-1 (kindly provided by Hoffman-LaRoche) or TMPD to a final concentration of 245 μM and 1 mM, respectively. Activities were determined assuming a value of 237 μM O_2 for air-saturated buffer at 37 °C.

5.2.6 Heme analysis:

The heme *b* contents of both wild type and mutant purified cytochrome *bd* were measured by the pyridine hemochromogen assay, using an extinction coefficient for the wavelength pair 556.5−540 nm = 23.98 mM^{-1} cm^{-1} (Berry and Trumpower 1987). The heme *d* content was determined from the reduced minus "as isolated" difference spectrum with the $\Delta\varepsilon_{628-607\ nm}$ = 10.8 mM^{-1} cm^{-1} (Borisov, Arutyunyan et al. 1999). The concentration of the wild type cytochrome *bd* was determined from the reduced minus as isolated difference spectrm, using $\Delta\varepsilon_{560-580\ nm}$ = 21.4 mM^{-1} cm^{-1} (Tsubaki, Hori et al. 1995). Since the "as isolated" enzyme contains varying amounts of ferrous heme *d*-oxy complex and oxoferryl heme *d* species, the heme *d* content was also determined by the absolute spectrum of the fully reduced enzyme, using the extinction coefficient $\Delta\varepsilon_{628\text{-}670\ nm}$ = 25 mM^{-1} cm^{-1} (Borisov, Arutyunyan et al. 1999). The concentration of the mutant protein was determined by the BCA assay using wild type cytochrome *bd* as standard.

5.2.7 UV-Vis spectroscopic measurements:

All the absorbance spectra in the UV-Vis region were obtained with a DW2000 spectrophotometer (Aminco) using a 1 cm pathlength cuvette. The series of absorbance spectra for mid-point potential measurements were taken using UV-2101PC scanning spectrophotometer (Shimadzu).

5.2.8 Electrochemistry and FTIR difference spectroscopy:

The FTIR difference of wild type and E107Q mutant *bd* oxidases spectra were obtained using the techniques previously described in chapter 4. In the case of S140 and

N148 mutants, a 3-bounce attenuated total reflectance (ATR) attachment with a 3 mm diamond prism (SensIR now Smiths Detection) was used with a BioRad (now Varian Inc.) FTS-575C FTIR spectrophotometer equipped with liquid nitrogen cooled MCT detector. A thin film containing the enzyme was adhered to the surface of the diamond prism. First step is the detergent removal from the purified enzyme and pellet the enzyme. 10 ml of 250 mM enzyme solution was diluted 300-fold with water. The solution was concentrated using an Amicon 50 K membrane concentrator to a final volume of 500 ml. This dilution and concentration was repeated. The final suspension of enzyme was pelleted using a counter-top centrifuge. The pellet was re-suspended in 10 ml of water and could be stored at -80 °C. To prepare the protein film, 6 ml of this sample was pipetted onto the ATR diamond prism and air-dried for a few minutes. This caused the protein to stick firmly to the crystal surface. The protein film was re-hydrated by first humidifying the air around the film until a stable FTIR spectrum is recorded. Then 1 ml solution of the perfusion buffer (30 mM HEPES, 20 mM KCl, 5 mM $MgCl_2$, pH 8.5, in H_2O) is put on the film in order to re-wet the sample. The protein concentration is estimated to be approximately 500 mM. The sample was sealed with an acrylic lid, designed to allow the space above the film to be perfused with buffer of any composition. In this way, the redox status of the enzyme was altered, as previously described, to obtain the fully reduced and fully oxidized states. Upon changing the buffer composition, the state of the enzyme in the film was monitored by visible spectroscopy using a home-built apparatus with an Ocean Optics USB2000 spectrometer. The absorption spectrum in the visible was obtained by reflectance off the surface of the sample on the diamond ATR crystal. Thus, one can record the visible spectrum simultaneously with the infrared spectrum as the buffer

composition is changed. In general, the sample was equilibrated with a buffer by flowing the solution over the sample for about 1 h. A peristaltic pump (Cole-Parmer, Masterflex C/L) and a valve controller (Hamilton) are used for the flow and exchange of buffers. All experiments were performed at 22 °C with a flow speed of 0.33 ml/min.

The oxidized enzyme was obtained by flowing the perfusion buffer (30 mM HEPES, 20 mM KCl, 5 mM $MgCl_2$, pH 8.5) including 1 mM ferricyanide over the sample. To reduce the enzyme, an aliquot of a freshly prepared solution of dithionite (3 mM final concentration) was added to the perfusion buffer. Each FTIR spectrum consisted of 512 interferograms which were averaged. This ‘‘single-beam’’ (detector response) spectrum (512 averaged interferograms) was recorded in one state and, after changing buffers, recorded in the second state. Triangle apodization was used for the Fourier transformation. The oxidized and reduced single-beam spectra were ratioed to obtain the absorbance difference spectrum (-log10 (oxidized/reduced)). This oxidation reduction cycle was repeated to improve the signal to noise ratio (S/N) for each sample and the spectra from at least 2 samples were averaged. All experiments performed with 4 cm^{-1} spectral resolution.

5.2.9 Sequence analysis and topology model generation:

The homologous sequences of subunit I of cytochrome *bd* were kindly provided by Dr. James Hemp in Grennis lab, Urbana, University of Illinois. The sequence alignment was performed by BioEdit Sequence Alignment Editor Ver.7.0.9.0 (Hall 1999). The topology model of subunit I was generated by membrane topology prediction tool TMHMM 2.0 program (http://www.cbs.dtu.dk/services/TMHMM/). The graph was

created by TOPO2 program based on the TMHMM result (http://www.sacs.ucsf.edu/TOPO-run/wtopo.pl).

5.3 Results:

5.3.1 Complementation test, heme analysis and optical spectra:

The complementation test carried out on minimal plate containing antibiotics exhibited a bi-polar pattern for S140 and N148 mutants. All the S140 mutations result in failure of aerobic growth, while N148 mutants show normal terminal oxidase behavior as wild type enzyme (**Table 5.1**). Unlike N148 mutants that have normal hemes content and wild type spectra, mutations at S140 show impaired heme b_{595} / heme *d* active center.

5.3.2 Ubiquinol-1 / TMPD oxdiase activity of S140 and N148 mutants:

Consistent with the results from complementation test, heme analysis and optical spectra, none of the S140 mutants shows any ubiquinol-1 oxidase activity, while some of them, S140L and S140T, retain around 40-50% TMPD activity, indicating a perturbed but relatively functional binuclear active site. All the mutations at N148 behave like wild type in the activity assay (**Table 5.1**).

5.3.3 FTIR spectra of wild type and S140T mutant:

Although most of the S140 mutants could be isolated with the heme content intact and approximating that of the wild type oxidase, S140T gives the best yield of protein in the customized fermentation system, which provided enough enzyme for the FTIR experiment. **Figure 5.2** shows the oxidized-minus-reduced FTIR difference spectra of

wild type, the S140T and N148D mutant cytochrome *bd* oxidases. The spectra include the contributions of all hemes, the bound quinone, the backbone and all residues reorganising or changing protonation state concomitant with the redox reaction. The positive signals correspond to the oxidized form and the negative signals to the reduced state. The spectra of wild type oxidase have been previously described in (Zhang, Oettmeier et al. 2002) and include the contributions of several protonated acidic residues (i.e., COOH). It is noted that anaerobically grown *E. coli* contains primarily menaquinone as a component of its respiratory chain, whereas aerobically grown cells utilize ubiquinone. Cytochrome *bd* can utilize either menaquinol or ubiquinol as a substrate. The S140T mutant enzyme, isolated from microaerobically grown cells, exhibits clear perturbations in the spectral region that is typical for protonated acidic residues, 1730 to 1750 cm^{-1} (Venyaminov and Kalnin 1990).

As shown in **Figure 5.2**, the FTIR redox difference spectra of the N148D mutant oxidase show no difference from that of the wild type oxidase. In the case of S140T mutant oxidase, besides the impairment of the positive band at 1759 cm^{-1} and the negative band at 1751 cm^{-1}, the absence of the positive band at 1736 cm^{-1} is also highlighted in double difference spectra in **Figure 5.3**. Compared with the double difference FTIR spectra of E107Q mutant given in the last chapter (**Figure 4.4**), there is a 2 cm^{-1} red-shift of the entire sigmoid shaped band in the S140T mutant spectra. This is most readily interpreted as being due to the reorganization of the environment around a protonation state change of E107. Different from the E107Q, the positive band at 1759 cm^{-1} indicates the mutation at S140T perturbs some unknown protonated acidic residue other than E107, which could be E99 due to its critical location in the membrane. The

basic conclusion is that S140 may be involved in the protonation of E107 / E99 at the pH of the experiment (pH 8.5).

5.4 Discussion and conclusions:

Like the well established model for the two proton transfer pathways, D-channel and K-channel in heme-copper oxidase, many non-acidic amino acids contribute to the proton translocation process both structurally and catalytically, other than those well-known highly conserved acidic residue. The story should be somehow consistent in the cytochrome *bd* oxidase. Previously (chapter 3 and 4), several critical acidic residues, E445, E99, E107 and D29 have been reported to be critical to the proton translocation. In the current work, two more strictly conserved non-acidic residues, S140 and N148 entered our view due to their unique location in the membrane.

Sitting right next to E99 and E107 in the transmembrane helix IV of subunit I (**Figure 5.1**), S140 and N148 are highly conserved (> 92%) in over 1000 sequences and more strictly conserved in the *E. coli* subfamily (100%) (James Hemp, unpublished data). While N148 mutants show wild type-like properties in all the aspects, the mutations at S140 lost all the ubiquinol-1 oxidase activity but retain the TMPD oxidase activity partially. The relatively intact heme b_{595} / heme *d* active center in S140 mutants as well as its close proximity to E107 make them a good subject for further investigation by FTIR.

The S140T mutant was well expressed in our customized microaerobic incubation system and also sufficiently stable for FTIR difference spectroscopy. The results (**Figure 5.2**) show a substantial difference between the spectra of the wild type and the S140T mutant. The double difference spectra (**Figure 5.3**) clearly show that perturbation of an

acidic residue at 1736 cm^{-1} in the oxidized form of the enzyme, and at 1751 cm^{-1} when the enzyme is fully reduced. This sigmoid shaped band is exactly the same as we observed in E107Q mutant (Yang, Zhang et al. 2007) despite of a 2 cm^{-1} red-shift of the entire signal. The position of the absorption demonstrates that this protonated acidic amino acid is in a hydrophobic environment, which is also consistent with the previous result on E107 (Yang, Zhang et al. 2007). It's reasonable to believe that the mutation at S140 perturbs the protonation state of E107. Furthermore, the positive band at 1759 cm^{-1} also indicates that there could be some acidic residues other than E107 have also been perturbed by S140T mutant. Based on the topology of subunit I of cytochrome *bd* oxidase, E99 could be one of the most possible candidates.

As the last chapter in this trilogy of proton channel investigation, two highly conserved non-acidic residues located in the membrane have been studied by FTIR spectroscopy. One of them, S140 may participate in facilitating protons transportation inside the membrane besides stabilizing the heme b_{595} / heme *d* binuclear active center. Further investigations with different approaches (i.e. electrometric measurement) might be helpful to reveal more details about this unique site of cytochrome *bd* oxidase in proton uptake from cytoplasm.

5.5 Figures and tables:

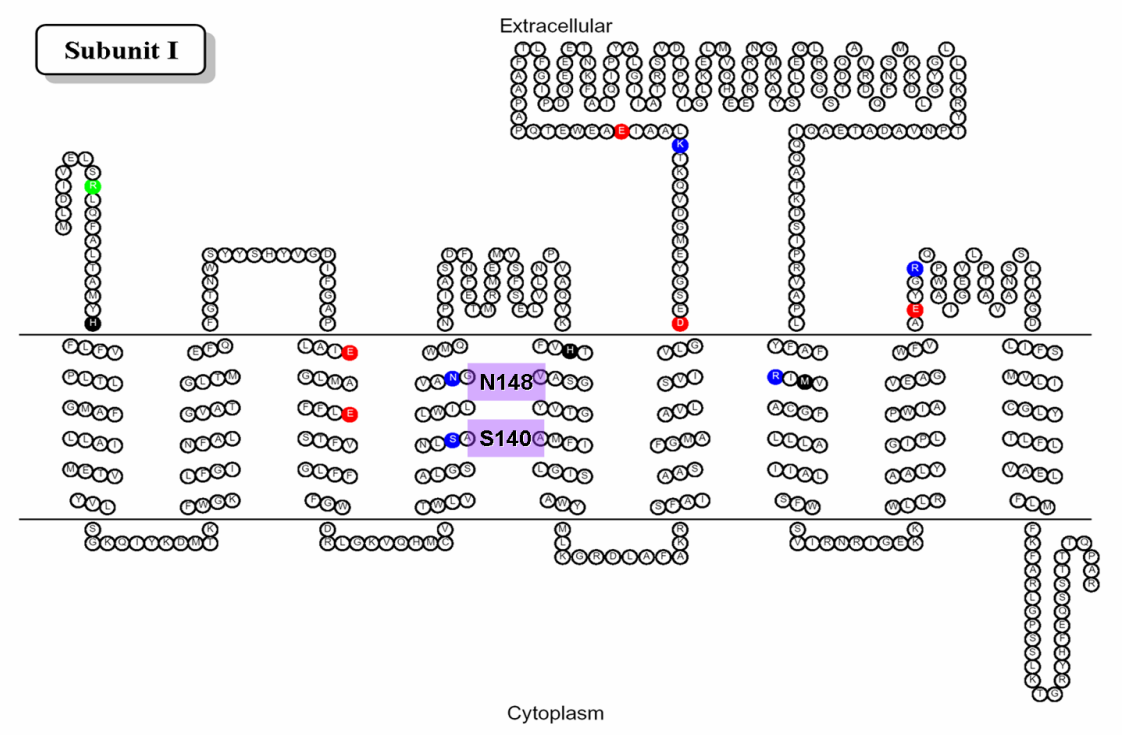

Figure 5.1 Membrane topology model of subunit I of cytochrome *bd* oxidase from *E. coli* with S140 and N148 marked out.

Table 5.1 Summary of the properties of the cytochrome *bd* S140 and N148 mutants

	Complementation of aerobic growth	Heme content (UV-Vis spectra)	UQ_1H_2 oxidase activity[a]	TMPD oxidase activity[b]
Wild type	Yes	All hemes present	100%	100%
S140A	No	Little heme *d*/heme b_{595}	0%	0%
S140L	No	Near wild type	0%	42%
S140T	No	Near wild type	0%	47%
S140H	No	No heme d/heme b_{595}	0%	0%
S140C	No	Little heme d/heme b_{595}	0%	0%
N148A	Yes	All hemes present	100%	100%
N148D	Yes	All hemes present	100%	100%

[a] 100% of ubiquinol-1 oxidase activity corresponds to a turnover of about $1450e^{-1}$/sec.
[b] 100% of TMPD oxidase activity corresponds to a turnover of about $100e^{-1}$/sec.

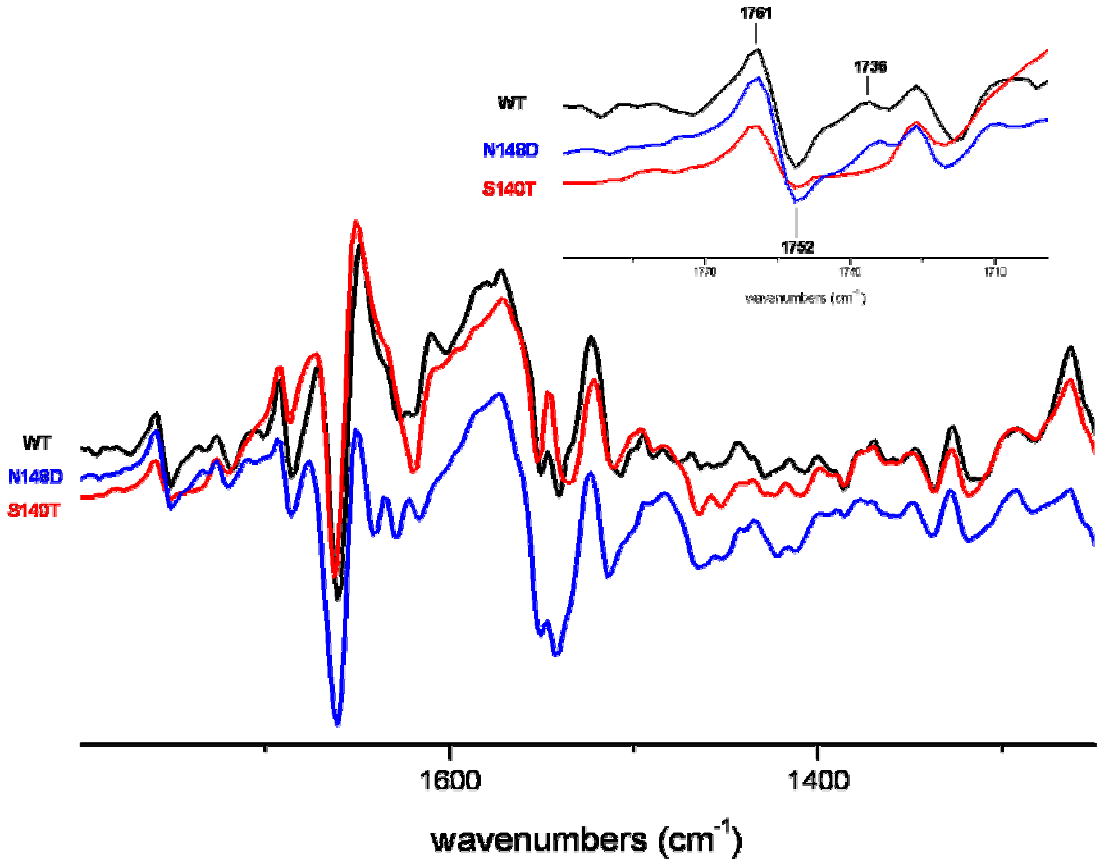

Figure 5.2 Oxidized-*minus*-reduced FTIR difference spectra of wild type, S140T and N148D.
Both wild type and S140T mutant were grown anaerobically, while N148D was from aerobic culture. (Inset) An enlarged look into the region above 1700 cm^{-1}.

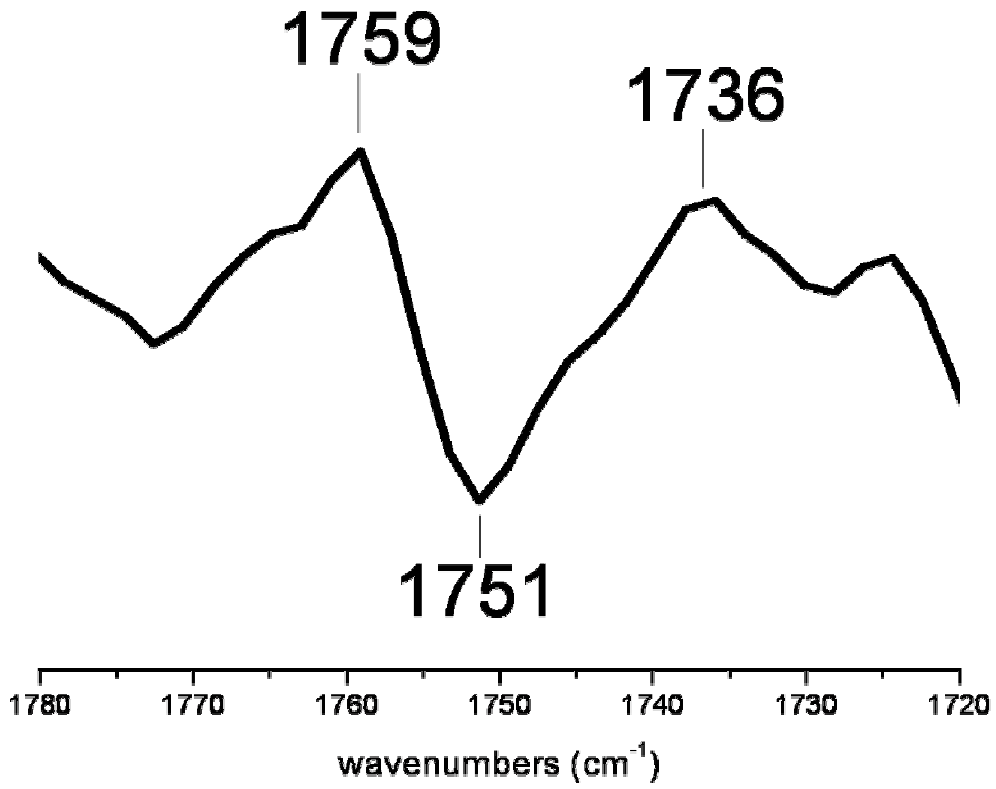

Figure 5.3 Wild type-*minus*-S140T double difference spectrum.
The negative band at 1751 cm^{-1} and positive band at 1736 cm^{-1} are assigned to perturbed E107, while 1759 cm^{-1} may come from E99.

CHAPTER 6: PROBING A POTENTIAL QUINOL BINDING SITE BY FTIR SPECTROSCOPIC STUDY

6.1 Introduction:

Unlike the majority of the cytochrome oxidases that oxidized cytochrome *c*, the terminal oxidases in *E. coli*, cytochrome bo_3 and cytochrome *bd* oxidase, accept electrons directly from the quinol pool in the membrane. Under different growth conditions, different quinine types are found in the membrane of *E. coli*. Ubiquinone-8 is predominately found under aerobic growing conditions, while demethylmenaquinone-8 and menaquinone-8 are observed at reduced oxygen levels (Hollander 1976; Bentley and Meganathan 1987). With the help of crystal structure, combined with site-directed mutagenesis work, several residues in cytochrome bo_3 have been identified to be involved in ubiquinone binding. Among them, the acidic residues serve important roles, especially D75, whose protonation has been shown to be directly involved in quinol binding (Hellwig, Barquera et al. 2001).

Compared to the quinone binding work in cytochrome bo_3, relatively little progress has been made in cytochrome *bd*, largely due to the lack of a crystal structure. As mentioned in previous chapters, limited proteolysis demonstrated that the Q-loop between helix VI and VII is somehow critical in quinol binding and oxidation (Lorence, Carter et al. 1988). Following the successful path of cytochrome bo_3, several highly conserved acidic amino acids have been found in or near the Q-loop from over 1000 sequences, including E257 (**Figure 6.1**) and D239.

FTIR difference spectroscopy of the wild type cytochrome *bd* has previously implicated at least one acidic residue as being involved in quinone binding and more than one acidic residue was shown to be perturbed upon reducing the hemes (Zhang, Oettmeier et al. 2002; Yamazaki, Kandori et al. 1999). This approach is extended in the current work reported in this chapter. FTIR difference spectroscopy of the E257A mutant oxidase shows that E257 in the wild type oxidase is not involved in the protonated/deprotonated change due to the oxidation/reduction of the metal centers. By contrast, E257A mutant appears to be located at or near the quinone binding site, as previously proposed (Mogi, Akimoto et al. 2006).

6.2 Materials and methods:

6.2.1 Strains and plasmids:

E. coli strain GO105 (*cyd*AB::*kan*, *cyo*, *rec*A), which lacks both cytochrome bo_3 and cytochrome *bd* quinol oxidases (Kaysser, Ghaim et al. 1995) was used as the host strain for expressing both the wild type and mutant cytochrome *bd* on a plasmid. To obtain wild type cytochrome *bd*, plasmid pTK1 (Zuberi 1993) was introduced to the strain. This plasmid is a derivative of pBR322 and contains the whole operon of wild type *bd* as well as ampicillin resistance gene for selection. Mutants of cytochrome *bd* were also expressed using this same plasmid system.

6.2.2 Site-directed mutagenesis using Quik-Change method:

The Stratagene Quik-Change mutagenesis kit was used to construct mutants. Plasmid pTK1 was used as template. The oligonucleotide primers were synthesized by

Roy J. Carver Biotechnology Center (Urbana, IL) with melting temperature around 80 °C based on the Stratagene formula, and were diluted in pure water to 100 ng/μL for Quik-Change reaction. Thermocyclings were conducted on PTC-100 Programmable Thermal Controller (MJ Research Inc.). The protocol was as follows: 95 °C for 1 min, 1 cycle; 18 cycles of 95 °C for 1 min, 54 °C for 1 min, and 68 °C for 8 min; then 68 °C for 7 min, 1 cycle. The samples were digested with 1 μL *Dpn*I for 3 ~ 4 hours. All mutants were confirmed by DNA sequencing.

6.2.3 Complementation test for the mutant cytochrome *bd*:

The complementation test was carried out as follows: Plasmid DNA from confirmed mutants was used to transform GO105 using TSS method (Chung, Niemela et al. 1989). Cells were grown anaerobically for selection of ampicillin and kanamycin resistance. The strains exhibiting both amplicillin and kanamycin resistance were restreaked to obtain single colonies, and were grown on M63 (Cohen and Rickenberg 1956) minimal plates supplemented with 0.3 % lactate and 0.3 % succinate. Also added were 100 μg/mL ampicillin and 50 μg/mL kanamycin to maintain the plasmid and the strain. Complementation was defined by aerobic growth within 48 ~ 72 hours of incubation at 37 °C.

6.2.4 Cell growth and protein sample preparation:

Large scale cell growth of strains that grow aerobically (i.e. expressing wild type or E107D mutant) was carried out in 24 2-liter flasks shaking at 220 rpm 37 °C using two Innova 4330 incubator shakers (New Brunswick Scientific). Strains expressing wild type

and those inactive mutants, which could not grow aerobically, were grown at the Fermentation Facility at the University of Illinois, or the OSU Fermentation Facility at 37 °C, pH 7, in a 20-liter fermenter using LB containing 100 μg/mL Amp, 50 μg/mL Kan, and 0.3 % glucose. Both wild type and mutant cytochrome *bd* oxidases were purified from the membrane of GO105/pTK1 as described previously (Miller and Gennis 1986), with the modification that the hydroxyapatite column was omitted. Fractions were collected from the Fast-Flow Sepharose DEAE column with an A_{412}/A_{280} ratio greater than 0.5. The pooled fractions were concentrated using an Amicon concentrator with a 50 kDa molecular weight cut-off filter and then dialyzed three times against 50 mM sodium phosphate buffer, pH 7.8, containing 5 mM EDTA, 0.05% N-lauroylsarcosine. Both wild type and mutant cytochrome *bd* samples were then examined, using the same dialysis buffer for appropriate dilution unless specified otherwise.

6.2.5 Ubiquinol-1 and TMPD oxidase activity assay:

Cytochrome *bd* wild type and mutants were assayed both in isolated membranes, in which there is no other quinol oxidase, and with the purified enzyme. For membranes, samples were homogenized in 25 mM Tris HCl, 1 mM EDTA disodium salt, pH 7.5. Purified protein samples were dialyzed against 50 mM NaPi buffer, pH 7.8, containing 5 mM EDTA disodium salt and 0.05 % N-lauroyl sarcosine. Various dilutions of either the homogenized membrane samples or pure protein samples were added to 1.8 mL of the respective buffer containing either 2 mM dithiothreitol or 4 mM ascorbate that had been equilibrated to 37 °C in a Clark-type oxygen electrode (Yellow Springs Instrument CO.). A baseline was taken and the reaction was initiated by addition of ubiquinol-1 (kindly

provided by Hoffman-LaRoche) or TMPD to a final concentration of 245 μM and 1 mM, respectively. Activities were determined assuming a value of 237 μM O_2 for air-saturated buffer at 37 °C.

6.2.6 Heme analysis:

The heme *b* contents of both wild type and mutant purified cytochrome *bd* were measured by the pyridine hemochromogen assay, using an extinction coefficient for the wavelength pair 556.5−540 nm = 23.98 mM^{-1} cm^{-1} (Berry and Trumpower 1987). The heme *d* content was determined from the reduced minus "as isolated" difference spectrum with the $\Delta\varepsilon_{628-607\ nm}$ = 10.8 mM^{-1} cm^{-1} (Borisov, Arutyunyan et al. 1999). The concentration of the wild type cytochrome *bd* was determined from the reduced minus as isolated difference spectra, using $\Delta\varepsilon_{560-580\ nm}$ = 21.4 mM^{-1} cm^{-1} (Tsubaki, Hori et al. 1995). Since the "as isolated" enzyme contains varying amounts of ferrous heme *d*-oxy complex and oxoferryl heme *d* species, the heme *d* content was also determined by the absolute spectrum of the fully reduced enzyme, using the extinction coefficient $\Delta\varepsilon_{628\text{-}670\ nm}$ = 25 mM^{-1} cm^{-1} (Borisov, Arutyunyan et al. 1999).

6.2.7 UV-Vis spectroscopic measurements:

All the absorbance spectra in the UV-Vis region were obtained with a DW2000 spectrophotometer (Aminco) using a 1 cm pathlength cuvette. The series of absorbance spectra for mid-point potential measurements were taken using UV-2101PC scanning spectrophotometer (Shimadzu).

6.2.8 Electrochemistry and FTIR difference spectroscopy:

FTIR difference spectra recorded at 5 °C as a function of applied potential with BioRad (now Varian, Inc.) FTS-6000 FTIR. Each FTIR difference spectrum consisted of 256 intereferograms at 4 cm^{-1} resolution and approximately 20 spectra were averaged to give better signal to noise. Triangular apodization is used for Fourier transformation. Equilibration at the applied potential is achieved in less than 10 min. FTIR spectra monitored until no change detected. Experimental conditions for *bd* quinol oxidase and electrochemical cell set-up is described in detail previously (Mansfield and Wiggins 1990; Mantele 1996). A mixture of 13 different mediators added to 40 μM final concentration 1,1'-dicarboxylferrocene, dimethylparaphenylendiamine (DMPPD), ferricyanide, quinhydrone, tetramethylparaphenylendiamine (TMPPD), tetrachlorobenzoquinone, 2,6-dichlorophenol indophenol, ruthenium hexamine chloride, 1,2-naphthoquinone, menadione, 2-hydroxy-1,4-naphthoquinone, benzyl viologen, methyl viologen.

6.2.9 Sequence analysis and topology model generation:

The homologous sequences of subunit I of cytochrome *bd* were kindly provided by Dr. James Hemp in Grennis lab, Urbana, University of Illinois. The sequence alignment was performed by BioEdit Sequence Alignment Editor Ver.7.0.9.0 (Hall 1999). The topology model of subunit I was generated by membrane topology prediction tool TMHMM 2.0 program (http://www.cbs.dtu.dk/services/TMHMM/). The graph was created by TOPO2 program based on the TMHMM result (http://www.sacs.ucsf.edu/TOPO-run/wtopo.pl).

6.3 Results:

6.3.1 Complementation test, ubiquinol-1/TMPD activity assay, heme analysis and UV-Vis spectra:

Like most of other mutants at critical sites, the E257A mutant cytochrome *bd* oxidase does not support the aerobic growth on minimal plate. It also lacks ubiquinol oxidase activity but retains significant TMPD oxidase activity (**Table 6.1**). Spectroscopically, E257A mutant is similar to the wild type enzyme, indicating no perturbation of the heme content.

6.3.2 FTIR spectra of wild type and E257A mutant:

Data from the Mogi group (Mogi, Akimoto et al. 2006) indicate that E257 is at or near the ubiquinol binding site, as one might predict based on its location in the Q-loop. For this purpose, the E257A mutant was examined by FTIR spectroscopy. The redox difference spectrum, shown in **Figure 6.2** is very similar to that of the anaerobically grown wild type oxidase in the 1730 cm^{-1} – 1750 cm^{-1} region (Zhang, Oettmeier et al. 2002). Hence, it is concluded that E257 is not contributing to the redox-coupled spectroscopic changes. Either E257 is not protonated (i.e., not absorbing in the 1750 cm^{-1} region of the spectrum) or, if it is protonated, its environment is not altered by the redox changes.

Previously reported site-directed mutagenesis of E257 has implicated this residue as being at or near the quinol binding site (Mogi, Akimoto et al. 2006). The FTIR redox difference spectrum (**Figure 6.2**) shows that the E257A mutant oxidase retains the bound quinone, which is primarily menaquinone. This is demonstrated by the presence of the

absorption band at 1633 cm^{-1}, which is assigned to the C=O stretch of a bound quinone (Zhang, Oettmeier et al. 2002). Another band indicating bound quinone is at 1611 cm^{-1} is present in the E257A mutant spectrum, which is due to C=C mode (Zhang, Oettmeier et al. 2002). The 1635 cm^{-1} and 1611 cm^{-1} bands are shifted in the E257A mutant spectrum to 1633 cm^{-1} and 1614 cm^{-1}, respectively. Both these shifts may result from a perturbation of the bound quinone. With the wild type cytochrome *bd*, the 1635 cm^{-1} band is absent when the enzyme is bound to the inhibitor aurachin D (Zhang, Oettmeier et al. 2002). Presumably, the inhibitor either displaces or alters the binding of the quinone to the protein. The same observation has been made with aurachin C 1-10, which is the N-hydroxy derivative of aurachin D and is somewhat less potent inhibitors of cytochrome *bd* (Miyoshi, Takegami et al. 1999; Meunier, Madgwick et al. 1995). **Figure 6.2** shows the redox difference spectra of the wild type and the E257A mutant oxidase, in the presence and absence of aurachin C 1-10. The 1633 cm^{-1} band is clearly observed in the redox FTIR difference spectrum of the E257A mutant oxidase. This indicates that under the conditions of this experiment, the quinine (mainly menaquinone) remains bound to the enzyme in the presence of aurachin C 1-10. Under conditions the equivalent band in the wild type oxidase is diminished in magnitude, suggesting partial displacement of the bound quinone. It is concluded that the either binding of aurachin C 1-10 to the E257A mutant oxidase is altered or the effect of the inhibitor binding on the bound quinone is altered by the E257A mutation.

6.4 Discussion and conclusions:

Mutations in E257 (E257A and E257Q) have been examined by Japanese group (Mogi, Akimoto et al. 2006) and it was concluded that this residue is involved in the binding of the substrate ubiquinol. These mutations each result in about a 3 to 4-fold increase in the K_m of ubiquinol-1. E257A had a V_{max} that was about 30% of the wild type value, whereas E257Q had a slightly higher V_{max}.

In the current work, the E257A mutant was further examined. Under the conditions of our assay, the E257A mutant is inactive with ubiquinol-1 as the substrate, and the heme content is normal. The FTIR redox difference spectrum (**Figure 6.2**) is similar to that of the wild type enzyme isolated from anaerobically grown cells. In particular, in the region around 1750 cm^{-1}, the similarity indicates that E257 is not contributing to the spectroscopic perturbations due to the oxidation/reduction of the metal centers. Hence, E257 can be ruled out as the acidic residue whose protonation state is altered depending on whether ubiquinone or menaquinone is bound to the protein.

In addition, the FTIR redox difference spectrum of the E257A mutant shows that quinone remains bound to the protein. Hence, the loss of function is not due to the elimination of the bound quinone (primarily menaquinone). The data from Mogi et al show that E257 is not essential for the interaction of the enzyme with ubiquinol-1, although mutants do increase the K_m by several folds. In the experiments reported here, the presence of endogenous quinone, mostly menaquinone-8, is reported. The E257A mutant may alter the way in which the quinone binds to the protein and reduce the rate of catalysis. Under our assay conditions (100 μM ubiquinol-1) we have virtually no oxidase activity. Using the values reported for the V_{max} and K_m by Mogi et al (2006) we would

expect about 5% of the oxidase activity compared to the wild type. The reason for the discrepancy, which may be insignificant, will require further investigation.

Figure 6.2 also shows the FTIR redox difference spectrum of the E257A mutant in the presence of aurachin C 1-10. The 1633 cm^{-1} band is not eliminated by aurachin C 1-10, indicating that either aurachin C 1-10 is not binding under the conditions of the experiment or the binding is perturbed in such a way that the bound quinone is not displaced. With the wild type oxidase, aurachin C 1-10 under the same conditions results in a spectrum in which the 1633 cm^{-1} band is not present (**Figure 6.2**). Mogi et al have shown that the binding of aurachin D to the E257A mutant is not abolished but is perturbed and the data in **Figure 6.2** are consistent with this result. Hence, E257 may retain its candidacy as part of the quinol binding motif in cytochrome *bd* oxidase.

6.5 Figures and tables:

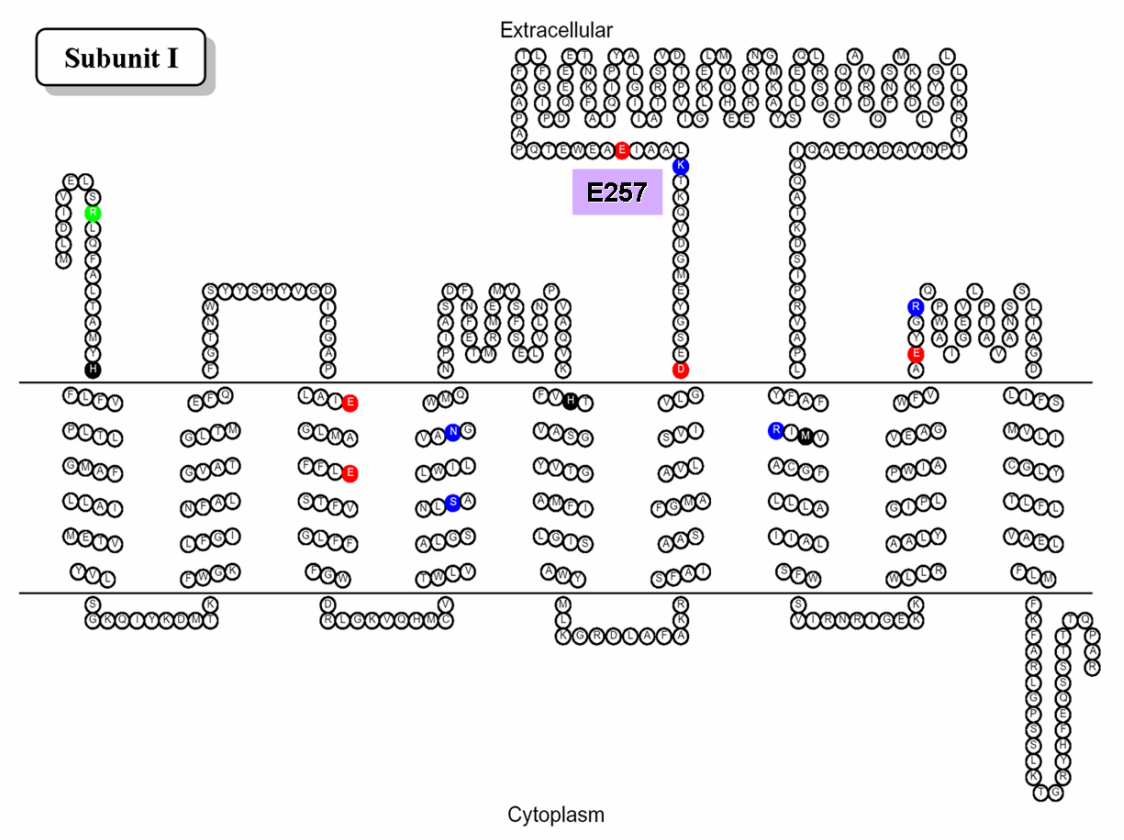

Figure 6.1 Membrane topology model of subunit I of cytochrome *bd* oxidase from *E. coli* with E257 marked out.

Table 6.1 Summary of the properties of the cytochrome *bd* E257 mutants

	Complementation of aerobic growth	Heme content (UV-Vis spectra)	UQ_1H_2 oxidase activity[a]	TMPD oxidase activity[b]
Wild type	Yes	All heme present	100%	100%
E257A	No	All heme present	0%	50%
E257Q	No	All heme present	0%	72%

[a] 100% of ubiquinol-1 oxidase activity corresponds to a turnover of about $1450e^{-1}$/sec.
[b] 100% of TMPD oxidase activity corresponds to a turnover of about $100e^{-1}$/sec.

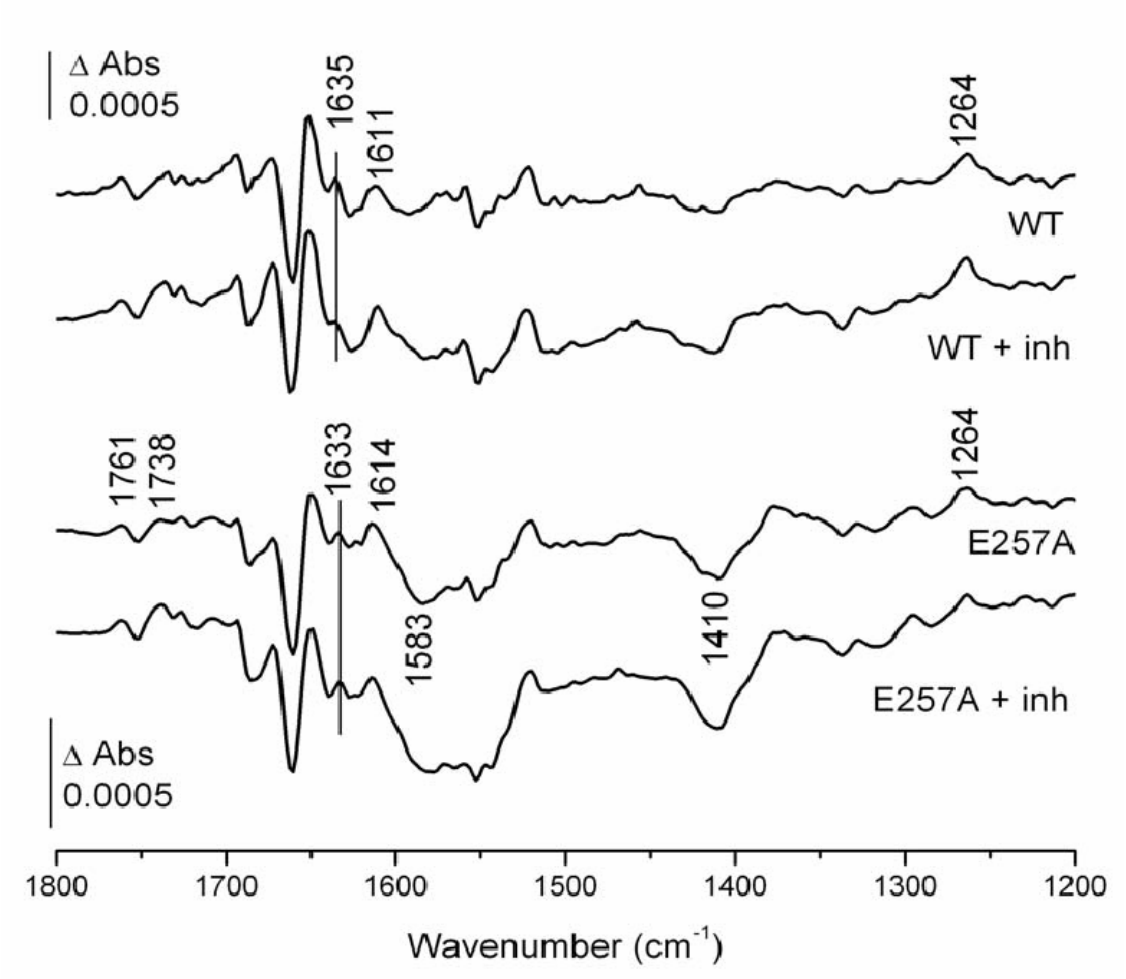

Figure 6.2 Oxidized-*mius*-reduced FTIR difference spectra of the wild type and E257A mutant of cytochrome *bd* (+708 mV to -292 mV vs. SHE) with and without the inhibitor aurachin C 1-10.

The 1635 cm^{-1} band in the spectrum of the wild type oxidase is from the bound quinone. This is shifted to 1633 cm-1 in the mutant, showing that the quinone remains bound to the E257A mutant oxidase, though there is a perturbation of this C=O mode.. In the presence of aurachin C 1-10, the band is significantly reduced in intensity, in the wild type oxidase, but is not altered in the E257A mutant. Hence, aurachin 1-10 does not displace the bound quinone. The strong negative features at about 1583 and 1410 cm^{-1} are often observed with mutants of cytochrome *bd*.

CHAPTER 7:SITE-DIRECTED MUTATION OF AN HIGHLY CONSERVED ACIDIC RESIDUE PERTURBS QUINONE BINDING AND HEME B_{595} PROPERTIES

7.1 Introduction:

The FTIR study reported in the last chapter confirmed the importance of E257 in the quinone binding in cytochrome *bd* oxidase. Although it may not participate the quinol / enzyme interaction directly as the binding site, E257 is critical to maintain the binding pocket functional. Hence, the search for the quinol binding site in cytochrome *bd* oxidase is still open to other candidates. As mentioned previously, the hydrophilic Q-loop between helix VI and VII is involved in quinol binding and oxidation (Lorence, Carter et al. 1988). Other than E257, which is located right in the Q-loop, D239, another strictly conserved acidic residue, is also close to this region (**Figure 7.1**). Sitting at the interface of membrane and periplasm, this amino acid from the N-terminus of Q-loop could be an even better binding site for the quinol from the "quinol pool" in the membrane.

In this chapter, two mutations have been made at D239 site, D239A and D239N. While losing their ubiquinol oxidase activity as expected, both of them exhibited unusually high TMPD oxidase activity. Redox titration demonstrated that one of the mutant, D239N, perturbed the midpoint redox potential (E_m) of all the heme groups in a manner of making the E_m of heme b_{595} the highest among three. Instead of FTIR, Stopped-Flow was introduced in this study to help us get a better vision in terms of the role of heme b_{595} in rapid enzyme turnover as well as quinol binding. Based on the data, a

plausible new intermediate has been introduced in the modified catalysis model of cytochrome *bd* oxidase (Yang, Borisov et al. 2008).

7.2 Materials and methods:

7.2.1 Strains and plasmids:

E. coli strain GO105 (*cyd*AB::*kan*, *cyo*, *rec*A), which lacks both cytochrome bo_3 and cytochrome *bd* quinol oxidases (Kaysser, Ghaim et al. 1995) was used as the host strain for expressing both the wild type and mutant cytochrome *bd* on a plasmid. To obtain wild type cytochrome *bd*, plasmid pTK1 (Zuberi 1993) was introduced to the strain. This plasmid is a derivative of pBR322 and contains the whole operon of wild type *bd* as well as ampicillin resistance gene for selection. Mutants of cytochrome *bd* were also expressed using this same plasmid system.

7.2.2 Site-directed mutagenesis using Quik-Change method:

The Stratagene Quik-Change mutagenesis kit was used to construct mutants. Plasmid pTK1 was used as template. The oligonucleotide primers were synthesized by Roy J. Carver Biotechnology Center (Urbana, IL) with melting temperature around 80 °C based on the Stratagene formula, and were diluted in pure water to 100 ng/μL for Quik-Change reaction. Thermocyclings were conducted on PTC-100 Programmable Thermal Controller (MJ Research Inc.). The protocol was as follows: 95 °C for 1 min, 1 cycle; 18 cycles of 95 °C for 1 min, 54 °C for 1 min, and 68 °C for 8 min; then 68 °C for 7 min, 1 cycle. The samples were digested with 1 μL *Dpn*I for 3 ~ 4 hours. All mutants were confirmed by DNA sequencing.

7.2.3 Complementation test for the mutant cytochrome *bd*:

The complementation test was carried out as follows: Plasmid DNA from confirmed mutants was used to transform GO105 using TSS method (Chung, Niemela et al. 1989). Cells were grown anaerobically for selection of ampicillin and kanamycin resistance. The strains exhibiting both amplicillin and kanamycin resistance were restreaked to obtain single colonies, and were grown on M63 (Cohen and Rickenberg 1956) minimal plates supplemented with 0.3 % lactate and 0.3 % succinate. Also added were 100 μg/mL ampicillin and 50 μg/mL kanamycin to maintain the plasmid and the strain. Complementation was defined by aerobic growth within 48 ~ 72 hours of incubation at 37 °C.

7.2.4 Cell growth and protein sample preparation:

Large scale cell growth of strains that grow aerobically (i.e. expressing wild type or E107D mutant) was carried out in 24 2-liter flasks shaking at 220 rpm 37 °C using two Innova 4330 incubator shakers (New Brunswick Scientific). Strains expressing wild type and those inactive mutants, which could not grow aerobically, were grown at the Fermentation Facility at the University of Illinois, or the OSU Fermentation Facility at 37 °C, pH 7, in a 20-liter fermenter using LB containing 100 μg/mL Amp, 50 μg/mL Kan, and 0.3 % glucose. Both wild type and mutant cytochrome *bd* oxidases were purified from the membrane of GO105/pTK1 as described previously (Miller and Gennis 1986), with the modification that the hydroxyapatite column was omitted. Fractions were collected from the Fast-Flow Sepharose DEAE column with an A412/A280 ratio greater than 0.5. The pooled fractions were concentrated using an Amicon concentrator with a 50

kDa molecular weight cut-off filter and then dialyzed three times against 50 mM sodium phosphate buffer, pH 7.8, containing 5 mM EDTA, 0.05% N-lauroylsarcosine. Both wild type and mutant cytochrome *bd* samples were then examined, using the same dialysis buffer for appropriate dilution unless specified otherwise.

7.2.5 Ubiquinol-1 and TMPD oxidase activity assay:

Cytochrome *bd* wild type and mutants were assayed both in isolated membranes, in which there is no other quinol oxidase, and with the purified enzyme. For membranes, samples were homogenized in 25 mM Tris HCl, 1 mM EDTA disodium salt, pH 7.5. Purified protein samples were dialyzed against 50 mM NaPi buffer, pH 7.8, containing 5 mM EDTA disodium salt and 0.05 % N-lauroyl sarcosine. Various dilutions of either the homogenized membrane samples or pure protein samples were added to 1.8 mL of the respective buffer containing either 2 mM dithiothreitol or 4 mM ascorbate that had been equilibrated to 37 °C in a Clark-type oxygen electrode (Yellow Springs Instrument CO.). A baseline was taken and the reaction was initiated by addition of ubiquinol-1 (kindly provided by Hoffman-LaRoche) or TMPD to a final concentration of 245 μM and 1 mM, respectively. Activities were determined assuming a value of 237 μM O_2 for air-saturated buffer at 37 °C.

7.2.6 Heme analysis:

The heme *b* contents of both wild type and mutant purified cytochrome *bd* were measured by the pyridine hemochromogen assay, using an extinction coefficient for the wavelength pair 556.5 − 540 nm = 23.98 mM^{-1} cm^{-1} (Berry and Trumpower 1987). The

heme *d* content was determined from the reduced minus "as isolated" difference spectrum with the $\Delta\varepsilon_{628-607\ nm}$ = 10.8 mM^{-1} cm^{-1} (Borisov, Arutyunyan et al. 1999). The concentration of the wild type cytochrome *bd* was determined from the reduced minus as isolated difference spectra, using $\Delta\varepsilon_{560-580\ nm}$ = 21.4 mM^{-1} cm^{-1} (Tsubaki, Hori et al. 1995). Since the "as isolated" enzyme contains varying amounts of ferrous heme *d*-oxy complex and oxoferryl heme *d* species, the heme *d* content was also determined by the absolute spectrum of the fully reduced enzyme, using the extinction coefficient $\Delta\varepsilon_{628-670\ nm}$ = 25 mM^{-1} cm^{-1} (Borisov, Arutyunyan et al. 1999).

7.2.7 UV-Vis spectroscopic measurements:

All the absorbance spectra in the UV-Vis region were obtained with a DW2000 spectrophotometer (Aminco) using a 1 cm pathlength cuvette. The series of absorbance spectra for mid-point potential measurements were taken using UV-2101PC scanning spectrophotometer (Shimadzu).

7.2.8 Redox titration of wild type cytochrome *bd* and D239 mutants:

Both wild type and D239 mutant cytochrome *bd* samples were prepared as described in above. The redox titration was carried out using the ultra-thin layer spectroelectrochemical cell for UV-Vis spectroscopy as previously described (Mansfield and Wiggins 1990; Mantele 1996) and kindly provided by Dr. Werner Mantele (University of Frankfurt, Germany). The gold-grid working electrode was chemically modified by 2 mM cysteamine solution as reported before (Hellwig, Behr et al. 1998) to a total concentration of 40 μM each. At this concentration and with the pathlength below

10 μm, no spectral contribution from the mediators in the visble region could be detected in the control experiment with samples lacking the protein. As a supporting electrolyte, 100 mM KCl was added. Approximately 10 ~ 15 μL of protein samples were added to fill the spectroelectrochemical cell. Absorbance changes were monitored at multiple wavelengths using a UVPC-2101 spectrophotometer (Shimadzu). The equilibration time took was less than 10 min under the conditions as described above. Redox titrations were performed by stepwise setting the potential and recording the spectrum after sufficient equilibration. All measurements were obtained at 5 °C and were repeated at least twice. The absorbance change at 628 nm was used for generating the heme *d* titration curve, both 440 nm and 595 nm were used for generating the heme b_{595} titration curve, and both 428 nm and 560 nm were used for generating the heme b_{558} tiration curve. The midpoint potentials (Em) were obtained by interactive fitting to a Nernst equation using the program offered by Origin (Microcal).

7.2.9 Stopped-Flow spectroscopic and kinetic measurements:

All the work was performed at 20 ˚C using an Applied Photophysics model SX with a photodiode array detector as well as single-wavelength detection. The flow system was flushed thoroughly with Argon-saturated buffer (50 mM sodium phosphate, 5 mM EDTA and 0.05% N-lauroylsarcosine, pH 7.8) before the experiments. The whole system was kept anaerobic by flowing Argon during the experiments. The mixing ratio of the two solutions being mixed was all 1:1. For all experiments reported, at least three runs were performed for each time scale ranging from 2 s to 1 min, and 1600 spectra were

collected from 300 nm to 1200 nm. All concentrations reported are the initial concentrations before mixing.

Since each species of heme *d* in the catalytic cycle of cytochrome *bd* have been characterized optically, the formation and the decay of the heme *d* species can be monitored spectrophotometrically. The reduction by ubiquinol of the "as isolated" enzyme was carried out by generated the "as isolated" enzyme *in situ*. This was done by typically starting with one solution containing 5 μM enzymes with an excess concentration of 200 μM ubiquinone and 6 mM DTT in Argon-saturated buffer (50 mM sodium phosphate, 5 mM EDTA disodium salt and 0.05% N-lauroyl sarcosine, pH 7.8). This solution was rapidly mixed with an equal volume of a solution containing approximately 5 μM O_2 in the same buffer. The conditions were adjusted so that the O_2 rapidly oxidized the enzyme which was then, in turn, reduced by the excess ubiquinol-1 that was present. The oxidation reaction was too fast to resolve but most of the reduction was monitored to obtain rate constants. Spectroscopic analysis of the product of the reaction of O_2 with the reduced enzyme showed that it contained approximately 80% oxoferryl and 20% ferrous-oxy complex.

To investigate the inhibition of D239N mutant cytochrome *bd* by aurachin C 1-10, 5 μM enzymes was incubated with 1 μM aurachin C 1-10 for 10 minutes in Argon-saturated buffer (50 mM sodium phosphate, 5 mM EDTA and 0.05 % N-lauroyl sarcosine, pH 7.8) before mixing with oxygen-limited buffer.

7.2.10 Data analysis:

The data were first analyzed with the use of Pro-Kineticist software package "ProK for PC" (Applied Photophysics) and selected data were imported into Origin 7 (Microcal) for further analysis and preparation of the figures.

7.2.11 Sequence analysis and topology model generation:

The homologous sequences of subunit I of cytochrome *bd* were kindly provided by Dr. James Hemp in Grennis lab, Urbana, University of Illinois. The sequence alignment was performed by BioEdit Sequence Alignment Editor Ver.7.0.9.0 (Hall 1999). The topology model of subunit I was generated by membrane topology prediction tool TMHMM 2.0 program (http://www.cbs.dtu.dk/services/TMHMM/). The graph was created by TOPO2 program based on the TMHMM result (http://www.sacs.ucsf.edu/TOPO-run/wtopo.pl).

7.3 Results:

7.3.1 Complementation test, heme analysis and ubiquinol-1/TMPD oxidase activity:

D239 was replaced by both alanine and by asparagine (**Table 7.1**). Neither the D239A nor D239N mutants support the aerobic cell growth. The UV-visible spectra of both purified mutants are similar to the wild type, indicating no impact on the heme content. This is double confirmed by heme analysis. Both D239A and D239N show no ubiquinol oxidase activity. Considering the location of D239, which is near the Q-loop interface with the membrane (**Figure 7.1**), it suggests a plausible perturbation at the ubiquinol binding site. Despite losing ubiquinol oxidase activity, D239 mutants have

better TMPD oxidase activity, especially D239A, which is three times more active than wild type. This indicates an intact and fully, if not better, functional heme b_{595} and heme *d* bi-nuclear center.

7.3.2 Electrochemical measurement of the heme mid-point potentials:

The midpoint potentials of three hemes were determined for the D239N mutant and compared to those of the wild type. The results show a large decrease in the midpoint potential heme *d* from the wild type value of 240 mV (vs. NHE) to 100 mV, which also leads to a relative higher midpoint potential heme b_{595} value of 154 mV compared to that of heme *d* from the D239N mutant (**Table 7.1**).

7.3.3 Fast kinetics of D239N mutant by Stopped-Flow:

Figure 7.2 shows the time course of D239N mutant hemes *b* and heme *d* absorbance changes in 2 seconds as well as those of wild type cytochorme *bd*. An extremely slow tail of D239N hemes b oxidation was observed in the first 0.7 second (**Figure 7.2, right panel**), indicating the perturbation of quinol binding site caused by this mutation. The D239N mutant also showed slow re-reduction of hemes b (**Figure 7.2, right panel**) and heme *d* (**Figure 7.2, left panel**), which support our interpretation as well.

A positive control has been done by adding aurachin C 1-10, a strong quinol binding site inhibitor, to fully reduced wild type cytochrome *bd* enzyme. **Figure 7.3** shows the comparison between the control and D239N mutant. A 10-minute incubation with aurachin C 1-10 before mixing resulted in slow re-reduction of both hemes *b*

(**Figure 7.3, right panel, black**) and heme *d* (**Figure 7.3, left panel, black**). No slow oxidation of hemes *b* similar to the D239N mutant (**Figure 7.3, right panel, red**) has been observed in the control. Moreover, the heme *d* in the control showed a slightly faster re-reduction rate than that of D239N mutant (**Figure 7.3, left panel, red**). These differences between D239N and control indicate that more damage on the catalytic cycle has been caused by the mutant other than just blocking the quinol binding site.

Figure 7.4 shows the first spectrum after mixing fully reduced D239N with oxygen taken at 0.6 ms. The peak at 562 nm and 628 nm as well as the shoulder at 680 nm indicate a mixture of reduced hemes *b*, reduced heme *d* and oxoferryl heme *d*. The development of optical changes at 650 nm during the first 10 ms of the reaction (**Figure 7.5**) also indicates the formation of ferrous oxy (A) complex. Thus, the mixture right after mixing could consists of oxoferryl (F), ferrous oxy (A) and reduced (R) enzymes.

7.4 Discussion and conclusions:

D239 and Quinol Binding Site. Although D239 is not totally conserved in over 1000 sequences we have examined, this aspartate is completely conserved within the family of *bd*-type oxidases with the "long Q-loop". This large hydrophilic loop between transmembrane Helix VI and VII in the periplasmic side has been shown to play an important role in quinol binding. The highly conserved D239 is located at the N-terminus of the Q-loop, which makes it a potential candidate of quinol binding site. Both the D239A and D239N mutants lack ubiquinol oxidase activity, but exhibit high TMPD oxidase activity. During further investigation of D239N mutant oxidase by oxidation / re-reduction assay, both slow oxidation and re-reduction of hemes b are observed, indicating

a perturbation at the quinol binding site by the mutation. However, due to the lack of crystal structure of cytochrome *bd* oxidase, whether D239 is the quinol binding site or just part of it requires further investigation.

Role of Heme b_{595}. The role of heme b_{595} in the catalysis is not fully understood, but there is evidence that it may form a bi-nuclear center together with heme *d*, to facilitate the oxygen reduction. Based on current thinking of the electron transfer pathway in cytochrome *bd*, electrons provided by quinol enter the enzyme by first passing heme b_{558}, then go through heme b_{595}, and eventually arrive at heme *d* to reduce the bound oxygen to water. As an evidence, the midpoint potentials of three hemes in wild type increase in the order of heme b_{558}, heme b_{595} and heme *d*. In D239N mutant oxidase, the midpoint potentials of all the hemes are substantially reduced by the mutation. Moreover, in the mutant, heme b_{595} has the highest midpoint potential.

In the early stage (0.6 ms) of the oxidation / re-reduction assay of D239N, we find the solution after mixing consists of small amount of reduced hemes b and reduced heme *d* as well as large portion of oxoferryl heme *d* (**Figure 7.4, inset**). According to current reaction scheme (**Figure 7.6**), oxoferryl heme *d* corresponds to F state enzyme, but reduced heme *d* can come from either R1 or R3 states. The quantification of the mixture shows more reduced hemes b than heme *d* in a 2 to 1 ratio (15% vs. 8%). Thus, in our first hypothesis, reduced heme *d* in the solution reflects the presence of R3 state enzyme, indicating some fully reduced enzyme has not yet reacted with oxygen even at 0.6ms after mixing. To explain the presence of R3 state enzyme, there are three possibilities: i) there is not enough oxygen; ii) there is enough oxygen, but the reaction is too fast, so the R3 state enzyme is the product of re-reduction; iii) there is enough oxygen, but the

reaction is too slow, some R3 state enzyme is still waiting to be oxidized. Based on the spectra change in the first 10ms (**Figure 7.5**), the increasing peak at 650nm indicates the formation of ferrous oxy (A) state enzyme or, A3 state specifically, which is consistent with the oxidation of D239N heme *d* in the first 10ms (**Figure 7.2, right panel**). Thus, the third assumption should be correct, and at 0.6ms, there are R3, A3 and F state enzymes in the mixture, even though we cannot rule out the possible presence of peroxy (P) state due to the limitation of our instrument. All of these above seem to be a reasonable scenario that can justify itself, but it's not likely to be the truth.

Based on **Figure 7.5**, the formation of ferrous oxy state indicates excess amount of oxygen in the system. As we know in the activity assay, D239 mutants show even superior TMPD oxidase activity to wild type, which indicates no effect on the oxygen affinity of the bi-nuclear center. In other words, the abnormal high midpoint potential of heme b_{595} does not impair the oxygen binding ability of heme *d*, at least, when the enzyme is fully reduced. The fully reduced (R3) enzyme would be converted to A3 state in no time whenever there is oxygen. So, in our alternative hypothesis, the reduced heme *d* observed in **Figure 7.4** can only come from R1 state enzyme.

In normal catalysis of wild type cytochrome *bd* oxidase (**Figure 7.6**), the two-electron reduction of oxoferryl (F) species generates R1 state having reduced heme *d* and leaving both hemes b oxidized due to the highest midpoint potential of heme *d*. While in the D239N mutant, higher midpoint potential of heme b_{595} makes a relatively stable transition state, Rb possible, which has reduced heme b_{595} and oxidized heme *d* (**Figure 7.7**). In this new model, one-quinol reduction of F state results in a mixture of more Rb and less R1 states at equilibrium below:

$$b_{558}^{+3}b_{595}^{+2}d^{+3} \leftrightarrow b_{558}^{+3}b_{595}^{+3}d^{+2} \quad (1)$$

$$b_{558}^{+3}b_{595}^{+3}d^{+2} \rightarrow b_{558}^{+3}b_{595}^{+3}d^{+2} = O_2 \quad (2)$$

$$b_{558}^{+3}b_{595}^{+3}d^{+2} = O_2 + QH_2 \rightarrow b_{558}^{+2}b_{595}^{+2}d^{+2} = O_2 \quad (3)$$

The existence of Rb state is usually covered either by fast reduction like in **Figure 7.2** (**right panel**) or by fast oxidation, like the plateau of aurachin C 1-10 inhibited wild type *bd* curve in **Figure 7.3** (**right panel, red**). In our D239N mutant, on one hand, the impaired quinol binding ability slows down the reduction of oxoferryl enzyme; on the other hand, higher midpoint potential pushes the equilibrium (1) to the left and prevents fast decay of Rb state. The comprehensive consequence is the slow oxidation of hemes b in **Figure 7.3** (**right panel**) until oxygen is out at around 0.7 second.

The reaction curve of heme *d* in **Figure 7.3** (**left panel**) and the formation of ferrous oxy enzyme in **Figure 7.5** can also be explained by our new hypothesis. The significant amount of reduced heme *d* at 0.6 ms observed from spectrum in **Figure 7.4** indicates an impaired oxygen affinity. Under the double effect of lower oxygen binding ability and more difficult quinol binding (reaction (3)), R1 state enzyme accumulated in a short time and consequently accelerated reaction (2), which resulted in decline of reduced heme *d* (the first 10 ms in **Figure 7.3, left panel**) is the tail of this process). The consumption of previous accumulated R1 state enzyme caused by reaction (2) further forced the equilibrium (1) shifted to the right until the whole system achieved a new

equilibrium eventually (see the relatively flat part of the curve, or Phase I, in **Figure 7.3, left panel**).

The mutations at D239 impair the quinol binding ability. D239N, one of the mutants, further perturbs the rapid catalysis by increasing the midpoint potential of heme b_{595}, confirms its importance in the internal electron transfer pathway, and also implies a role of heme b_{595} in the oxygen affinity regulation. Details of this regulation require further investigation.

7.5 Figures and tables:

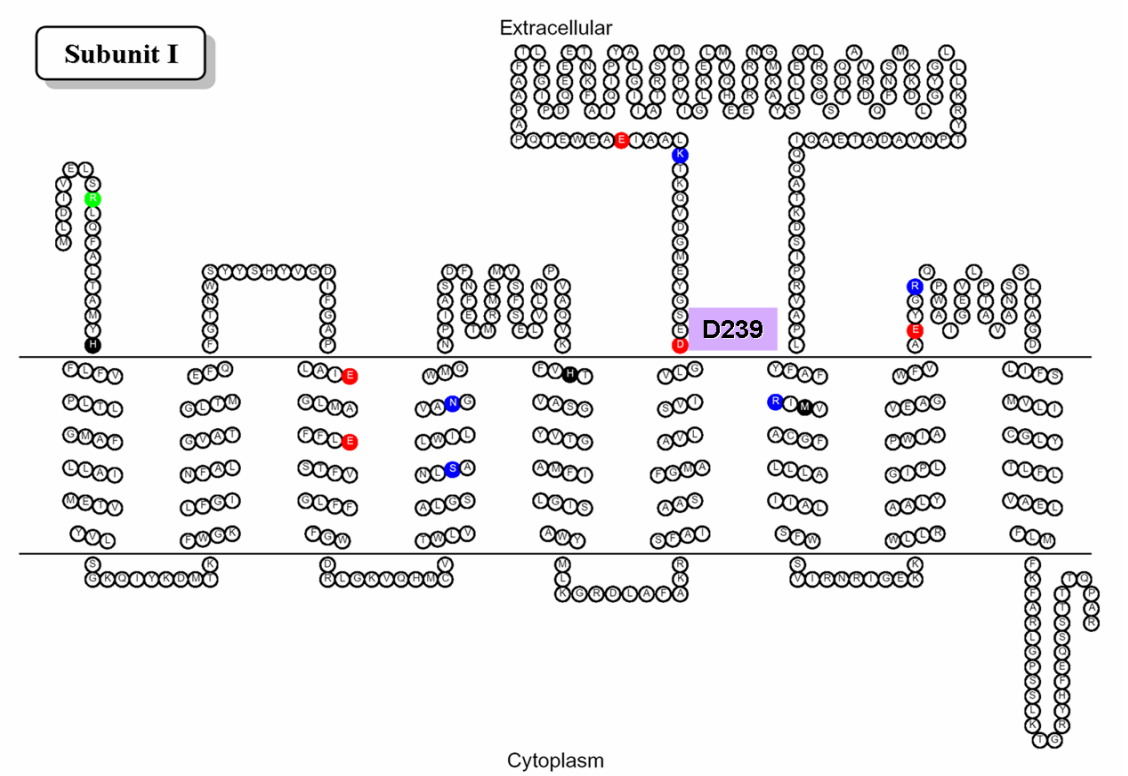

Figure 7.1 Membrane topology model of subunit I of cytochrome *bd* oxidase from *E. coli* with D239 marked out.

Table 7.1 Summary of the properties of the cytochrome *bd* D239 mutants

	Complementation of aerobic growth	Heme content (UV-Vis Spectra)	UQ_1H_2 oxidase activity[a]	TMPD oxidase activity[b]	E_m (vs. NHE[c])
WT	Yes	All hemes present	100%	100%	b_{558}: 100 ± 20 mV b_{595}: 222 mV *d*: 240±12 mV
D239A	No	All hemes present	0	300%	N/A
D239N	No	All hemes present	0	120%	b_{558}: 65 ± 11 mV b_{595}: 154 mV *d*: 100 mV

[a] 100% of ubiquinol-1 oxidase activity corresponds to a turnover of about $1450e^{-1}$/sec.
[b] 100% of TMPD oxidase activity corresponds to a turnover of about $100e^{-1}$/sec.
[c] Normal Hydrogen Electrode

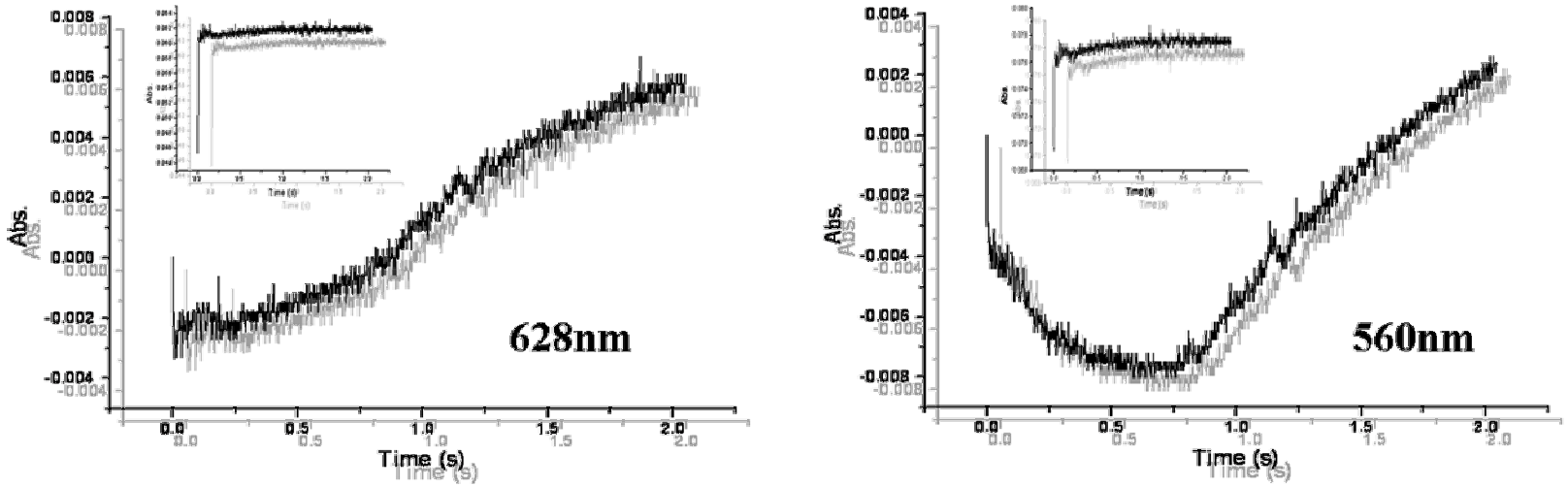

Figure 7.2 Effects of wild type (insets) and D239N mutation on hemes oxidation / re-reduction by ubiquinol observed at 562-minus-578 nm (hemes *b*) and 628-minus-719 nm (heme *d*) on a 2 s time scale.
30% of wild type hemes *b* is reduced in 10 ms at rate constant k = 290 ± 2.19 s^{-1}. A slow hemes *b* oxidation lasting for 0.7 s followed by slow re-reduction in D239N mutant enzyme is observed. After a 10 ms tail of oxidation, D239N heme *d* experienced a two-phase re-reduced in 2 s: slow phase (0.01 to 0.7 s) and fast phase (0.7 to 2 s).

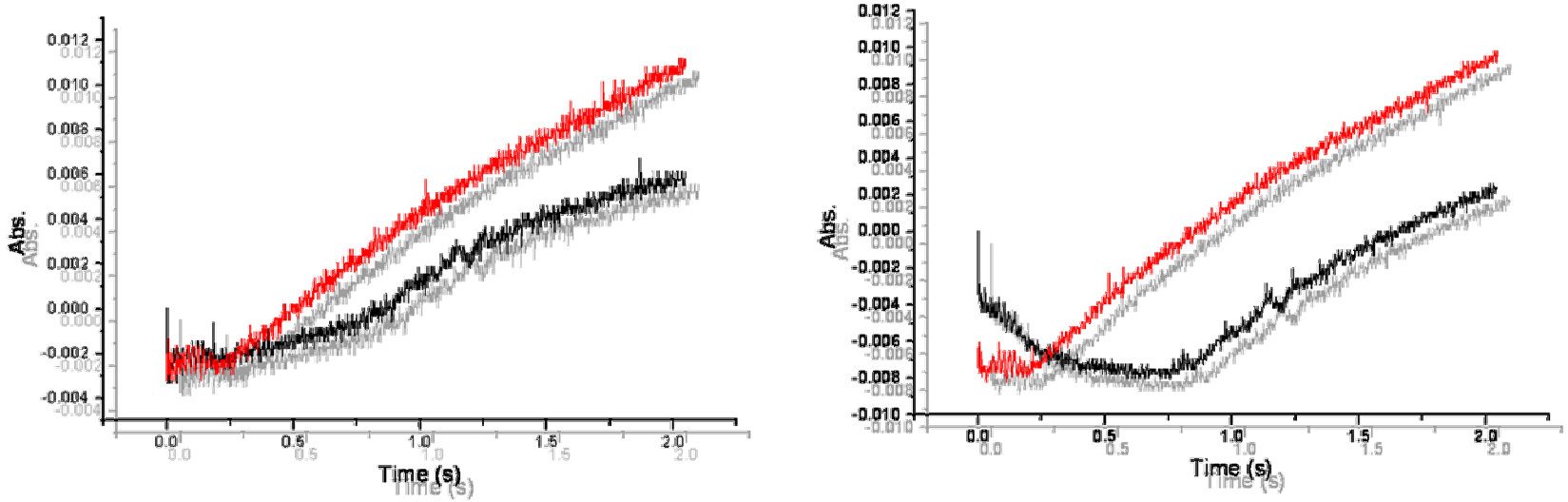

Figure 7.3 Comparison of optical time courses for the oxidation / re-reduction of D239N mutation (black) and inhibited wild type (red) *E. coli* cytochrome *bd*.
Left. Inhibited wild type enzyme shows a single-phase faster heme *d* re-reduction other than the two-phase re-reduction in D239N mutant.
Right. Followed by a plateau caused by excessive oxygen, aurachin C 1-10 inhibited wild type shows a slightly faster hemes *b* re-reduction than D239N mutant. No D239N-type slow oxidation is observed in the inhibited wild type enzyme.

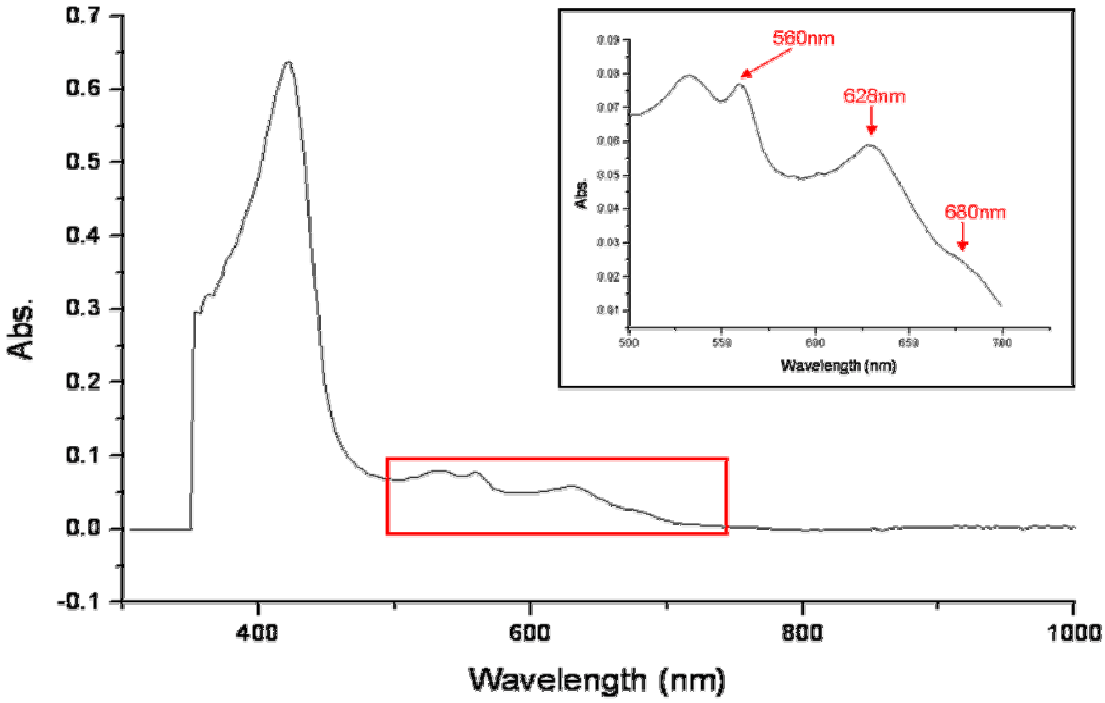

Figure 7.4 Spectrum at 0.6 ms after mixing fully reduced D239N mutant enzyme plus excess ubiquinol with oxygen.
Absorptions at 560, 628 and 680 indicate a mixture of reduced hemes *b*, reduced and oxoferryl hemes d at 0.6 ms after mixing.

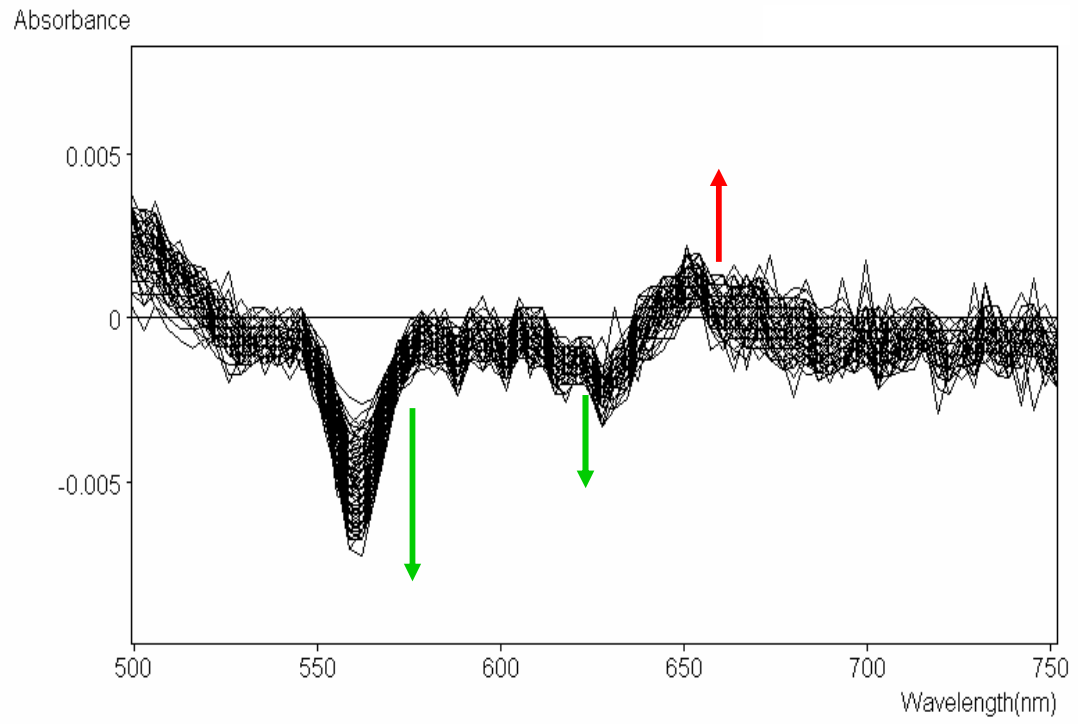

Figure 7.5 Spectra change in early stages of reaction.
From the absorbance time wavelength surface of optical changes, selected spectra taken from 0 to 10 ms are shown, in 0.6 ms increments. The direction of signal development in time is indicated by *arrows* (Green: 560 nm, 628 nm; Red: 650 nm).

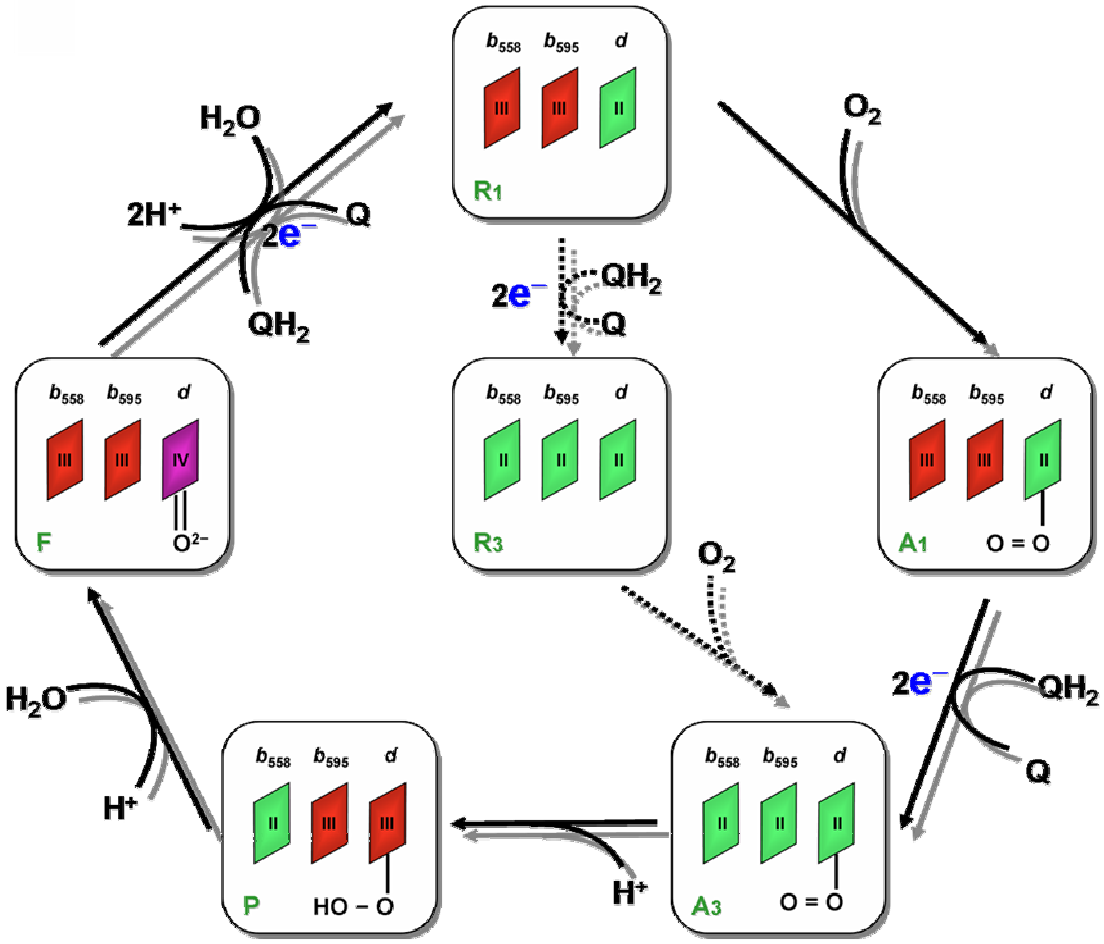

Figure 7.6 Reaction schemes of wild type cytochrome *bd*.
The three rhombuses represent hemes b_{558}, b_{595} and *d*, respectively. The Roman numeral denotes the charge of each heme. Catalytic cycle is connected by solid arrows while the dashed ones refer to the non-catalytic intermediates introduced in the experiment.

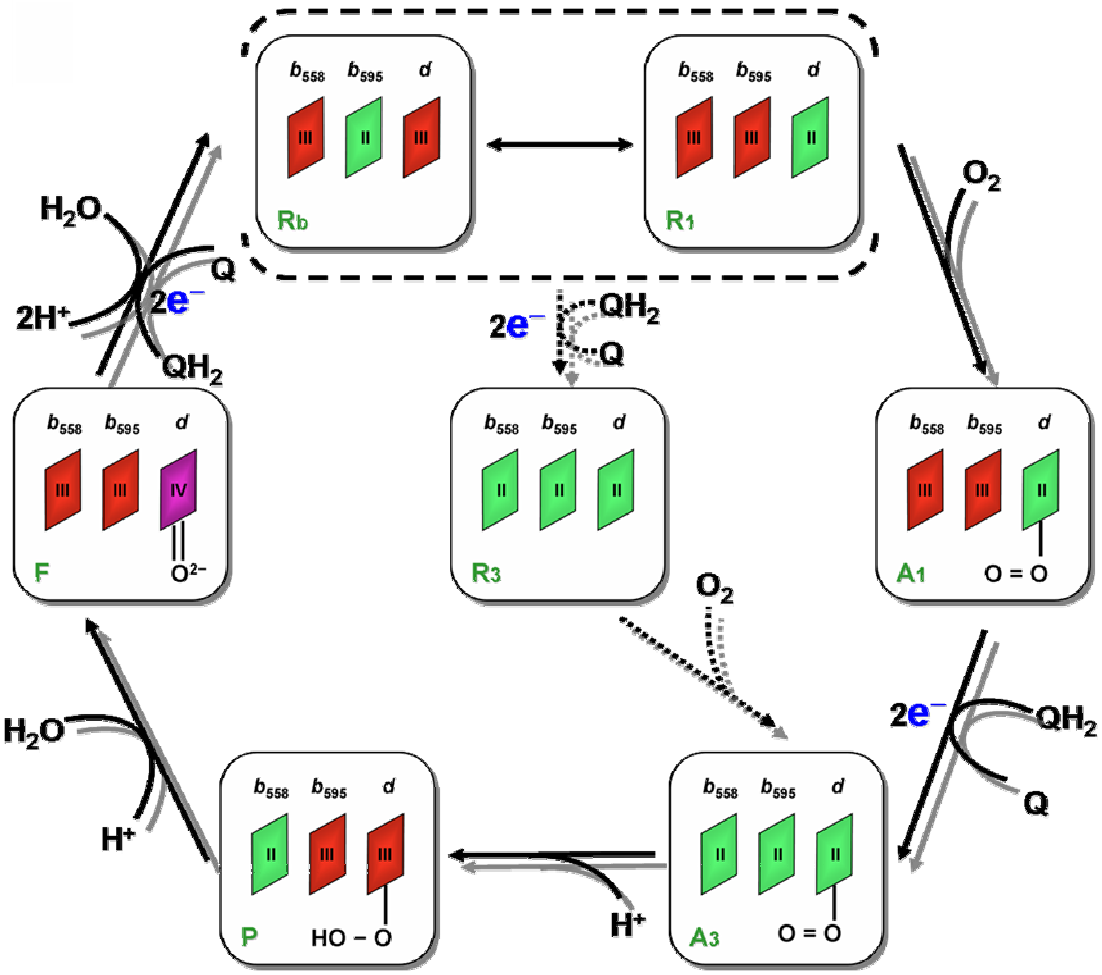

Figure 7.7 Plausible reaction schemes of D239 mutant cytochrome *bd*.
The three rhombuses represent hemes b_{558}, b_{595} and *d*, respectively. The Roman numeral denotes the charge of each heme. Catalytic cycle is connected by solid arrows while the dashed ones refer to the non-catalytic intermediates introduced in the experiment.

CHAPTER 8:CONCLUSIONS

Cytochrome *bd* quinol oxidase is a unique respiratory terminal oxidase in many ways. Being the only well-studied representative in the tri-heme oxidase family, cytochrome *bd* oxidase is optimally expressed under microaerobic growth condition. Two hemes, instead of one heme and one copper ion, comprise the binuclear reaction center where oxygen molecule is reduced to water. Besides the difference in structure, cytochrome *bd* does not function as a proton pump, which is one of the most characteristic features in heme-copper oxidase superfamily. The high tolerance of cyanide inhibition also distinguishes cytochrome *bd* from other terminal oxidases. It has been nearly thirty years since cytochrome *bd* oxidase has been discovered. Although many properties of this enzyme have been well characterized, there are still more hiding behind the curtain, such as its X-ray structure, the ligand of heme *d*, the role of heme b_{595}, the substrate binding site, and the in-membrane electron / proton transfer. In this dissertation, some of those questions above have been addressed based on my Ph.D. work. All the results are summarized in this chapter as well as their potential influence on the future research of cytochrome *bd* oxidase.

Cytochrome *bd* catalyzes the two-electron oxidation of ubiquinol or menaquinol and the four-electron reduction of oxygen to water under different growth conditions. Other than the recently observed peroxy complex (Fe^{3+}–OOH), four different states of heme *d* have been well characterized spectroscopically: fully oxidized ferric form (Fe^{3+}), fully reduced ferrous form (Fe^{2+}), one-oxygen-bound ferrous-oxy complex (Fe^{2+}–O_2), and the oxoferryl form (Fe^{4+}=O^{2-}). In previous studies, people have been questioned the

presence of either all-ferric form or ferrous-oxy complex in the rapid turnover of the enzyme. In my work, the rates of reduction of fully oxidized and oxoferryl forms of cytochrome *bd* by ubiquinol-1 and TMPD have been measured by Stopped-Flow techniques. My data pointed out that reduction of all-ferric form enzyme is too slow to be considered as one step in the catalytic cycle, whereas the observed rates of reduction of the oxoferryl form and ferrous-oxy complex of cytochrome *bd* are consistent with the catalytic turnover. Based on the observations, we established a new model of the catalytic cycle which does not include all-ferric form of the enzyme as an intermediate. This is also the first successful intention of using ubiquinol as substrate of cytochrome *bd* oxidase in the fast kinetics study, which could profoundly change the future experiment design.

A re-visit of a previous reported mutant, E445A, uncovered the dithionite-resistant heme b_{595} caused by the mutation and revealed the critical role of heme b_{595} in the enzyme catalysis. Electrometric and time-resolved optical studies preferred a new hypothetic model of electron-proton coupling within the enzyme, indicating a "must-exist" proton uptake pathway with conveying proton from cytoplasm to the heme b_{595} / heme *d* binuclear center. Couple of protonatable groups has been adding to the model and postulated to be part of the proton channel.

Benefited from the increasing database of available cytochorme *bd* oxidase sequences, many highly conserved residues have been identified and mapped out on the two-dimensional topology. Due to the limit knowledge on the crystal structure, site-directed mutagenesis has been and will still be a powerful tool for us in the foreseeable future studies on cytochrome *bd* oxidase. Two highly conserved acidic residues, E99 and

E107, have been intensively studied by mutagenesis due to their unique locations in the transmembrane helices, where are also close to the proposed active site near the periplasmic side of membrane. Although most of the mutations severely destabilized the di-heme center, we managed to obtain sharp FTIR redox difference spectra from mutant E107Q. The comparison study with wild type and E107Q assigned the absorption bands from the COOH group of E107 at 1753 and 1738 cm^{-1}, showing that E107 is protonated at pH 7.6, and that that it is perturbed by the reduction of the heme b_{595} / heme *d* binuclear center at the active site. Regarding the FTIR results and close proximity of both E99 and E107 to heme *d*, they are promising candidates for the protonatable groups mentioned in E445 study. However, their exact roles in the proton translocation require further investigation.

As the last part of this proton channel trilogy, two highly conserved non-acidic residues, S140 and N148, have also been discovered and studied by mutagenesis. Despite of N148 mutants' wild type features, mutations at S140 results in ubiquinol oxidase activity loss as well as perturbation on the active site. One of the two TMPD active mutants, S140T, was examined by FTIR spectroscopy and found to be involved in the proton uptake by affecting the protonation states of E107 and other unknown COOH group (probably E99). The structural and catalytic importance of S140 is waiting for more details from other approaches, like electrometric measurement and Flow-Flash.

Probing the quinone binding site of cytochrome *bd* quinol oxidase is always one of the best interests in research on this enzyme. A combined experiment with strong binding site inhibitor, aurachin C 1-10, by FTIR studies, suggested that E257, a strictly conserved amino acid in Q-loop, could contribute to the quinol binding. It's not likely to

be the direct binding site of substrate, but rather control the bound quinone release after oxidation reaction.

D239, another conserved residue at the very beginning of the N-terminus of Q-loop, may also play an important role in the quinol binding business based on the kinetics study of its mutants with stopped-flow techniques. More interestingly, other than quinol binding, D239N perturbs the midpoint potentials of heme groups and makes the heme b_{595} having the highest midpoint potential of three. Global analysis of the data gave the possibility of a new sub-intermediate in the catalytic cycle, whose existence calls for more experimental data support.

In summary, my work has demonstrated that the fully oxidized form of cytochrome *bd* oxidase does not participate in the rapid catalysis. Several critical sites have been identified as part of the plausible proton translocation pathway based on a novel hypothesis. Two acidic residues may involve in quinone binding mechanism, which requires further study. Fast mixing techniques, such as stopped-flow and flow-flash, as well as time-resolved electrometrics, were introduced in the kinetics study. FTIR spectroscopy together with electrochemical control has been proven to be extremely powerful in probing the proton channel within cytochrome *bd* quinol oxidase, and it will be of continued use in the research on other respiratory complexes.

LIST OF SYMBOLS AND ABBREVIATIONS

Amp	ampicillin
Amp^R / Amp^S	ampicillin resistant / sensitive
Ag / AgCl	silver-silver chloride electrode
AP	alkaline phosphatase
Asc	ascorbate
as iso	as isolated state, air-oxidized state
ATP	adenosine triphosphate
BCA	Bicinchoninic Acid
$BQCl_4$	tetrachlorobenzoquinone
°C	temperature in Celsius
CCD	charge coupled device
CO	carbon monoxide
CN^-	cyanide
Cytochrome bd, cyt bd	cytochrome bd quinol oxidase
D_2O	deuterium water
DMK	demethylmenaquinone
DTT	dithiothreitol
DEAE	diethylaminoethyl
e	electron
E_m	midpoint potential
E.coli	*Escherichia coli*
EDTA	ethylenediaminetetraacetic acid
ENDOR	electron nuclear double resonance

EPR	electron paramagnetic resonance
Fe	iron
Ferryl	iron (IV)
FTIR	Fourier transform infrared spectroscopy
g-value	gyromagnetic ratio
GHz	gigahertz
H^+	proton
HPLC	high performance liquid chromatography
HQNO	2-n-heptyl-4-hydroxquinoline-N-oxide
i.d.	internal diameter
K	temperature in Kelvin
Kan	kanamycin
kD	kilodalton
KHz	kilohertz
Ki	inhibition constant
KPi	potassium phosphate
LB	Luria broth
M	molar
Min	minute
MQ	menaquinone
mL	milliliter
mM	millimolar
mW	milliwatt
µM	micromolar
µL	microliter

nm	nanometer
NaCl	sodium chloride
NaPi	sodium phosphate
NMR	nuclear magnetic resonance
NPP	nitrophenylphosphate
O.D.	optical density
ONPG	ortho-nitrophenyl-β-D-galactopyranoside
ox	oxidized
Oxy	oxygenated species
PCR	polymerase chain reaction
PMS	phenazine methosulfate
PMSF	phenylmethylsulfonylfluoride
RR, rR	resonance Raman spectroscopy
red	reduced
TMPD	N, N, N', N'-tetramethyl-p-phenylenediamine
Tris	tris[hydroxymethyl]aminomethane
UQ_1	ubiquinone-1
UQ_1H_2	ubiquinol-1
UV-Vis	ultraviolet-visible
WT, wt	wild type

BIBLIOGRAPHY

Abramson, J., S. Riistama, G. Larsson, A. Jasaitis, M. Svensson-Ek, L. Laakkonen, A. Puustinen, S. Iwata and M. Wikstrom (2000). "The Structure of the Ubiquinol Oxidase from *Escherichia coli* and Its Ubiquinone Binding Site." Nature Structural Biology 7: 910-917.

Anraku, Y. and R. B. Gennis (1987). "The Aerobic Respiratory Chain of *Escherichia coli*." TIBS 12: 262-266.

Arutyunyan, A. M., V. B. Borisov, V. I. Novoderezhkin, J. Ghaim, J. Zhang, R. B. Gennis, A. A. Konstantinov (2008). "Strong Excitonic Interactions in the Oxygen-reducing Site of *bd*-type Oxidase: The Fe-to-Fe Distance Between Hemes *d* and b_{595} is 10 A." Biochemistry 47(6): 1752-1759.

Banci, L., I. Bertini, E. A. Pease, M. Tien and P. Turano (1992). "Proton NMR Investigation of Manganese Peroxidase from *Phanerochaete chrysosporium*. A Comparison with Other Peroxidases." Biochemistry 31: 10009-10017.

Bartoschek, S., M. Johansson, B. H. Geierstanger, J. G. Okun, C. R. Lancaster, E. Humpfer, L. Yu, C. A. Yu, C. Griesinger and U. Brandt (2001). "Three Molecules of Ubiquinone Bind Specifically to Mitochondrial Cytochrome bc1 Complex." J. Biol. Chem. 38: 35231-35234.

Bayman, F., D. E. Robertson, P. L. Dutton and W. Mantele (1999). "Electrochemical and Spectroscopic Investigatio of Cytochrome bc1 Complex from *Rhodobacter capsulatus*." Biochemistry 38: 13188-13199.

Belevich, I., V. B. Borisov, M. I. Verkhovsky (2007). "Discovery of the True Peroxy Intermediate in the Catalytic Cycle of Terminal Oxidases by Real-time Measurement." J. Biol. Chem. 282(39): 28514-28519.

Belevich, I., V. B. Borisov, J. Zhang, K. Yang, A. A. Konstantinov, R. B. Gennis, M. I. Verkhovsky (2005). "Time-resolved Electrometric and Optical Studies on Cytochrome *bd* Suggest a Mechanism of Electron-proton Coupling in the Di-heme Active Site." Proc. Natl. Acad. Sci. USA 102: 3657-3662.

Bentley, R. and R. Meganathan (1987). *Escherichia coli* and *Salmonella typhimurium*. Washington, D.C., American Society for Microbiology.

Berry, E. A. and B. L. Trumpower (1987). "Simulataneous Determination of Hemes *a*, *b*, and *c* from Pyridine Hemochrome Spectra." Anal. Bioch. 161: 1-15.

Bertini, I., H. Molinari and N. Niccolai (1991). NMR and Biomolecular Structure. New York City, NY, VCH Publishers Inc.

Bertini, I., A. Rosato and P. Turano (1999). "Solution Structure of Paramagnetic Metalloproteins." Pure Appl. Chem. 71: 1717-1725.

Bertini, I., P. Turano and A. J. Vila (1993). "Nuclear Magnetic Resonance of Paramagnetic Metalloproteins." Chem. Rev. 93: 2833-2932.

Borisov, V., A. M. Arutyunyan, J. P. Osborne, R. B. Gennis and A. A. Konstantinov (1999). "Magnetic Circular Dichroism Used to Examine the Interaction of *Escherichia coli* Cytochrome *bd* with Ligands." Biochemistry 38: 740-750.

Borisov, V. B., U. Liebl, F. Rappaport, J. L. Martin, J. Zhang, R. B. Gennis, A. A. Konstantinov, M. H. Vos (2002). "Interactions Between Heme *d* and Heme b_{595} in Quinol Oxidase *bd* from *Escherichia coli*: A Photoselection Study Using Femtosecond Spectroscopy." Biochemistry 41(5): 1654-1662.

Borisov, V. B., I. A. Smirnova, I. A. Krasnosel'skaya and A.A. Konstantinov (1994). "Oxygenated Cytochrome *bd* from *Escherichia coli* can be Converted into the Oxidized Form by Lipophilic Electron Acceptors." Biochemistry (Moscow) **59**: 437–443.

Branden, G., R. B. Gennis and P. Brzezinski (2006). "Transmembrane Proton Translocation by Cytochrome *c* Oxidase." Biochim. Biophys. Acta.

Brändén, M., F. L. Tomson, R. B. Gennis and P. Brzezinski (2002). "The Entry Point of the K-Proton-Transfer Pathway in Cytochrome *c* Oxidase." Bichemistry 41: 10794-10798.

Breton, J., C. Boullais, G. Berger, C. Mioskowski and E. Nabedry (1995). "Binding Sites of Quinones in Photosynthetic Bacterial Reaction Centers Investigated by Light-induced FTIR Difference Spectroscopy: Symmetry of the Carbonyl Interactions and Close Equivalence of the QB: Vibration s in *Rhodopseudomonas sphaeroides* and *Rhodobacter viridis* Probed by Isotope Labeling." Biochemistry 34: 11606-11616.

Breton, J., C. Boullais, J.-R. Burie, E. Nabedryk and C. Mioskowski (1994). "Binding Sites of Quinones in Photosynthetic Bacterial Reaction Centers Investigated by Light-induced FTIR Difference Spectroscopy: Assignment of the Interactions of Each Carbonyl of QA in *Rhodobacter sphaeroides* Using Site-Specific ^{13}C-Labeled Ubiquinone." Biochemistry 33: 14378-14386.

Breton, J., J.-R. Burie, C. Berthomieu, G. Berger and E. Nabedryk (1994). "The Binding Sites of Quinones in Photosynthetic Bacterial Reaction Centers Investigated by Light-induced FTIR Difference Spectroscopy: Assignment of the QA Vibrations in *Rhodobacter sphaeroides* Using ^{18}O- or ^{13}C-Labeled Ubiquinones and Vitamin K1." Biochemistry 33: 4953-4965.

Brondsted, L. and T. Atlung (1996). "Effect of Growth Conditions on Expression of the Acid Phosphatase (cyx-appA) Operon and the appY Gene, which Encodes a Transcriptional Activator of *Escherichia coli*." J. Bacteriol. 178: 1556-1564.

Calhoun, M. W., J. W. Thomas and R. B. Gennis (1994). "The Cytochrome Oxidase Superfamily of Redox-driven Proton Pumps." TIBS 19(8): 325-330.

Chung, C. T., S. L. Niemela and R. H. Miller (1989). "One-step Preparation of Competent *Escherichia coli*: Transformation and Storage of Bacterial Cells in the Same Solution." Proc. Natl. Acad. Sci. USA 86: 2172-2175.

Cohen, G. N. and H. V. Rickenberg (1956). "Concentration Specifique Reversible Des Amino Acides Chez *Escherichia coli*." Ann. Inst. Pasteur (Paris) 91: 693-720.

Cotter, P. A., V. Chepuri, R. B. Gennis and R. P. Gunsalus (1990). "Cytochrome *o* (*cyoABCDE*) and *d* (*cydAB*) Oxidase Gene Expression in *Escherichia coli* is Regulated by Oxygen, pH, and the fnr Gene Product." J. Bacteriol. 172(11): 6333-6338.

Crofts, A. R., S. Hong, N. Ugulava, B. Barquera, R. B. Gennis, M. Guergova-Kuras and E. A. Berry (1999). "Pathways for Proton Release during Ubihydroquinone Oxidation by the bc(1) Complex." Proc. Natl. Acad. Sci. USA 96: 10021-10026.

Cunningham, L., M. Pitt and H. D. Williams (1997). "The *cioAB* Genes from *Pseudomonas aeruginosa* Code for a Novel Cyanide-insensitive Terminal Oxidase Related to the Cytochrome *bd* Quinol Oxidases." Molecular Microbiology 24(3): 579-591.

Dassa, J., H. Fsihi, C. Marck, M. Dion, M. Kieffer-Bontemps and P. L. Boquet (1991). "A New Oxygen-regulated Operon in *Escherichia coli* Comprises the Genes for a Putative Third Cytochrome Oxidase and for pH 2.5 Acid Phosphatase (appA)." Mol. Gen. Genet. 229: 341-352.

D'Mello, R., S. Hill and R. K. Poole (1994). "Determination of the Oxygen Affinities of Terminal Oxidases in *Azotobacter vinelandii* Using the Deoxygenation of Oxyleghaemoglobin and Oxymyoglobin: Cytochrome bd is a Low-affinity Oxidase." Microbiol. 140: 1395-1402.

Dueweke, T. J. and R. B. Gennis (1990). "Epitopes of Monoclonal Antibodies Which Inhibit Ubiquinol Oxidase Activity of *Escherichia coli* Cytochrome *d* Complex Localize a Functional Domain." J. Biol. Chem. 265: 4273-4277.

Dueweke, T. J. and R. B. Gennis (1991). "Proteolysis of the Cytochrome *d* Complex with Trypsin and Chymotrypsin Localizes a Quinol Oxidase Domain." Biochemistry 30: 3401-3406.

Edwards, S. E., C. S. Loder, G. Wu, H. Corker, B. W. Bainbridge, S. Hill and R. K. Poole (2000). "Mutation of Cytochrome bd Quinol Oxidase Results in Reduced Stationary Phase Survival, Iron Deprivation, Metal Toxicity and Oxidative Stress in *Azotobacter vinelandii*." FEMS Microb. Lett. 185: 71-77.

Endley, S., D. McMurray and T. A. Ficht (2001). "Interruption of the cyd Locus in *Brucella aborus* Attenuates Intracellular Survival and Virulence in the Mouse Model of Infection." J. Bacteriol. 183: 2454-2462.

Engelman, D. M., T. A. Steitz and A. Goldman (1986). " Identifying Nonpolar Transbilayer Helices in Amino Acid Sequences of Membrane Proteins." Ann. Rev. Biophys. Biophys. Chem. 15: 321-353.

Fang, H., R.-J. Lin and R. B. Gennis (1989). " Location of Heme Axial Ligands in the Cytochrome *d* Terminal Oxidase Complex of *Escherichia coli* Determined by Site-directed Mutagenesis." J. Biol. Chem. 264(14): 8026-8032.

Fu, H. A., S. Iuchi and E. C. C. Lin (1991). "The Requirement of ArcA and Fnr for Peak Expression of the *cyd* Operon in *Escherichia coli* Under Microaerobic Conditions." Mol. Gen. Genet. 226: 209-213.

Garcia-Horsman, J. A., B. Barquera, J. Rumbley, J. Ma and R. B. Gennis (1994). "The Superfamily of Heme-Copper Respiratory Oxidases." J. Bacteriol. 176(18): 5567-5600.

Gennis, R. B. (1987). "The Cytochromes of *Escherichia coli*." FEMS Microb. Rev. 46: 387-399.

Gennis, R. B. (1998). "Multiple Proton-conducting Pathways in Cytochrome Oxidase and a Proposed Role for the Active-site Tyrosine." Biochim. Biophys. Acta. 1365: 241-248.

Georgiou, C. D., T. J. Dueweke and R. B. Gennis (1988). "B-Galactosidase Gene Fusions as Probes for the Cytoplasmic Regions of Subunits I and II of the Membrane-bound Cytochrome *d* Terminal Oxidase from *Escherichia coli*." J. Biol. Chem. 263(26): 13130-13137.

Gerard, H. C., J. Freise, Z. Wang, G. Roberts, D. Rudy, B. Kraub-Opatz, L. Kohler, H. Zeidler, H. R. Schumacher, J. A. Wittum-Hudson and A. P. Hudson (2002). "Chlamydia trachomatis Genes Whose Products are Related to Energy Metabolism are Expressed Differentially in Active vs. Persistent Infection." Microbes and Infection 4: 13-22.

Goff, H. and G. H. La Mar (1977). "High-spin Ferrous Porphyrin Complexes as Models for Deoxymyoglobin and Hemoglobin: A Proton Nuclear Magnetic Resonance Study." J. Am. Chem. Soc. 99: 6599-6606.

Goldman, B. S., K. K. Gabbert and R. G. Kranz (1996). "The Temperature-sensitive Growth and Survival Phenotypes of *Escherichia coli cydDC* and *cydAB* Strains are Due to Deficiencies in Cytochrome *bd* and are Corrected by Exogenous Catalase and Reducing Agents." J. Bacteriol. 178(21): 6348-6351.

Goldman, B. S., K. K. Gabbert and R. G. Kranz (1996). " Use of Heme Reporters for Studies of Cytochrome Biosynthesis and Heme Transport." J. Bacteriol. 178(21): 6338-6347.

Govantes, F., A. V. Orjalo and R. P. Gunsalus (2000). "Interplay Between Three Global Regulatory Proteins Mediates Oxygen Regulation of the *Escherichia coli* Cytochrome *d* Oxidase (*cydAB*) Operon." Molecular Microbiology 38: 1061-1073.

Govantes, F., J. A. Albrecht and R. P. Gunsalus (2000). "Oxygen Regulation of the *Escherichia coli* Cytochrome *d* Oxidase (*cydAB*) Operon: Roles of Multiple Promoters and the Fnr-1 and Fnr-2 Binding Sites." Molecular Microbiology 37: 1456-1469.

Green, G. N., R. M. Lorence and R. B. Gennis (1986). "Specific Overproduction and Purification of the Cytochrome b_{558} Component of the Cytochrome *d* Complex from *Escherichia coli*." Biochemistry 25(9): 2309-2314.

Green, G. N., H. Fang, R.-J. Lin, G. Newton, M. Mather, C. Georgiou and R. B. Gennis (1988). "The Nucleotide Sequence of the *cyd* Locus Encoding the Two Subunits of the Cytochrome *d* Terminal Oxidase Complex of *Escherichia coli*." J. Biol. Chem. 263(26): 13138-13143.

Hall, T. A. (1999). "BioEdit: A User-friendly Biological Sequence Alignment Editor and Analysis Program for Windows 95/98/NT." Nucl. Acids. Symp. Ser. 41: 95-98.

Hao, W. and G. B. Golding (2006). "Asymmetrical Evolution of Cytochrome *bd* Subunits." J. Mol. Evol. 62: 132-142.

Hastings, S. F., P. Heathercote, W. J. Ingledew and S. E. J. Rigby (2000). "ENDOR Spectroscopic Studies of Stable Semiquinone Radicals Bound to the *Escherichia coli* Cytochrome bo_3 Quinol Oxidase." Eur. J. Biochem. 267: 5638-5645.

Hastings, S. F., T. M. Kaysser, F. Jiang, J. C. Salerno, R. B. Gennis and W. J. Ingledew (1998). "Identification of a Stable Semiquinone Intermediate in the Purified and Membrane Bound Ubiquinol Oxidase-cytochrome *bd* from *Escherichia coli*." Eur. J. Biochem. 255(1): 317-323.

Hata, A., Y. Kirino, K. Matsuura, S. Itoh, T. Hiyama, K. Konishi, K. Kita and Y. Anraku (1985). "Assignment of ESR Signals of *Escherichia coli* Terminal Oxidase Complexes." Biochim. Biophys. Acta. 810: 62-72.

Hellwig, P., B. Barquera and R. B. Gennis (2001). "Direct Evidence for the Protonation of Aspartate-75, Proposed to be at a Quinol Binding Site, Upon Reduction of Cytochrome bo_3 from *Escherichia coli*." Biochemistry 40: 1077-1082.

Hellwig, P., J. Behr, C. Ostermeier, O.-M. H. Richter, U. Pfitzner, A. Odenwald, B. Ludwig, H. Michel and W. Mantele (1998). "Involvement of Glutamic Acid 278 in the Redox Reaction of the Cytochrome *c* Oxidase from *Paracoccus denitrificans* Investigated by FTIR Spectroscopy." Biochemistry 37: 7390-7399.

Hellwig, P., T. Mogi, F. L. Tomson, R. B. Gennis, J. Iwata, H. Miyoshi and W. Mantele (1999). "Vibrational Modes of Ubiquinone in Cytochrome bo_3 from *Escherichia coli* Identified by Fourier Transform Infrared Difference Spectroscopy and Specific ^{13}C Labeling." Biochemistry 38: 14683-14689.

Herzberg, G. (1962). Molecular Spectra and Molecular Structure: II. Infrared and Raman Spectra of Polyatomic Molecules. Princeton, NJ, D. Van Nostrand Company.

Hielscher, R., T. Wenz, S. Stolpe, C. Hunte, T. Friedrich and P. Hellwig (2006). "Monitoring Redox-dependent Contribution of Lipids in Fourier Transform Infrared Difference Spectra of Complex I from *Escherichia coli*." Biopolymers 82: 291-294.

Hill, B. C. and C. Greenwood (1983). "Spectroscopic Evidence for the Participation of Compound A (Fe_{a3}^{2+}-O_2) in the Reaction of Mixed-valence Cytochrome *c* Oxidase with Oxygen at Room Temperature." Biochem. J. 215: 659-667.

Hill, B. C., J. J. Hill and R. B. Gennis (1994). "The Room Temperature Reaction of Carbon Monoxide and Oxygen with the Cytochrome *bd* Quinol Oxidase from *Escherichia coli*." Biochemistry 33: 15110-15115.

Hill, J. J., J. O. Alben and R. B. Gennis (1993). "Spectroscopic Evidence for a Heme-heme Binuclear Center in the Cytochrome *bd* Ubiquinol Oxidase from *Escherichia coli*." Proc. Natl. Acad. Sci. USA 90: 5863-5867.

Hill, S., S. Viollet, A. T. Smith and C. Anthony (1990). "Roles for Enteric *d*-type Cytochrome Oxidase in N_2 Fixation and Microaerobiosis." J. Bacteriol. 172(4): 2071-2078.

Hirota, S., T. Mogi, Y. Anraku, R. B. Gennis and T. Kitagawa (1995). "Resonance Raman Study on Axial Ligands of Heme Irons in Cytochrome *bd*-type Ubiquinol Oxidase from *Escherichia coli*." Biospectroscopy 1: 305-311.

Hollander, R. (1976). "Correlation of the Function of Demethylmenaquinone in Bacterial Electron Transport with Its Redox Potential." FEBS Lett. 72: 98-100.

Hori, H., M. Tsubaki, T. Mogi and Y. Anraku (1996). "EPR Study of NO Complex of *bd*-type Ubiquinol Oxidase from *Escherichia coli*." J. Biol. Chem. 271(16): 9254-9258.

Huycke, M. M., V. Abrams and D. R. Moore (2002). "*Enterococcus faecalis* Produces Extracellular Superoxide and Hydrogen Peroxide that Damages Colonic Epithelial Cell DNA." Carcinogenesis 23(3): 529-536.

Huycke, M. M., D. Moore, W. Joyce, P. Wise, L. Shepard, Y. Kotake and M. S. Gilmore (2001). "Extracellular Superoxide Production by *Enterococcus faecalis* Requires Demethylmenaquinone and is Attenuated by Functional Terminal Quinol Oxidases." Molecular Microbiology 42(3): 729-740.

Inubushi, T. and T. Yonetani (1983). "Proton Nuclear Magnetic Resonance Study of Bovine Cytochrome Oxidase." FEBS Lett. 160: 287-290.

Iuchi, S. and E. C. C. Lin (1991). "Adaptation of *Escherichia coli* to Respiratory Conditions: Regulation of Gene Expression." Cell 66: 5-7.

Jasaitis, A., V. B. Borisov, N. P. Belevich, J. E. Morgan, A. A. Konstantinov and M. I. Verkhovsky (2000). "Electrogenic Reactions of Cytochrome *bd*." Biochemistry 39: 13800-13809.

Jiang, F. S., T. M. Zuberi, J. B. Cornelius, R. B. Clarkson, R. B. Gennis and R. L. Belford (1993). "Nitrogen and Proton ENDOR of Cytochrome *d*, Hemin, and Metmyoglobin in Frozen Solutions." J. Am. Chem. Soc. 115: 10293-10299.

Jones, R. W., J. H. Weiner and R. B. Gennis (1984). "Immunochemical Analysis of Membrane-bound Antigens from *Escherichia coli* which Have Succinate Dehydrogenase Activity." Bio. Soc. Trans.: 800-801.

Jünemann, S. (1997). "Cytochrome *bd* Terminal Oxidase." Biochim. Biophys. Acta. 1321: 107-127.

Jünemann, S., P. J. Butterworth and J. M. Wrigglesworth (1995). "A Suggested Mechanism for the Catalytic Cycle of Cytochrome *bd* Terminal Oxidase Based on Kinetic Analysis." Biochemistry 34: 14861-14867.

Jünemann, S. and J. M. Wrigglesworth (1994). "Antimycin Inhibition of the Cytochrome *bd* Complex From *Azotobacter vinelandii* Indicates the Presence of a Branched Electron Transfer Pathway for the Oxidation of Ubiquinol." FEBS Lett. 345: 198-202.

Jünemann, S., J. M. Wrigglesworth and P. R. Rich (1997). "Effects of Decyl-aurachin D and Reversed Electron Transfer in Cytochrome *bd*." Biochemistry 36(31): 9323-9331.

Kahlow, M. A., T. M. Loehr, T. M. Zuberi and R. B. Gennis (1993). "The Oxygenated Complex of Cytochrome *d* Terminal Oxidase: Direct Evidence for Fe-O_2 Coordination in a Chlorin-containing Enzyme by Resonance Raman Spectroscopy." J. Am. Chem. Soc. 115: 5845-5846.

Kahlow, M. A., T. M. Zuberi, R. B. Gennis and T. M. Loehr (1991). "Identification of a Ferryl Intermediate of *Escherichia coli* Cytochrome *d* Terminal Oxidase by Resonance Raman Spectroscopy." Biochemistry 30(49): 11485-11489.

Kaminski, P. A., C. L. Kitts, Z. Zimmerman and R. A. Ludwig (1996). "*Azorhizobium caulinodans* Uses Both Cytochrome *bd* (Quinol) and Cytochrome cbb_3 (Cytochrome *c*) Terminal Oxidases for Symbiotic N_2 Fixation." J. Bacteriol. 178(20): 5989-5994.

Kauffman, H. F. and B. F. Van Gelder (1973). "The Respiratory Chain of *Azotobacter vinelandii* II. The Effect of Cyanide on Cytochrome *d*." Biochim. Biophys. Acta. 314: 276-283.

Kauffman, H. F. and B. F. Van Gelder (1974). "The Respiratory Chain of *Azotobacter vinelandii* III. The Effect of Cyanide in the Presence of Substrates." Biochim. Biophys. Acta. 333: 218-227.

Kaysser, T. M., J. B. Ghaim, C. Georgiou and R. B. Gennis (1995). "Methionine-393 is an Axial Ligand of the Heme b_{558} Component of the Cytochrome *bd* Ubiquinol Oxidase from Escherichia coli." Biochemistry 34: 13491-13501.

Keating, K. A., G. N. La Mar, F.-Y. Shiau and K. M. Smith (1992). "^{1}H NMR Study of the Molecular and Electronic Structure of Paramagnetic Iron Chlorin Complexes of Myoglobin: Dynamic Heterogeneity of the Heme Pocket." J. Am. Chem. Soc. 114: 6513-6520.

Kelly, M. J. S., R. K. Poole, M. G. Yates and C. Kennedy (1990). "Cloning and Mutagenesis of Genes Encoding the Cytochrome *bd* Terminal Oxidase Complex in *Azotobacter vinelandii*: Mutants Deficient in the Cytochrome *d* Complex are Unable to Fix Nitrogen in Air." J. Bacteriol. 172(10): 6010-6019.

Kita, K., K. Konishi and Y. Anraku (1984). "Terminal Oxidases of *Escherichia coli* Aerobic Respiratory Chain II. Purification and Properties of Cytochrome b_{558}-*d* Complex from Cells Grown with Limited Oxygen and Evidence of Branched Electron-carrying Systems." J. Biol. Chem. 259(5): 3375-3381.

Kita, K., K. Konishi and Y. Anraku (1984). "Terminal Oxidases of *Escherichia coli* Aerobic Respiratory Chain I. Purification and Properties of Cytochrome b_{562}-*o* Complex from Cells in the Early Exponential Phase of Aerobic Growth." J. Biol. Chem. 259(5): 3368-3374.

Kitagawa, T. (1987). Biological Applications of Raman Spectroscopy. New York City, NY, John Wiley & Sons.

Kobayashi, K., S. Tagawa and T. Mogi (1999). "Electron Transfer Process in Cytochrome *bd*-type Ubiquinol Oxidase from *Escherichia coli* Revealed by Pulse Radiolysis." Biochemistry 38: 5913–5917.

Koland, J. G., M. J. Miller and R. B. Gennis (1984). "Potentiometric Analysis of the Purified Cytochrome *d* Terminal Oxidase Complex from *Escherichia coli*." Biochemistry 23(6): 1051-1056.

Konstantinov, A. A., S. Siletsky, D. Mitchell, A. Kaulen and R. B. Gennis (1997). "The Roles of the Two Proton Input Channels in Cytochrome *c* Oxidase from *Rhodobacter sphaeroides* Probed by the Effects of Site-Directed Mutations on Time-Resolved Electrogenic Intraprotein Proton Transfer." Proc. Natl. Acad. Sci. USA 94: 9085-9090.

Kranz, R. G. and R. B. Gennis (1983). "Immunological Characterization of the Cytochrome *o* Terminal Oxidase from *E. coli*." J. Biol. Chem. 258: 10614-10621.

Kranz, R. G. and R. B. Gennis (1984). "Characterization of the Cytochrome *d* Terminal Oxidase Complex of *Escherichia coli* Using Polyclonal and Monoclonal Antibodies." J. Biol. Chem. 259(12): 7998-8003.

Krasnoselskaya, I., A. M. Arutjunjan, I. S.mirnova, R. Gennis and A. A. Konstantinov (1993). "Cyanide-reactive Sites in Cytochrome *bd* Complex from *E. coli*." FEBS Lett. 327(3): 279-283.

Kusumoto, K., M. Sakiyama, J. Sakamoto, S. Noguchi and N. Sone (2000). "Menaquinol Oxidase Activity and Primary Structure of Cytochrome *bd* from the Amino-acid Fermenting Bacterium *Corynebacterium glutamicum*." Arch. Microbiol. 173: 390-397.

Kyte, J. and R. F. Doolittle (1982). "A Simple Method for Displaying the Hydropathic Character of a Protein." J. Mol. Biol. 157: 105-132.

La Mar, G. N. and J. S. de Ropp (1993). "NMR Methodology for Paramagnetic Proteins." Biol. Magn. Reson. 12: 1-78.

La Mar, G. N., W. D. J. Horrocks and R. H. Holm (1973). NMR of Paramagnetic Molecules: Principles and Applications. New York City, NY, Academic Press.

Loewen, P., J. Switala, I. von Ossowski, A. Hillar, A. Christie, B. Tattrie and P. Nicholls (1993). "Catalase HPII of *Escherichia coli* Catalyzes the Conversion of Protoheme to *cis*-Heme *d*." Biochemistry 32: 10159-10164.

Loisel-Meyer, S., M. P. Jimenez de Bagues, S. Kohler, J. P. Liautard and V. Jubier-Maurin (2005). "Differential Use of the Two High-oxygen-affinity Terminal Oxidases of *Brucella suis* for *In vitro* and Intramacrophagic Multiplication." Infect Immun. 73: 7768-7771.

Lorence, R. M., K. Carter, R. B. Gennis, K. Matsushita and H. R. Kaback (1988). "Trypsin Proteolysis of the Cytochrome *d* Complex of *Escherichia coli* Selectively Inhibits Ubiquinol Oxidase Activity While Not Affecting N, N, N', N'-Tetramethyl-p-phenylenediamine Oxidase Activity." J. Biol. Chem. 11: 5271-5276.

Lorence, R. M. and R. B. Gennis (1989). "Spectroscopic and Quantitative Analysis of the Oxygenated and Peroxy States of the Purified Cutochrome *d* Complex of *Escherichia coli*." J. Biol. Chem. 264: 7135-7140.

Lorence, R. M., G. N. Green and R. B. Gennis (1984). "Potentiometric Analysis of the Cytochromes of an *Escherichia coli* Mutant Strain Lacking the Cytochrome *d* Terminal Oxidase Complex." J. Bacteriol. 157(1): 115-121.

Lorence, R. M., M. J. Miller, A. Borochov, R. Faiman-Weinberg and R. B. Gennis (1984). "Effects of pH and Detergent on the Kinetic and Electrochemical Properties of the Purified Cytochrome *d* Complex of *Escherichia coli*." Biochim. Biophys. Acta. 790: 148-153.

Manoil, C. and J. Beckwith (1986). "A Generic Approach to Analyzing Membrane Protein Topology." Science 233: 17403-17408.

Mansfield, R. W. and T. E. Wiggins (1990). "Photoaffinity Labelling of the β-methoxyacrylate Binding Site in Bovine Heart Mitochondrial Cytochrome bc_1 Complex." Biochim. Biophys. Acta. 1015: 109-115.

Mantele, W. (1993). "Reaction-induced Infrared Difference Spectroscopy for the Study of Protein Function and Reaction Mechanisms." TIBS 18(6): 197-202.

Mantele, W. (1996). Biophysical Techniques in Photosynthesis. Boston, MA, Kluwer Academic Publishers.

Matsumoto, Y., M. Murai, D. Fujita, K. Sakamoto, H. Miyoshi, M. Yoshida and T. Mogi (2006). "Mass Spectrometric Analysis of the Ubiquinol-binding Site in Cytochrome *bd* from *Escherichia coli*." J. Biol. Chem. 281: 1905-1912.

Meinhardt, S. W., R. B. Gennis and T. Ohnishi (1989). "EPR Studies of the Cytochrome-*d* Complex of *Escherichia coli*." Biochim. Biophys. Acta. 975: 175-184.

Meunier, B., S. A. Madgwich, E. Reil, W. Oettmeier and P. R. Rich (1995). "New Inhibitors of the Quinol Oxidation Sites of Bacterial Cytochromes *bo* and *bd*." Biochemistry 34: 1076-1083.

Miller, M. J. and R. B. Gennis (1983). "The Purification and Characterization of the Cytochrome *d* Terminal Oxidase Complex of the *Escherichia coli* Aerobic Respiratory Chain." J. Biol. Chem. 258(15): 9159-9165.

Miller, M. J. and R. B. Gennis (1985). "The Cytochrome *d* Complex is a Coupling Site in the Aerobic Respiratory Chain of *Escherichia coli*." J. Biol. Chem. 260: 14003-14008.

Miller, M. J. and R. B. Gennis (1986). "Purification and Reconstitution of the Cytochrome *d* Terminal Oxidase Complex from *Escherichia coli*." Meth. Enz. 126: 138-145.

Minghetti, K. C. and R. B. Gennis (1988). "The Two Terminal Oxidases of the Aerobic Respiratory Chain of *Escherichia coli* Each Yield Water and Not Peroxide as a Final Product." Biochem. Biophys. Res. Commun. 155(1): 243-248.

Miyoshi, H., K. Takegami, K. Sakamoto, T. Mogi and H. Iwamura (1999). "Characterization of the Ubiquinol Oxidation Sites in Cytochrome *bo* and *bd* from *Escherichia coli* Using Aurachi C. Analogues." J. Biochem. 125: 138-142.

Mogi, T., S. Akimoto, S. Endou, T. Watanabe-Nakayama, E. Mizuochi-Asai and H. Miyoshi (2006). "Probing the Ubiquinol-binding Site in Cytochrome *bd* by Site-directed Mutagenesis." Biochemistry 45: 7924-7930.

Mogi, T., M. Tsubaki, H. Hori, H. Miyoshi, H. Nakamura and Y. Anraku (1998). "Two Terminal Quinol Oxidase Families in *Escherichia coli*: Variation on Molecular Machinery for Dioxygen Reduction." J. Biochem. Mol. Biol. Biophys. 2: 79-110.

Moller, S., M. D. R. Croning and R. Apweiler (2001). "Evaluation of Methods for the Prediction of Membrane Spanning Regions." Bioinformatics 17: 646-653.

Moss, D., E. Nabedryk, J. Breton and W. Mantele (1990). "Redox-linked Conformational Changes in Proteins Detected by a Combination of Infrared Spectroscopy and Protein Electrochemistry." Eur. J. Biochem. 187: 565-572.

Newton, G., C.-H. Yun and R. B. Gennis (1991). "Analysis of the Topology of the Cytochrome *d* Terminal Oxidase Complex of *Escherichia coli* by Alkaline Phosphatase Fusions." Mol. Microbiol. 5(10): 2511-2518.

Nicholls, D. G. and S. J. Ferguson (1992). Bioenergetics 2. New York City, NY, Harcourt Brace Jovanovich.

Ostermeier, C., A. Harrenga, U. Ermler and H. Michel (1997). "Structure at 2.7 Å Resolution of the *Paracoccus denitrificans* Two-Subunit Cytochrome *c* Oxidase Complexed with an Antibody F_v Fragment." Proc. Natl. Acad. Sci. USA 94: 10547-10553.

Oettmeier, W., K. Masson, M. Soll and E. Reil (1994). "Acridones and Quinolones as Inhibitors of Ubiquinone Functions in the Mitochondrial Respiratory Chain." Biochem. Soc. Trans. 22: 213-216.

Okamura, M. Y., M. L. Paddock, M. S. Graige and G. Feher (2000). "Proton and Electron Transfer in Bacterial Reaction Centers." Biochim. Biophys. Acta. 1458: 148-163.

Osborne, J. (1999). Structure and Function Relationships in Cytochrome bo_3 Oxidase and Cytochrome *bd*-I Oxidase from Escherichia coli. Ph.D. Thesis. Department of Biochemistry. Urbana-Champaign, University of Illinois: 109-114.

Osborne, J. P. and R. B. Gennis (1999). "Sequence Analysis of Cytochrome *bd* Oxidase Suggests a Revised Topology for Subunit I." Biochim. Biophys. Acta. 1410: 32-50.

Pinchas, S. and I. Laulicht (1977). Infrared Spectra of Labeled Compounds. London, Academic Press.

Poole, R. K. and S. Hill (1997). "Respiratory Protection of Nitrogenase Activity in *Azotobacter vinelandii* – Roles of the Terminal Oxidases." Bioscience Reports 17(3): 307-317.

Prince, R. C., P. L. Dutton and J. M. Bruce (1983). "Electrochemistry of Ubiquinones, Menaquinones and Plastoquinones in Aprotic Solvents." FEBS Lett. 160: 273-276.

Prinz, W. A. and J. Beckwith (1994). "Gene Fusion Analysis of Membrane Protein Topology: A Direct Comparison of Alkaline Phosphatase and beta-Lactamase Fusions." J. Bacteriol. 176: 6410-6413.

Provencher, S. and R. H. Vogel (1983). Regularization Techniques for Inverse Problems in Molecular Biology in: Numerical Treatment of Inverse Problems in Differential and Integral Equations. Boston, MA, Birkhäuser.

Pudek, M. R. and P. D. Bragg (1974). "Inhibition by Cyanide of the Respiratory Chain Oxidases of *Escherichia coli*." Arch. Biochem. Biophys. 164: 682-693.

Puustinen, A., M. Finel, T. Haltia, R. B. Gennis and M. Wikstrom (1991). "Properties of the Two Terminal Oxidases of *Escherichia coli*." Biochemistry 30: 3936-3942.

Reil, E., G. Hofle, W. Draber and W. Oettmeier (1997). "Quinolones and their N-oxides as Inhibitors of Mitochondrial Complexes I and III." Biochim. Biophys. Acta. 1318: 291-298.

Reil, E., M. Soll, K. Masson and W. Oettmeier (1994). "Synthesis of Quinolones and Acridones and Their Inhibitory Activity in NADH-Dehydrogenases and Cytochrome b/c1-Complexes." Biochem. Soc. Trans. 22: 62S.

Rice, C. W. and W. P. Hempfling (1978). "Oxygen-limited Continuous Culture and Respiratory Energy Conservation in *Escherichia coli*." J. Bacteriol. 134(1): 115-124.

Rigby, S. E. J., T. A. Alleyne, M. T. Wilson and G. R. Moore (1989). "A ^{1}H NMR Study of Bovine Cytochrome Oxidase." FEBS Lett. 257(1): 155-158.

Rothery, R. and W. J. Ingledew (1989). "The Cytochromes of Anaerobically Grown *Escherichia coli*." Biochem. J. 262: 437-443.

Sakamoto, J., E. Koga, T. Mizuta, C. Sato, S. Noguchi and N. Sone (1999). "Gene Structure and Quinol Oxidase Activity of a Cytochrome *bd*-type Oxidase from *Bacillus stearothermophilus*." Biochim. Biophys. Acta. 1411: 147-158.

Sakamoto, K., H. Miyoshi, K. Takegami, T. Mogi, Y. Anraku and H. Iwamura (1996). "Probing Substrate Binding Site of the *Escherichia coli* Quinol Oxidases Using Synthetic Ubiquinol Analogues." J. Biol. Chem. 271(47): 29897-29902.

Satterlee, J. D., S. Alam, Q. Yi, J. E. Erman, I. Constantinidis, D. J. Russell and S. J. Moench (1993). "Proton NMR Studies of Selected Paramagnetic Heme Proteins." Biol. Magn. Reson. 12: 275-298.

Savenkova, M. I., J. D. Satterlee, J. E. Erman, W. F. Siems and G. L. Helms (2001). "Expression, Purification, Characterization, and NMR Studies of Highly Deuterated Recombinant Cytochrome *c* Peroxidase." Biochemistry 40: 12123-12131.

Siebert, F., W. Maentele and W. Kreutz (1982). "Evidence for the Protonation of Two Internal Carboxylic Groups during the Photocycle of Bacteriorhodopsin. Investigation by Kinetic Infrared Spectroscopy." FEBS Lett. 141: 82-87.

Siegele, D. A., K. R. Imlay and J. A. Imlay (1996). "The Stationary-Phase-Exit Defect of *cydC* (*surB*) Mutants is Due to the Lack of a Functional Terminal Cytochrome Oxidase." J. Bacteriol. 178(21): 6091-6096.

Shi, L., C. D. Sohaskey, B. D. Kana, S. Dawes, R. J. North, V. Mizrahi and M. L. Gennaro (2005). "Changes in Energy Metabolism of Mycobacterium Tuberculosis in Mouse Lung and Under *In vitro* Conditions Affecting Aerobic Respiration." Proc. Natl. Acad. Sci. USA 102: 15629-15634.

Smith, A., S. Hill and C. Anthony (1990). "The Purification, Characterization and Role of the *d*-type Cytochrome Oxidase of *Klebsiella pneumoniae* during Nitrogen Fixation." J. Gen. Microbiol. 136: 171-180.

Spinner, F., M. R. Cheesman, A. J. Thomson, T. Kaysser, R. B. Gennis, Q. Peng and J. Peterson (1995). "The Haem b_{558} Component of the Cytochrome *bd* Quinol Oxidase Complex from *Escherichia coli* has Histidine-Methionine Axial Ligation." Biochem. J. 308: 641-644.

Sturr, M. G., T. A. Krulwich and D. B. Hicks (1996). "Purification of a Cytochrome *bd* Terminal Oxidase Encoded by the *Escherichia coli* app Locus from a Δ*cyo* Δ*cyd* Strain Complemented by Genes from *Bacillus firmus* OF4." J. Bacteriol. 178(6): 1742-1749.

Sun, J., M. A. Kahlow, T. M. Kaysser, J. P. Osborne, J. J. Hill, R. J. Rohlfs, R. Hille, R. B. Gennis and T. M. Loehr (1996). "Resonance Raman Spectroscopic Identification of a Histidine Ligand of b_{595} and the Nature o f the Ligation of Chlorin *d* in the Fully Reduced *Escherichia coli* Cytochrome bd Oxidase." Biochemistry 35: 2403-2412.

Sun, J., J. P. Osborne, M. A. Kahlow, T. M. Kaysser, R. B. Gennis and T. M. Loehr (1995). "Resonance Raman Studies of *Escherichia coli* Cytochrome *bd* Oxidase. Selective Enhancement of the Three Heme Chromophores of the "As-Isoloated" Enzyme and Characterization of the Cyanide Adduct." Biochemistry 34(38): 12144-12151.

Tamm, L. K. and S. A. Tatulian (1997). "Infrared Spectroscopy of Proteins and Peptides in Lipid Bilayers." Q. Rev. Biophys. 30: 365-429.

Thamrong-nawasawat, T. (2004). An Investigation of Cytochrome *bd* Quinol Oxidases of *V. cholerae*, *R. sphaeroides*, and *S. typhimurium*. Ph.D. Thesis. Department of Biochemistry. Urbana-Champaign, University of Illinois: 1-8.

Timkovich, R., M. S. Cork, R. B. Gennis and P. Y. Johnson (1985). "Proposed Structure of Heme *d*, a Prosthetic Group of Bacterial Terminal Oxidases." J. Am. Chem. Soc. 107: 6069-6075.

Tomson, F. L. (2002). Examining the Proton Channels in Heme-Copper Oxidases. Ph.D. Thesis. Department of Biochemistry. Urbana-Champaign, University of Illinois: 92.

Tseng, C.-P., J. Albrecht and R. P. Gunsalus (1996). "Effect of Microaerophilic Cell Growth Conditions on Expression of the Aerobic (*cyo*ABCDE and *cyd*AB) and Anaerobic (*nar*GHJI, *frd*ABCD, and *dms*ABC) Respiratory Pathway Genes in *Escherichia coli*." J. Bact. 178: 1094-1098.

Tsubaki, M., H. Hori, T. Mogi and Y. Anraku (1995). "Cyanide-binding Site of *bd*-type Ubiquinol Oxidase from *Escherichia coli*." J. Biol. Chem. 270(48): 28565-28569.

Tsubaki, M., T. Mogi and H. Hori (1999). "Azide- and Cyanide-binding to the *Escherichia coli bd*-type Ubiquinol Oxidase Studied by Visible Absorption, EPR and FTIR Spectroscopies." J. Biochem. 126: 510-519.

Tsubaki, M., T. Mogi and H. Hori (1999). "Fluoride-binding to the *Escherichia coli bd*-type Ubiquinol Oxidase Studied by Visible Absorption and EPR Spectroscopies." J. Biochem. 126: 98-103.

Tsubaki, M., T. Mogi, H. Hori, M. Sato-Watanabe and Y. Anraku (1996). "Infrared and EPR Studies on Cyanide Binding to the Heme-Copper Binuclear Center of Cytochrome *bo*-type Ubiquinol Oxidase from *Escherichia coli*." J. Biol. Chem. 271(8): 4017-4022.

Tsubaki, M., T. Uno, H. Hori, T. Mogi, Y. Nishimura and Y. Anraku (1993). "Cytochrome *d* Axial Ligand of the *bd*-type Terminal Quinol Oxidase from *Escherichia coli*." FEBS Lett. 335(1): 13-17.

Tsukihara, T., H. Aoyama, E. Yamashita, T. Takashi, H. Yamaguichi, K. Shinzawa-Itoh, R. Nakashima, R. Yaono and S. Yoshikawa (1996). "The Whole Structure of the 13-Subunit Oxidized Cytochrome c Oxidase at 2.8 Å." Science 272: 1136-1144.

Vos, M. H., V. B. Borisov, U. Liebl, J.-L. Martin and A. A. Konstantinov (2000). "Femtosecond Resolution of Ligand-heme Interactions in the High-affinity Quinol Oxidase *bd*: A Di-heme Active Site?" Proc. Natl. Acad. Sci. 97(4): 1554-1559.

Wang, R., S. J. Seror, M. Blight, J. M. Pratt, J. K. Broome-Smith and I. B. Holland (1991). "Analysis of the Membrane Organization of an *Escherichia coli* Protein Translocator, HlyB, a Member of a Large Family of Prokaryote and Eukaryote Surface Transport Proteins." J. Mol. Biol. 217: 441-454.

Wang, X. and Y. Lu (1999). "Proton NMR Investigation of the Heme Active Site Structure of an Engineered Cytochrome *c* Peroxidase that Mimics Manganese Peroxidase." Biochemistry 38: 9146-9157.

Way, S. S., S. Sallustio, R. S. Magliozzo and M. B. Goldberg (1999). "Impact of Either Elevated or Decreased Levels of Cytochrome *bd* Expression on *Shigella flexneri* Virulence." J. Bacteriol. 181: 1229-1237.

Yamamoto, Y., C. Poyart, P. Trieu-Cuot, G. Lamberet, A. Gruss and P. Gaudu (2005). "Respiration Metabolism of Group B Streptococcus is Activated by Environmental Haem and Quinone and Contributes to Virulence." Molecular Microbiology 56: 525-534.

Yamazaki, Y., H. Kandori and T. Mogi (1999). "Fourier-transform Infrared Studies on Conformation Changes in *bd*-type Ubiquinol Oxidase from *Escherichia coli* upon Photoreduction of the Redox Metal Centers." J. Biochem. 125: 1131-1136.

Yang, F.-D., L. Yu, C.-A. Yu, R. M. Lorence and R. B. Gennis (1986). "Use of an Azido-ubiquinone Derivative to Identify Subunit I as the Ubiquinol Binding Site of the Cytochrome *d* Terminal Oxidase Complex of *Escherichia coli*." J. Biol. Chem. 261(32): 14987.

Yang, K., J. Zhang, A. S. Vakkasoglu, R. Hielscher, J. P. Osborne, J. Hemp, H. Miyoshi, P. Hellwig, R. B. Gennis (2007). "Glutamate 107 in Subunit I of the Cytochrome *bd* Quinol Oxidase from *Escherichia coli* is Protonated and Near the Heme *d* / Heme b_{595} Binuclear Center." Biochemistry 46: 3270-3278.

Yang, K., V. B. Borisov, A. A. Konstantinov, R. B. Gennis (2008). "The Fully Oxidized Form of the Cytochrome *bd* Quinol Oxidase from E. coli Does Not Participate in the Catalytic Cycle: Direct Evidence from Rapid Kinetics Studies." FEBS Lett. 582: 3705-3709.

Zhang, J., B. Barquera, R. B. Gennis (2004). "Gene Fusions with Beta-Lactamase Show that Subunit I of the Cytochrome *bd* Quinol Oxidase from *E. coli* Has Nine Transmembrane Helices with the O_2 Reactive Site Near the Periplasmic Surface." FEBS Lett. 561(1-3): 58-62.

Zhang, J., P. Hellwig, J. P. Osborne, R. B. Gennis (2004). "Arginine 391 in Subunit I of the Cytochrome *bd* Quinol Oxidase from *Escherichia coli* Stabilizes the Rduced Form of the Hemes and is Essential for Quinol Oxidase Activity." J. Biol. Chem. 279(52): 53980-53987.

Zhang, J., P. Hellwig, J. P. Osborne, H.-W. Huang, P. Moënne-Loccoz, A. A. Konstantinov and R. B. Gennis (2001). "Site-directed Mutation of the Highly Conserved Region Near the Q-loop of the Cytochrome *bd* Quinol Oxidase from *Escherichia coli* Specifically Perturbs Heme b595." Biochemistry 40(29): 8548-8556.

Zhang, J., W. Oettmeier, R. B. Gennis and P. Hellwig (2002). "FTIR Spectroscopic Evidence for the Involvement of an Acidic Residue in Quinone Binding in Cytochrome *bd* from *Escherichia coli*." Biochemistry 41(14): 4612-4617.

Zhang, J., J. P. Osborne, R. B. Gennis and X. Wang (2004). "Proton NMR Study of the Heme Environment in Bacterial Quinol Oxidases." Arch. Biochem. Biophys. 421(2): 186-191.

Zhang, J. (2002). Mutagenesis and Spectroscopic Studies on Cytochrome *bd* Quinol Oxidase of *Escherichia coli*. Ph.D. Thesis. Department of Biochemistry. Urbana-Champaign, University of Illinois: 120-122.

Zuberi, T. M. (1993). Structural and Functional Studies of the Cytochrome d Oxidase Complex of *Escherichia coli*. Ph.D. Thesis. Department of Biochemistry. Urbana-Champaign, University of Illinois: 117.

VITA

Ke Yang was born on May 13, 1982 and was raised in Chongqing and Chengdu, People's Republic of China. He received his Bachelor of Science degree from Department of Bioscience, Sichuan University, Chengdu, in July 2003, after one-year exchange in University of Washington, Seattle. He enrolled in the graduate studies in the Biochemistry Department of University of Illinois at Urbana-Champaign in the Spring semester of 2004. On the way to obtain his Ph.D. degree in Biochemistry, he also received his Master of Science degrees from Biochemistry and Statistics, respectively. He is the co-author of the following publications:

1. Yang K., J. Zhang, A. S. Vakkasoglu, R. Hielscher, J. P. Osborne, J. Hemp, H. Miyoshi, P. Hellwig and R. B. Gennis (2007). "Glutamate 107 in Subunit I of the Cytochrome *bd* Quinol Oxidase from *Escherichia coli* is Protonated and Near the Heme *d* / Heme b_{595} Binuclear Center." Biochemistry 46: 3270-3278.

2. Yang K., V. B. Borisov, A. A. Konstantinov and R. B. Gennis (2008). "The Fully Oxidized Form of the Cytochrome bd Quinol Oxidase from *E. coli* Does Not Participate in the Catalytic Cycle: Direct Evidence from Rapid Kinetics Studies." FEBS Lett 582: 3705-3709.

3. Belevich I., V. B. Borisov, J. Zhang, K. Yang, A. A. Konstantinov, R. B. Gennis and M. I. Verkhovsky (2005). "Time-resolved Electrometric and Optical Studies on Cytochrome *bd* Suggest a Mechanism of Electron-proton Coupling in the Di-heme Active Site." Proc. Natl. Acad. Sci. USA 102: 3657-3662.